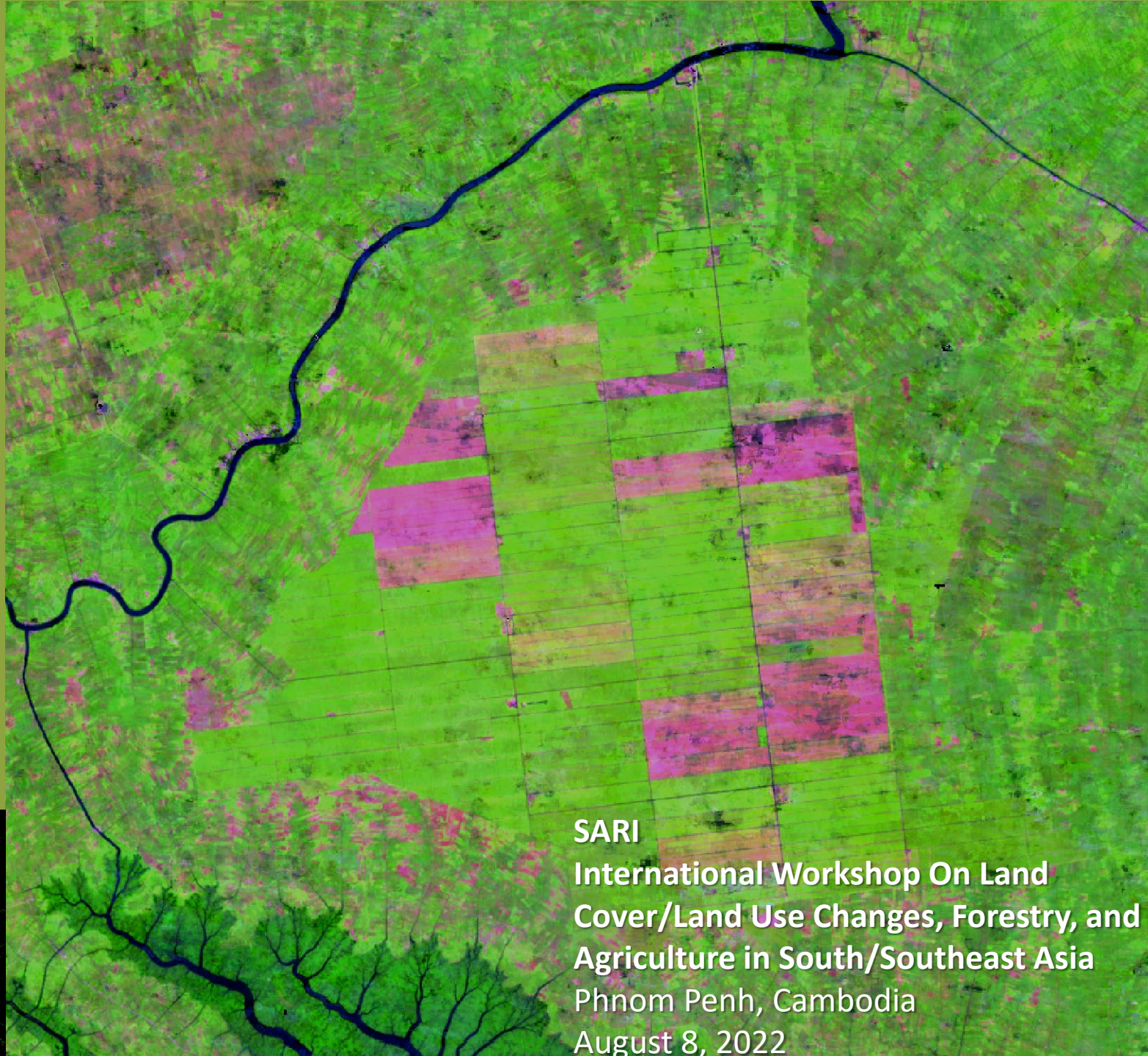


Oil Palm and Land Cover Change Dynamics in Indonesian Peatlands

Mark A. Cochrane

University of Maryland Center for
Environmental Science (UMCES)

Appalachian Laboratory



SARI

**International Workshop On Land
Cover/Land Use Changes, Forestry, and
Agriculture in South/Southeast Asia**

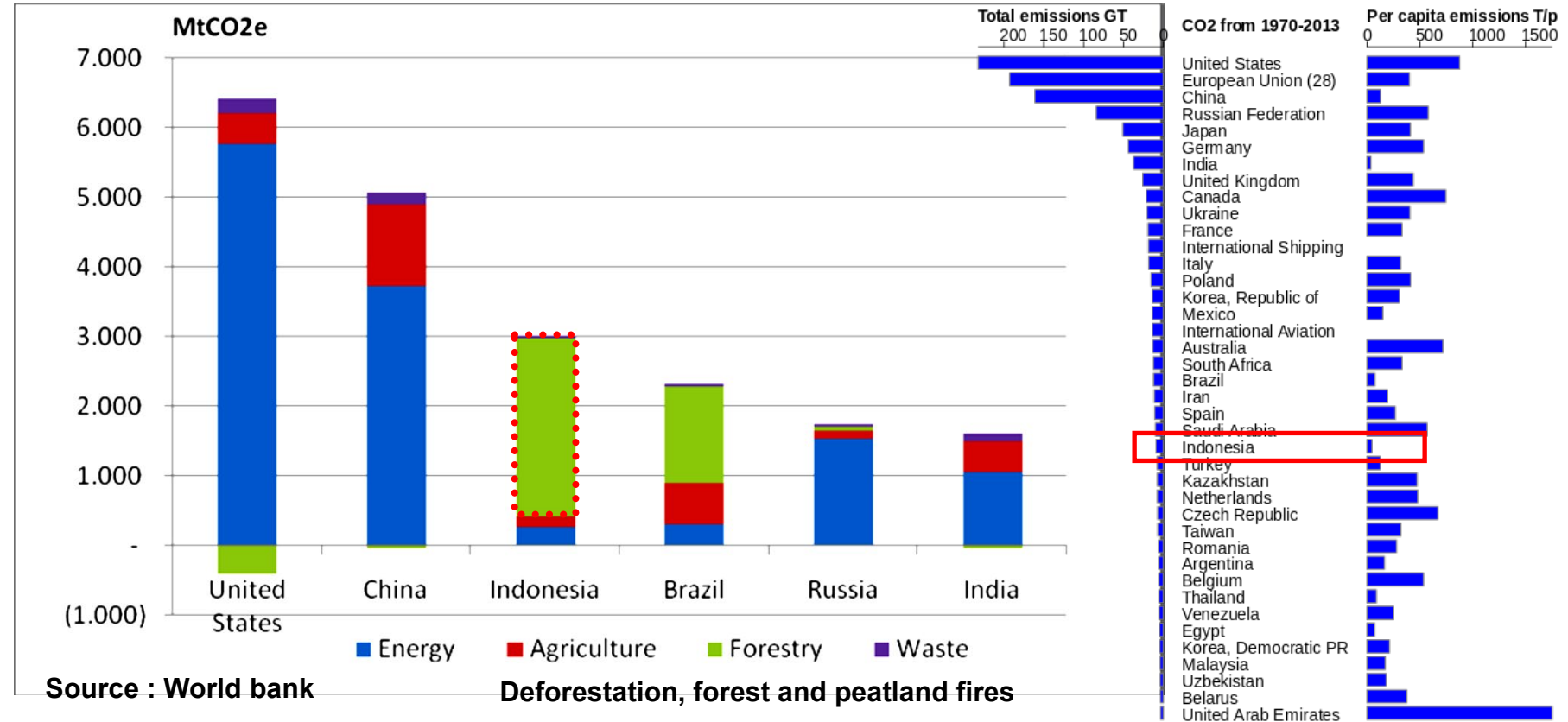
Phnom Penh, Cambodia

August 8, 2022

Indonesia : The worlds 3rd largest CO₂ emitter ?

2006 : Indonesian carbon emissions from deforestation and peatland fires : 1.9 Gt CO₂

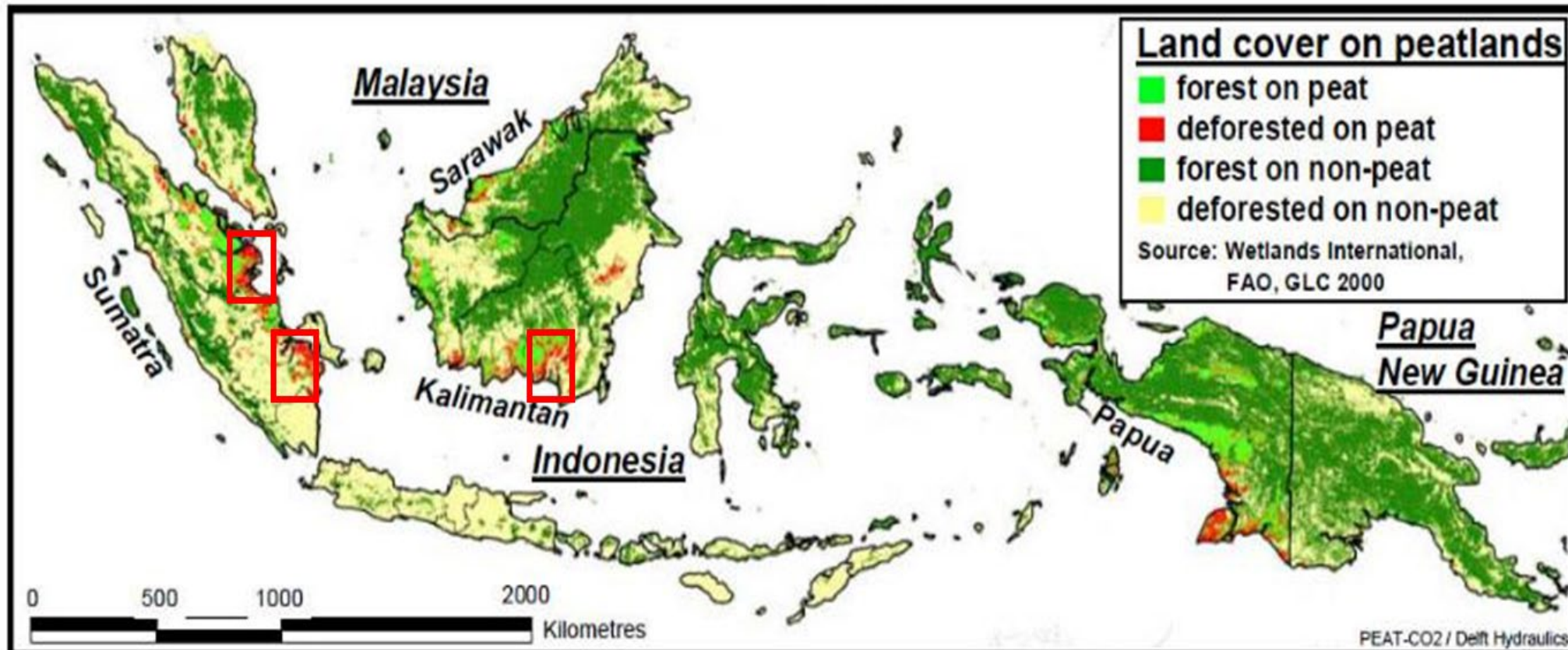
- Frequent wildfires have become a side-effect of peatland conversion
- In 2015, 2.6 million hectares burned, with the majority in peatlands of Sumatra and Indonesian Borneo (Kalimantan)
- Carbon releases exceeded Japan's annual emissions
- Severe regional air pollution, caused US\$16 billion in Indonesian economic losses and many premature deaths from smoke exposure

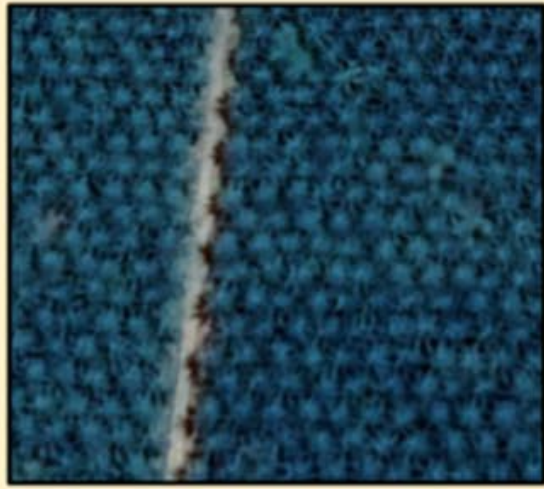


Forest clearing, conversion to agriculture and wildfires pushed Indonesia from 24th to 3rd in national carbon emissions

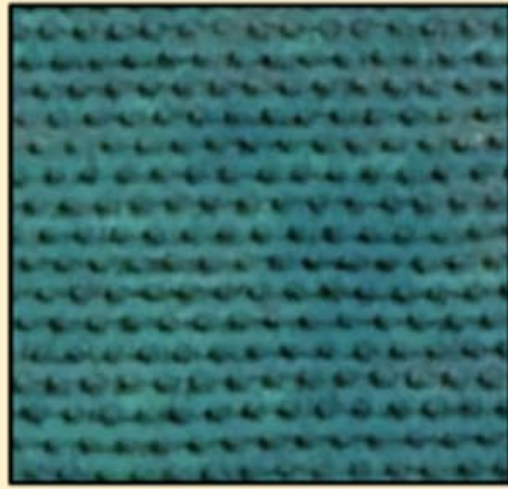
Land-Use Transitions in Indonesian Peatlands

- 1. Characterize the land-cover and land-use changes (LCLUC)*
- 2. Identify major drivers and impacts of those changes*
- 3. Develop strategies for managing the landscape sustainably*

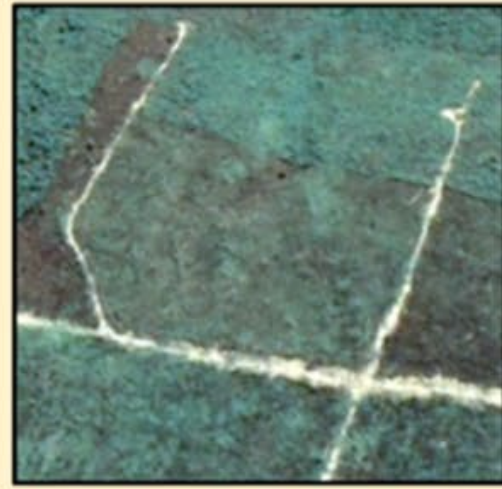




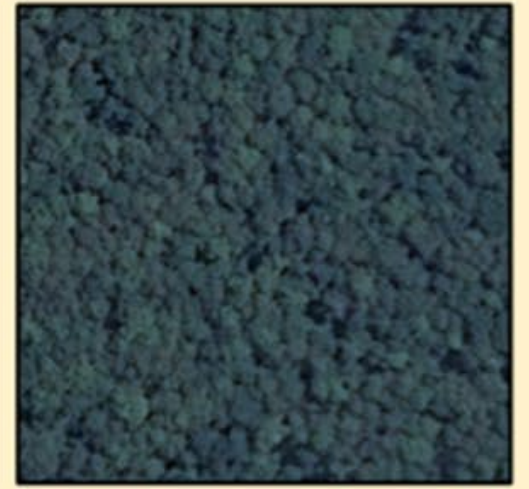
Mature oil palm



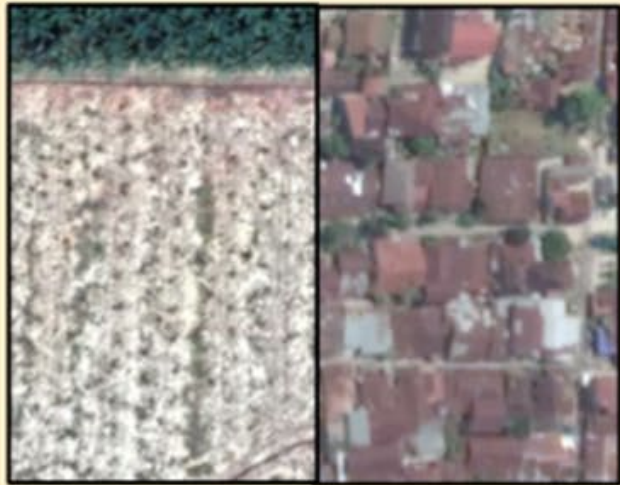
Young oil palm



Open dry land



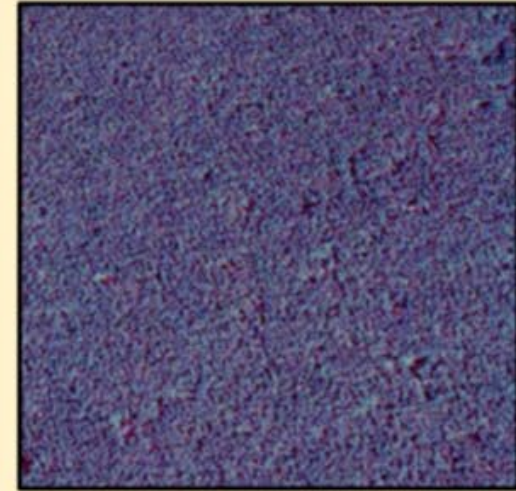
Forest



Bare soil (left) and
impervious surface (right)

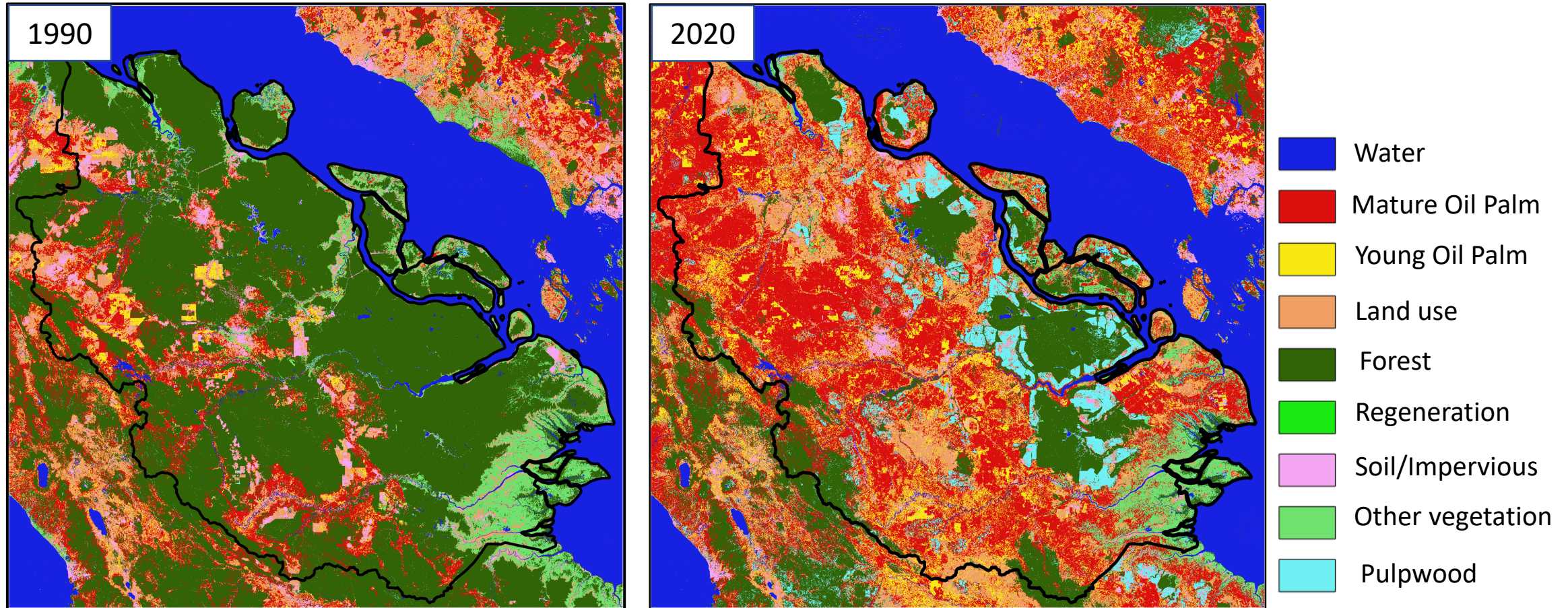


Other vegetation



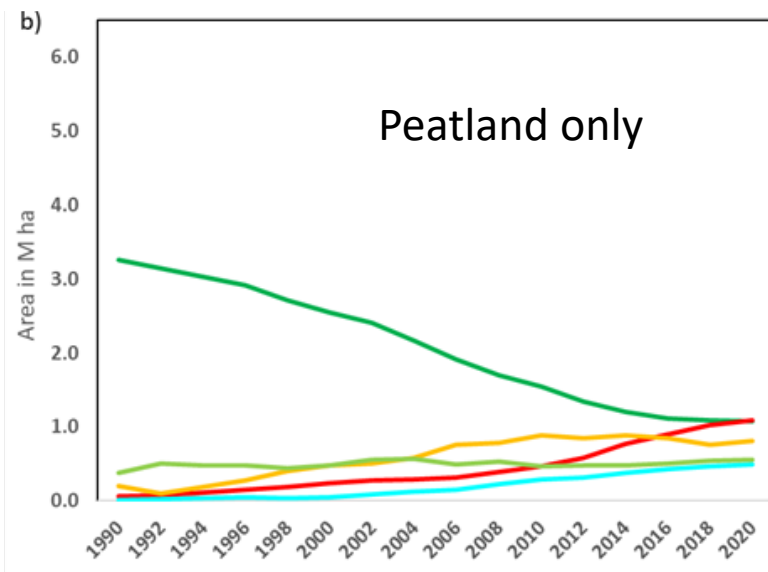
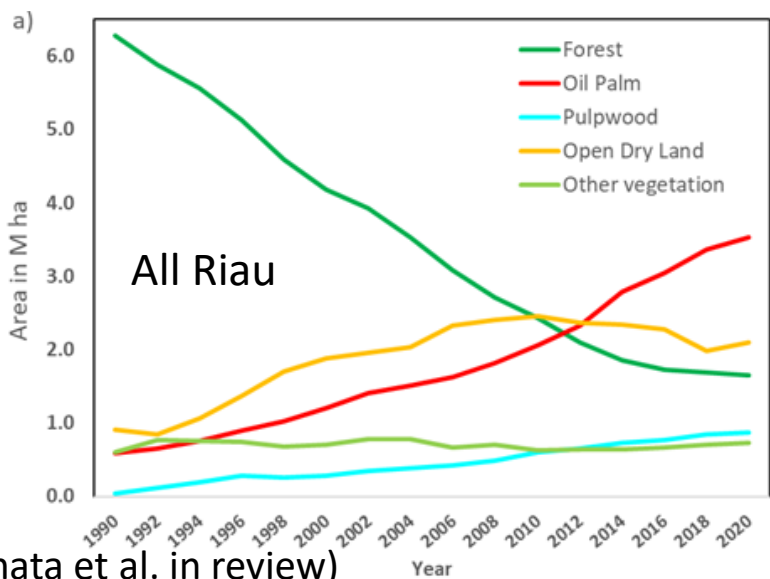
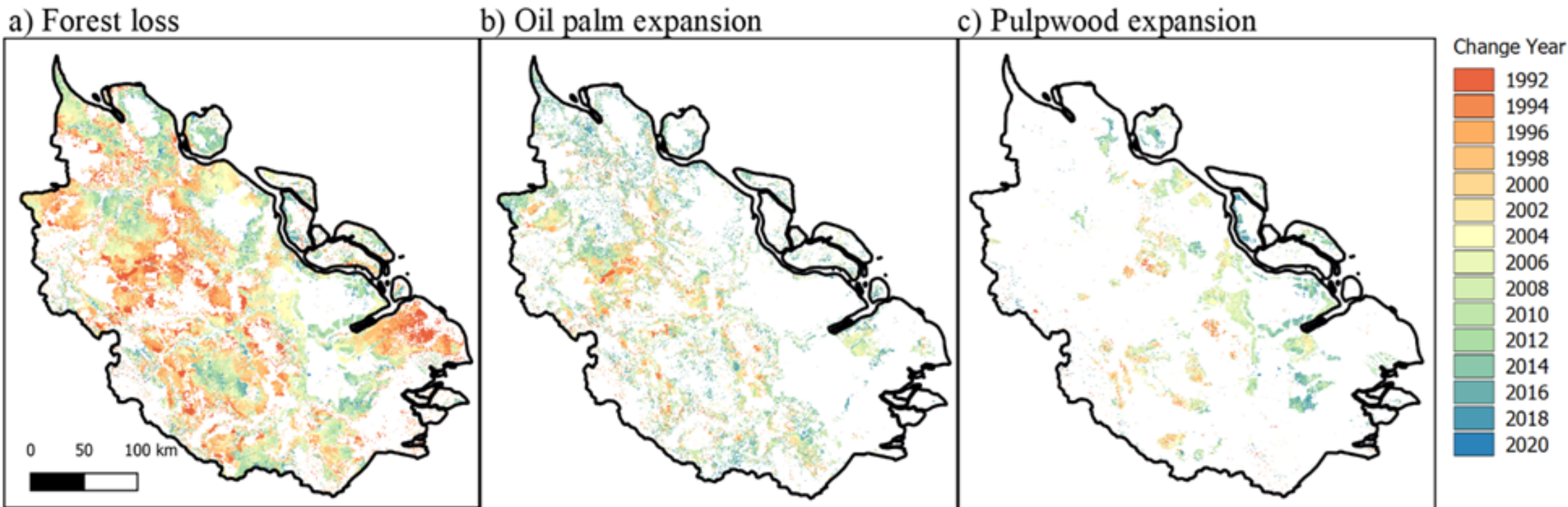
Pulpwood

Forest loss and expansion of oil palm plantation and other land cover types between 1990 and 2020



Land cover maps in Riau for 1990 and 2020 show the extensive amount of land cover change that has accompanied land use changes over the last 30 years

Forest loss and expansion of Oil Palm and Pulpwood plantations during 1990-2020



- Forest losses have largely been associated with the expansion of oil palm and pulpwood
- Open lands are also prevalent
- Increasing amounts of oil palm in sensitive peatland areas
- Deforestation rates have dropped recently

Deforestation over peatland area in Riau

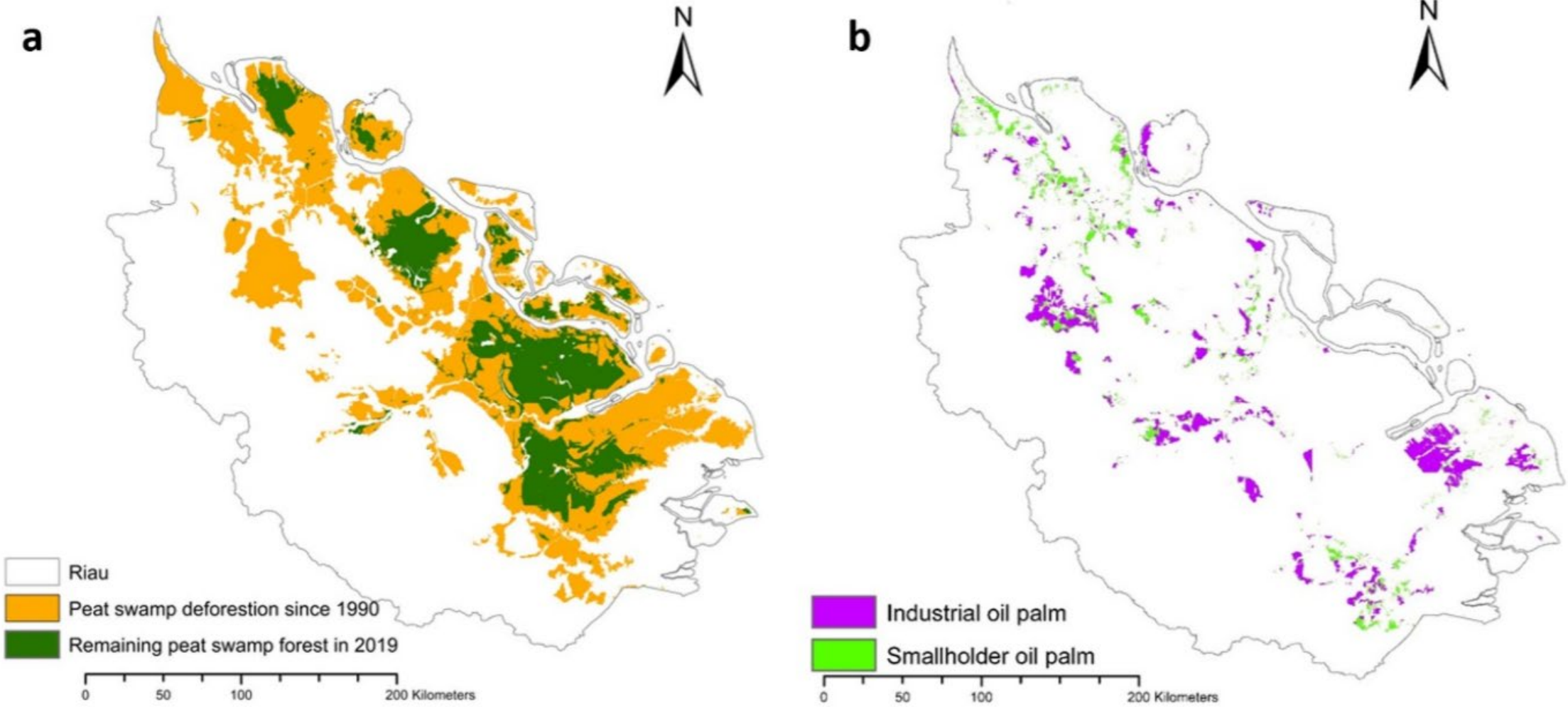
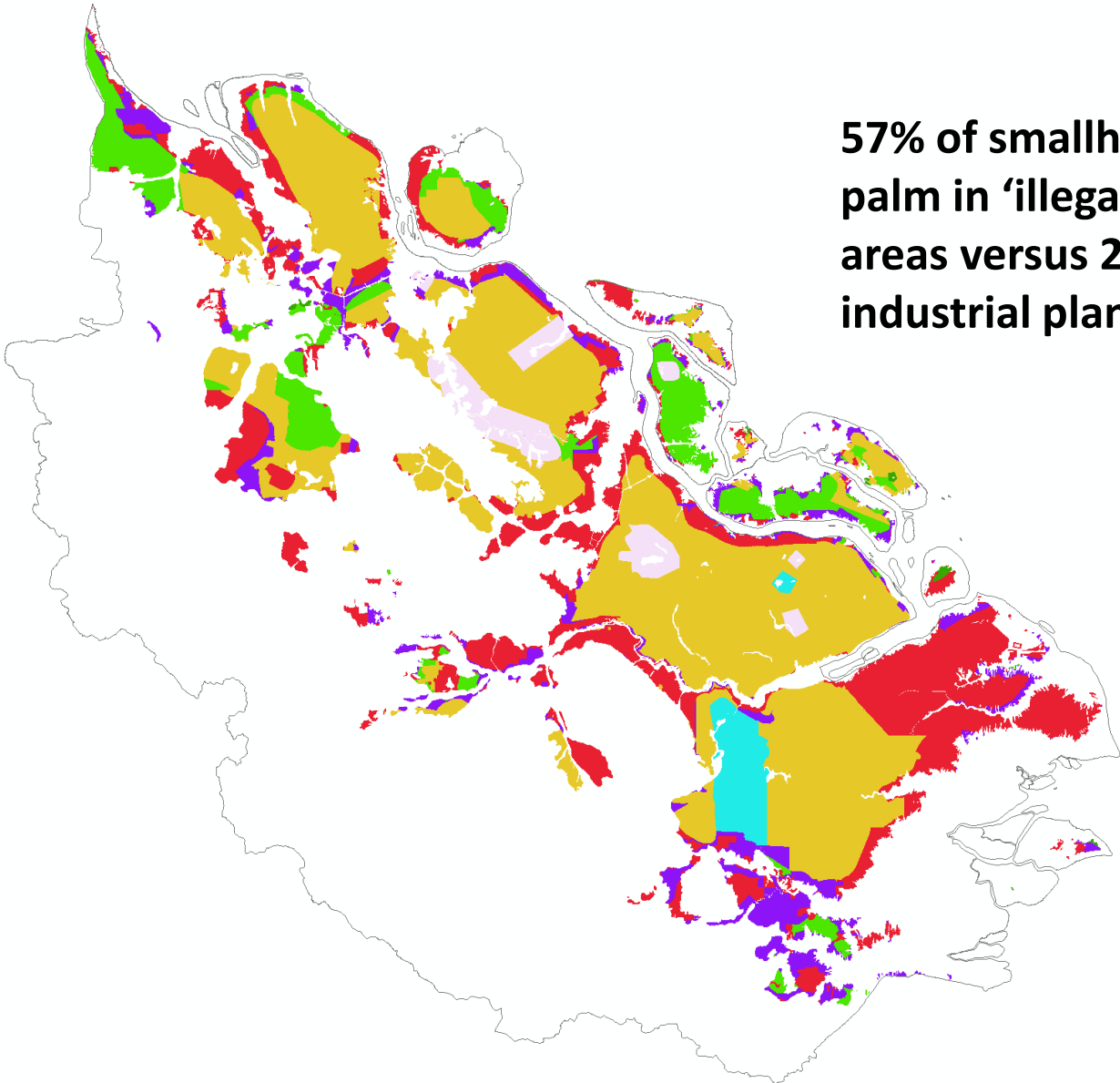


Figure 1. Maps of Riau, Indonesia showing (a) Peat swamp forest in 1990 and 2019 and (b) industrial and smallholder oil palm in 2019. Colored areas show only the areas that were peat swamp forest in 1990.

Land legal status over peat swamp forest in Riau

- Nature park
- Water
- Wildlife reserve
- Nature conservation area
- Limited production forest
- Conversion production forest
- Permanent production forest
- Protected forest
- APL(other use area)

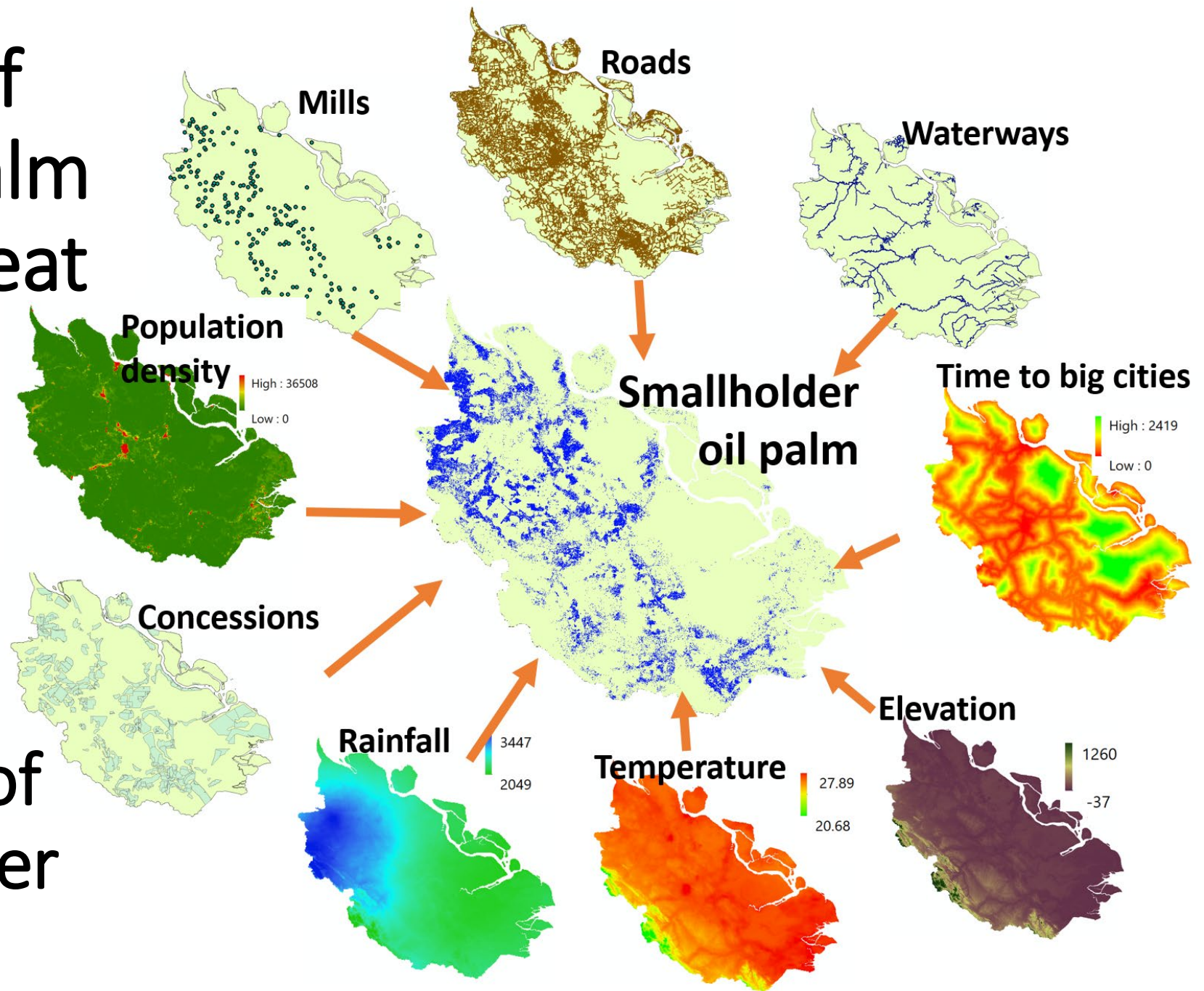


57% of smallholder oil palm in 'illegal' forest areas versus 26% of industrial plantations

Spatial patterns of
smallholder oil palm
expansion over peat
swamp forests

relate to

Socioeconomic and
biophysical drivers of
influence smallholder
oil palm expansion



Smallholder oil palms are clustered near service roads and residential roads and residential roads.

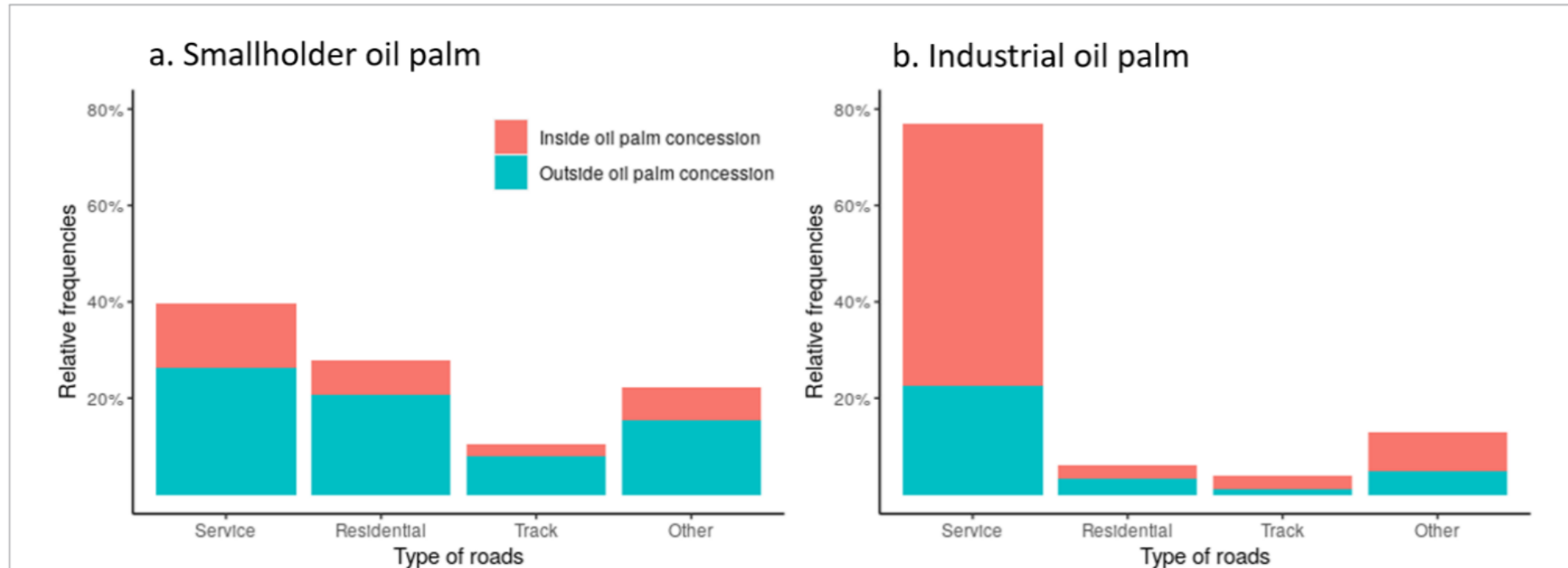


Figure 3. The nearest road type inside and outside of concession areas for (a) smallholder and (b) industrial oil palm on peat swamp forests in 2019. Service roads are for access to, or within an industrial estate, camp site, car park, alleys, etc. Residential stands for ‘roads which serve as an access to housing, without the function of connecting settlements’. Track represents roads for mostly agricultural or forestry uses. Other roads include primary, secondary, tertiary and unclassified highways, trunk, path, construction roads, etc.

High risk area of remaining peat swamp forest in Riau

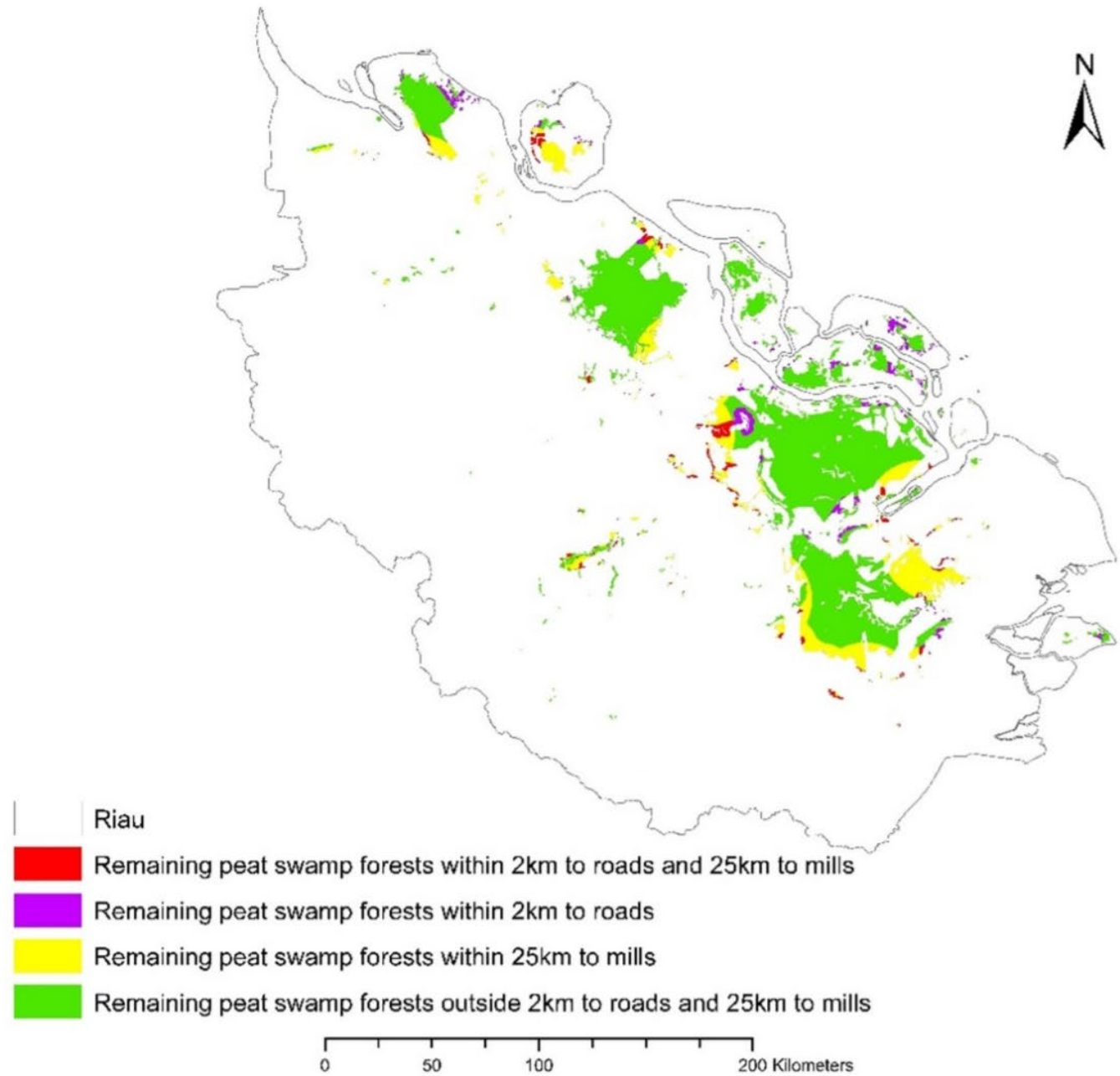
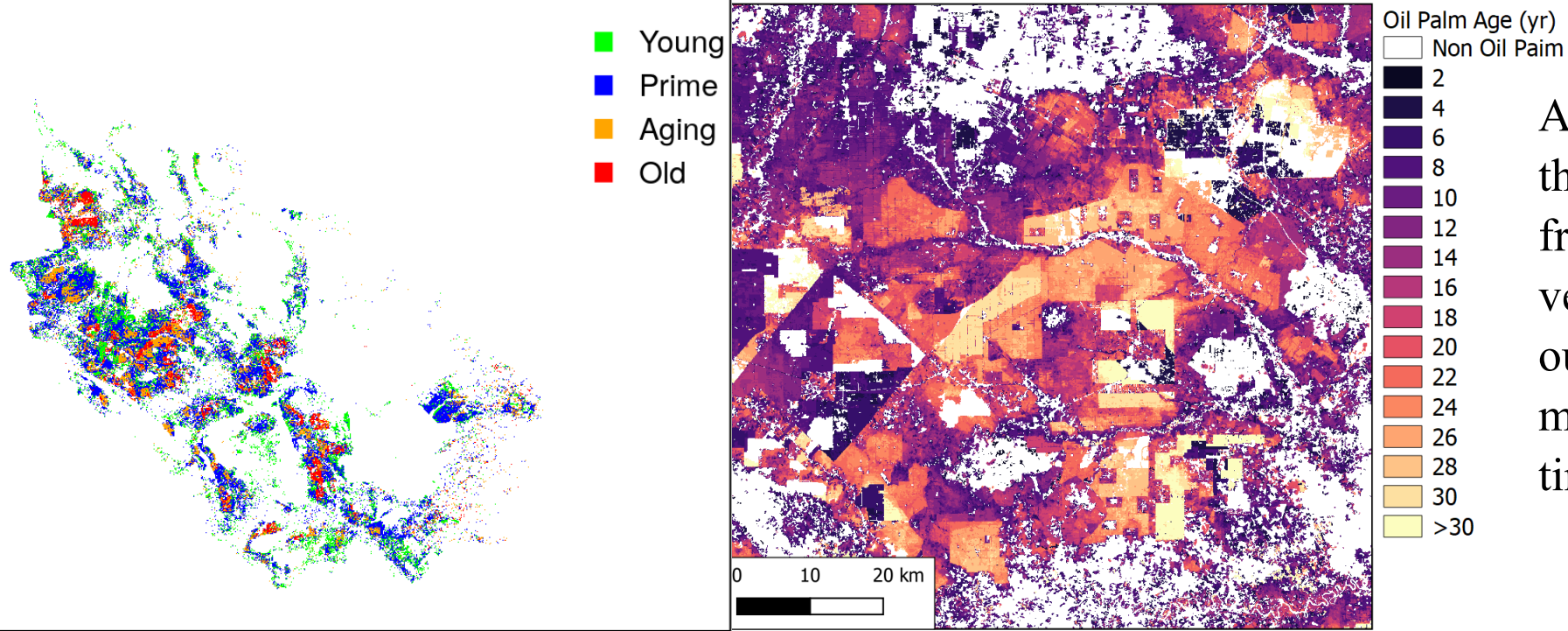


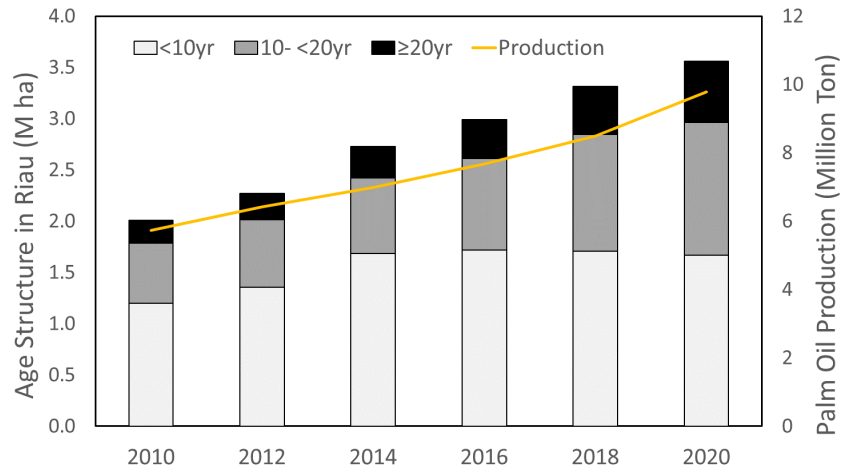
Figure 5. High risk area of remaining peat swamp forests to smallholder oil palm conversion in 2019.

Oil palm age map of Riau in 2020



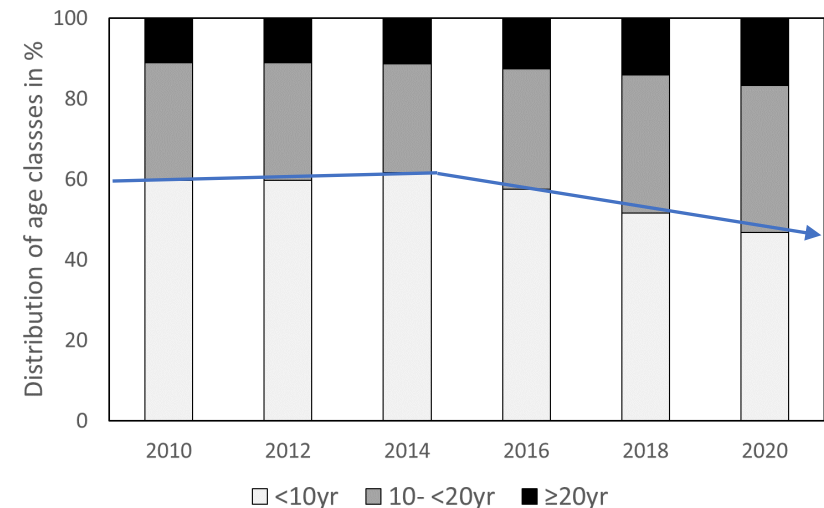
Age structure illustrates the general expansion from core areas with very old oil palm outward into more marginal regions over time

Changes in oil palm age structure in area and annual palm oil production (orange line), and as percentages (2010-2020)



Area and production have increased steadily

Since 2014 the rate of expansion has dropped



Oil palm area by age in Riau in 2017

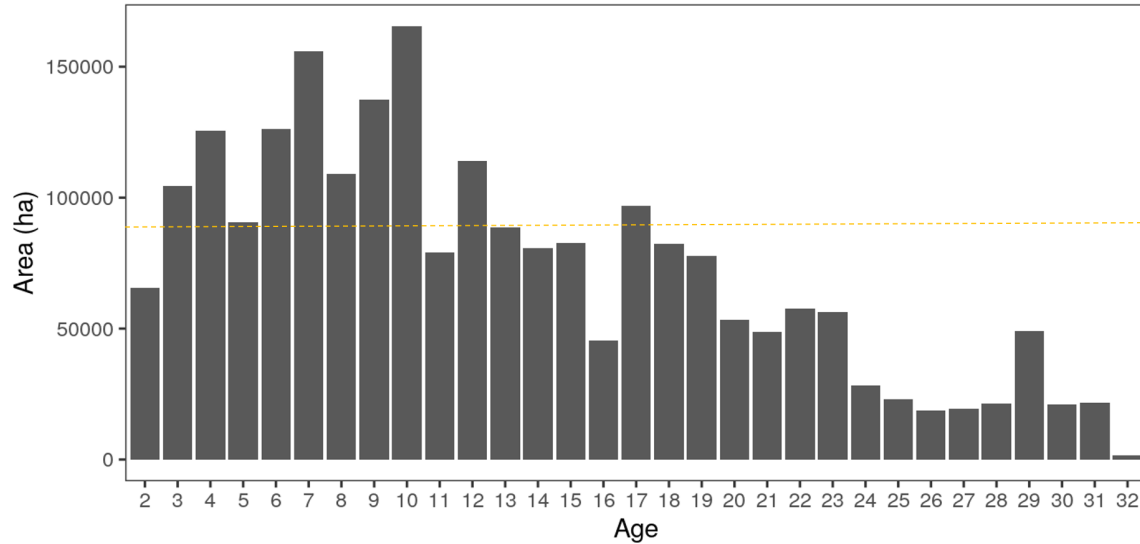
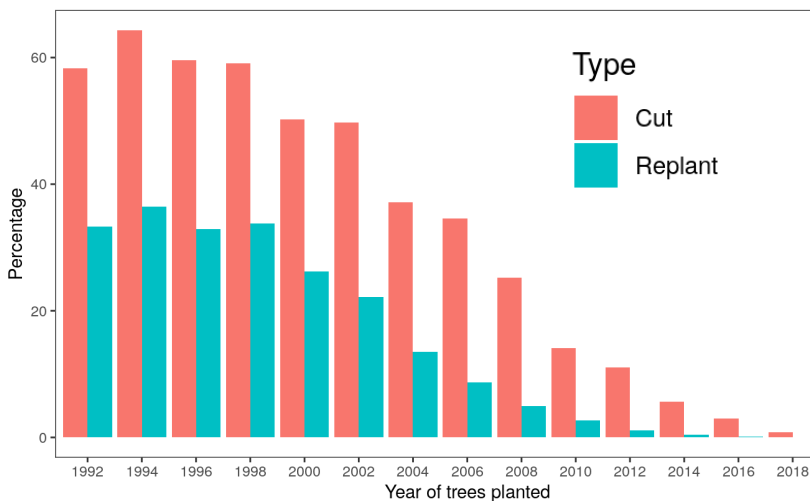


Figure above: Oil palm area by age in Riau in 2017 (Danylo et al., 2021). Orange dash line shows the level of 4% of total oil palm area in 2017.



Oil palm dynamic changes in cover as cutting and replanting occurs

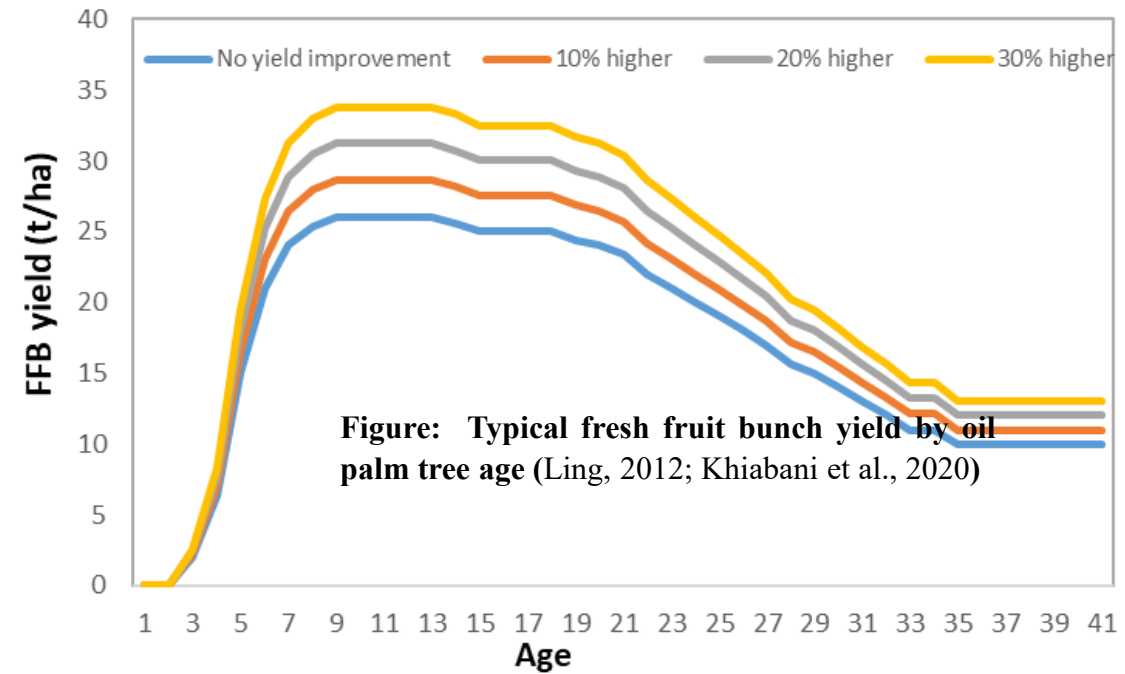
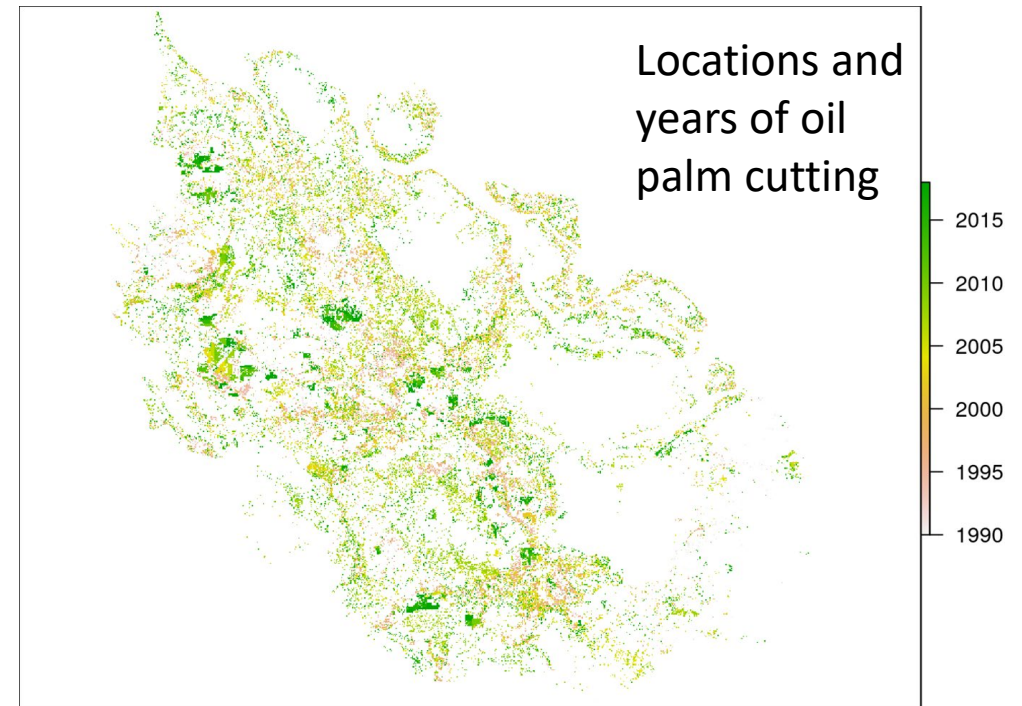


Figure: Typical fresh fruit bunch yield by oil palm tree age (Ling, 2012; Khiabani et al., 2020)



Oil palm production prediction till 2050

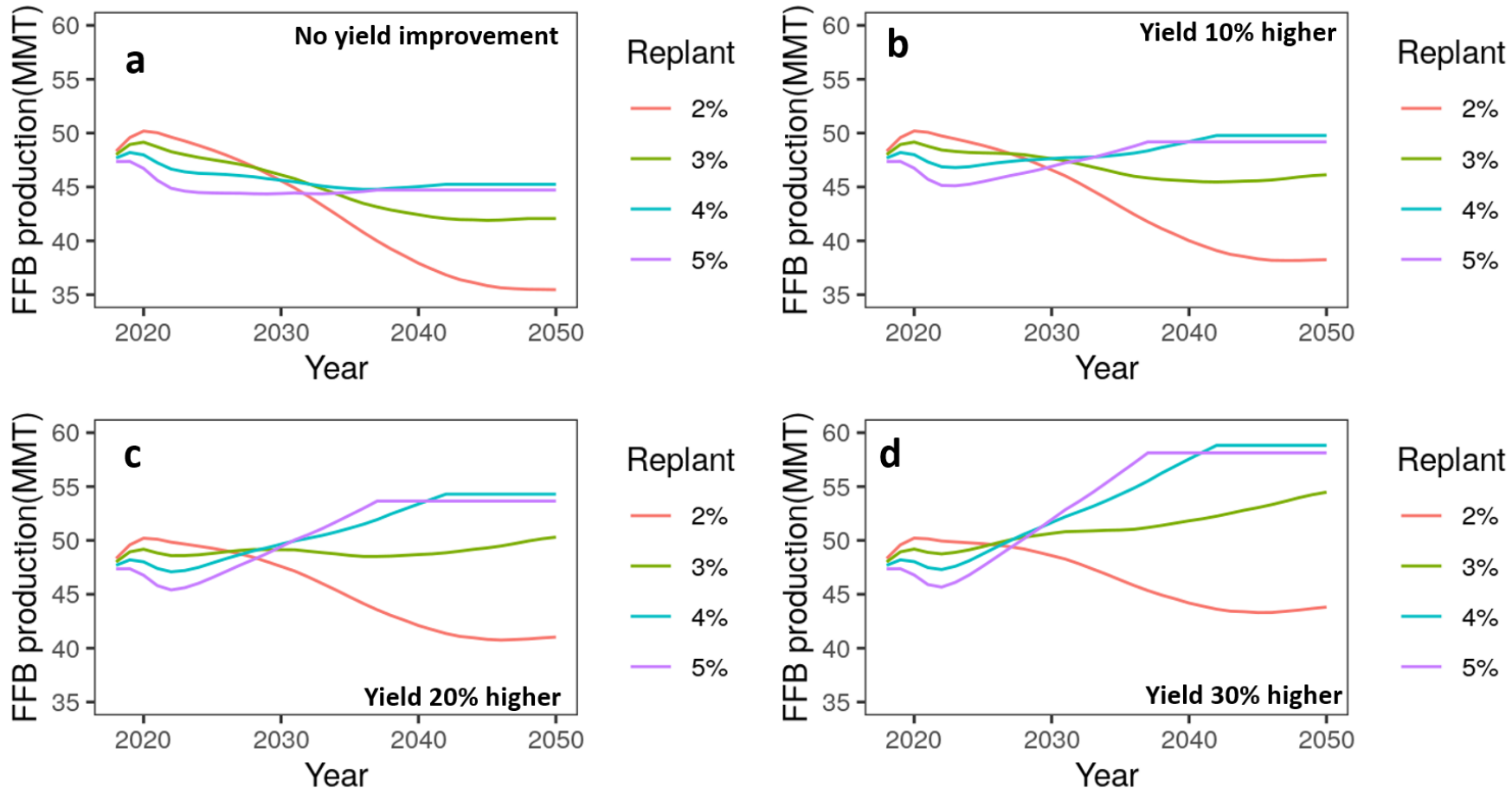


Figure 3. Projection of fresh fruit bunch (FFB) production (million metric ton) by year. Panel a shows the production trend under current yield with different replanting rate. Panel b shows the production trend with 10% higher yield for replanted trees. Panel c shows the production trend with 20% higher yield for replanted trees. Panel d shows the production trend with 30% higher yield for replanted trees.

Different replanting strategies

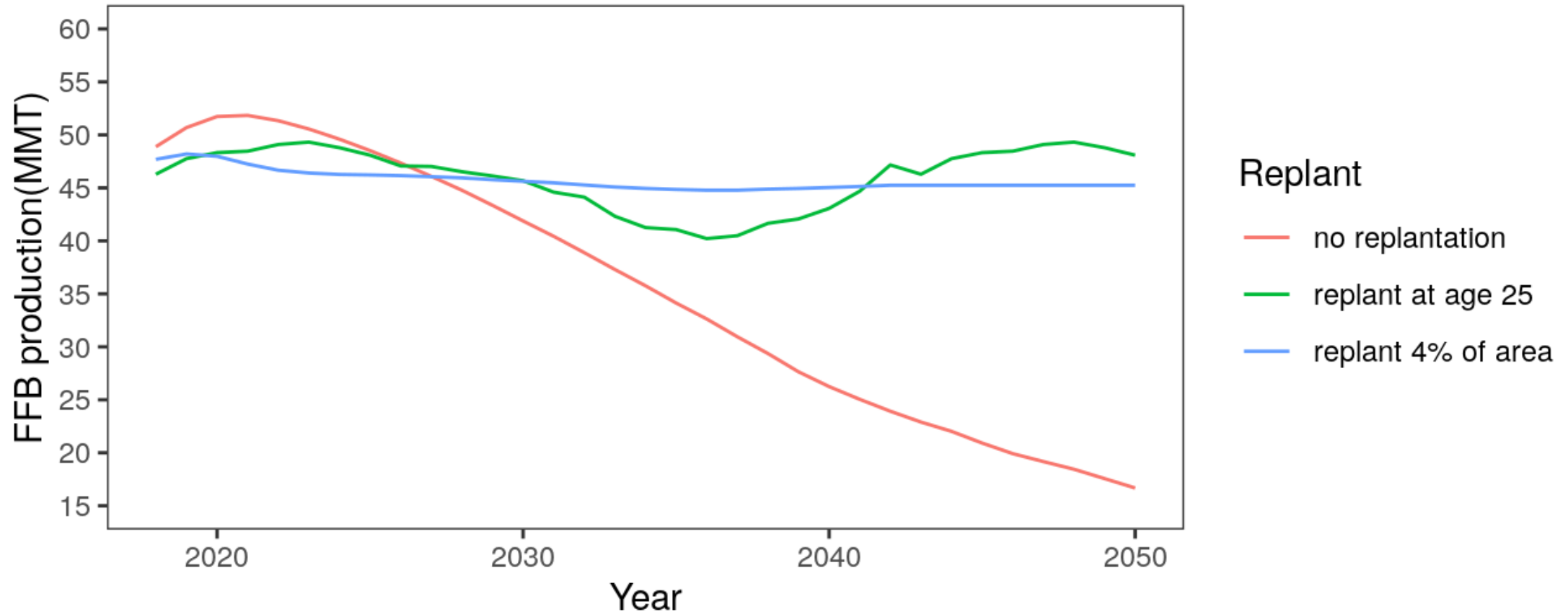
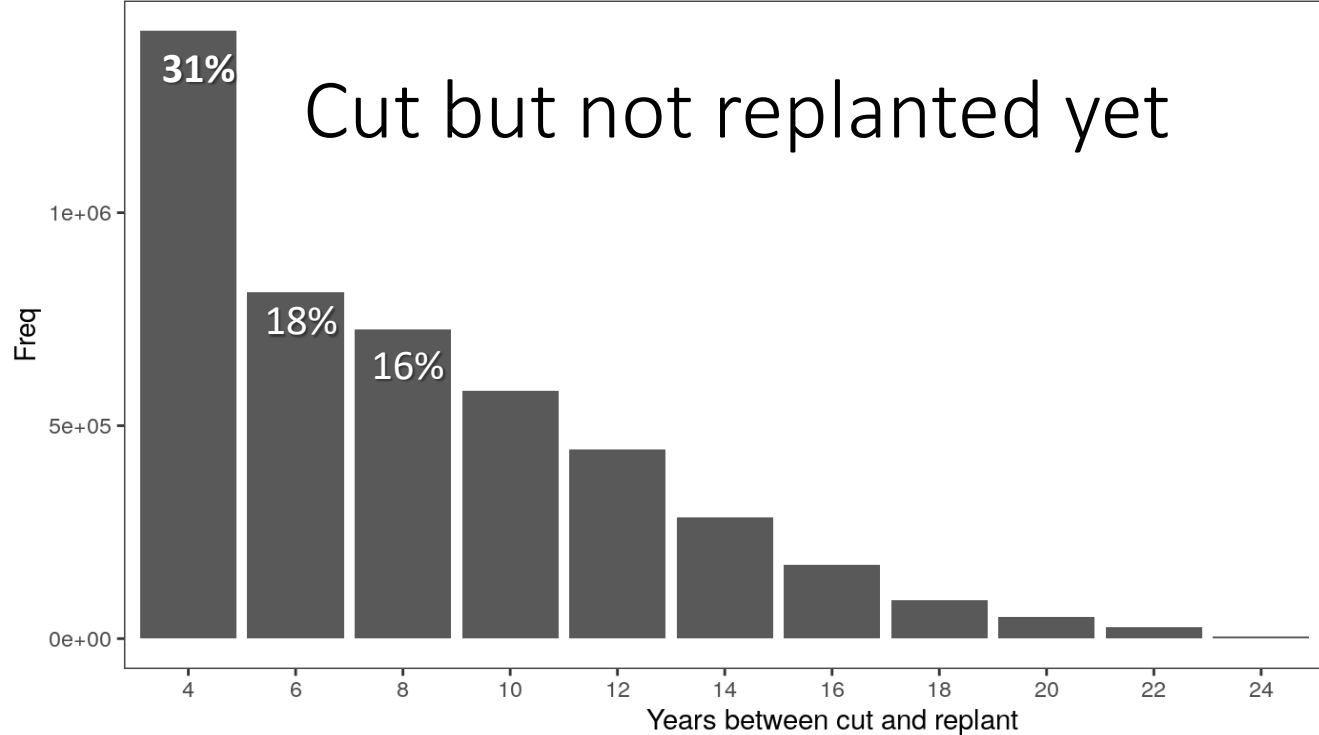
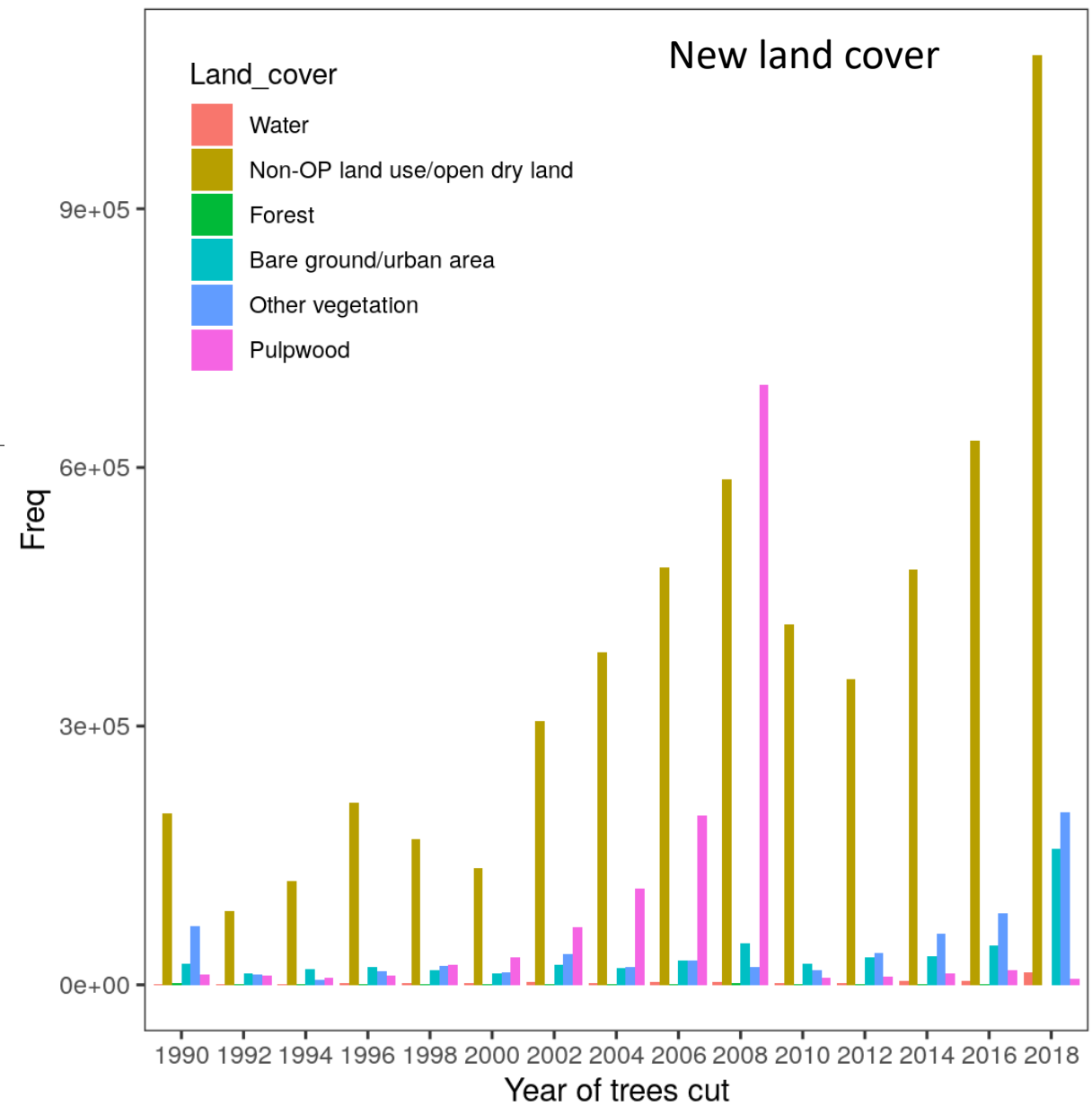


Figure XX. The production trend under different replanting strategies. It shows the production trend under 3 different replanting scenarios, including no replantation, replant at age 25, replant 4% of area each year. Under the scenario of no replantation, from age 35 to age 50, the yield is 10 tons per hectare, and become 0 after age 50 due to difficulties in harvesting

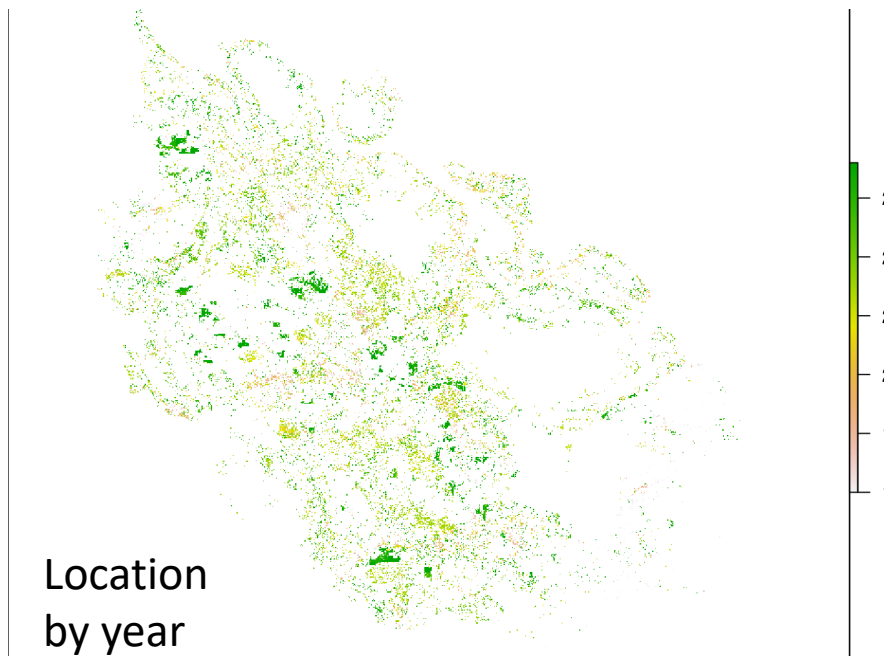
Cut but not replanted yet



Competing land uses



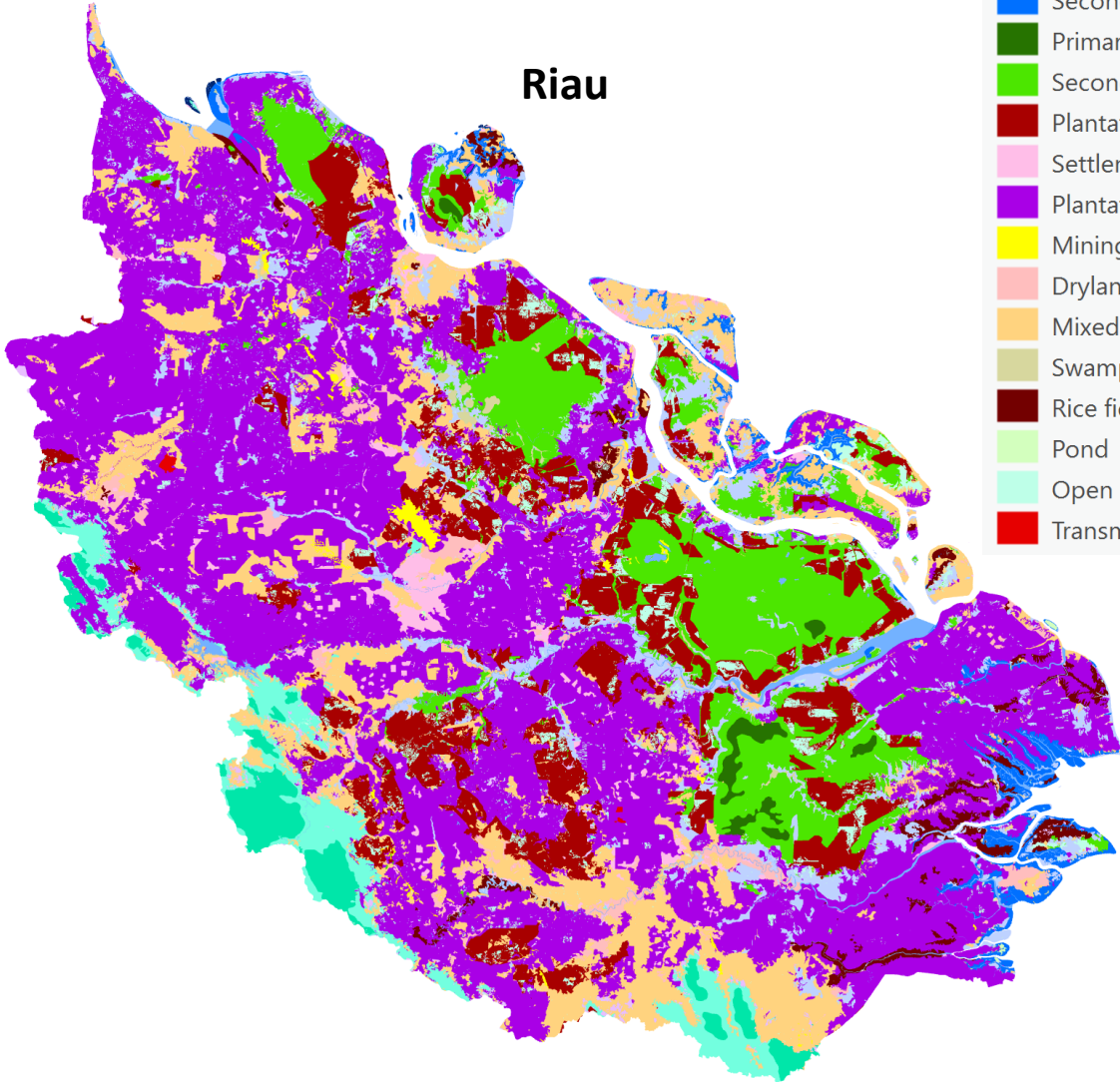
Location by year



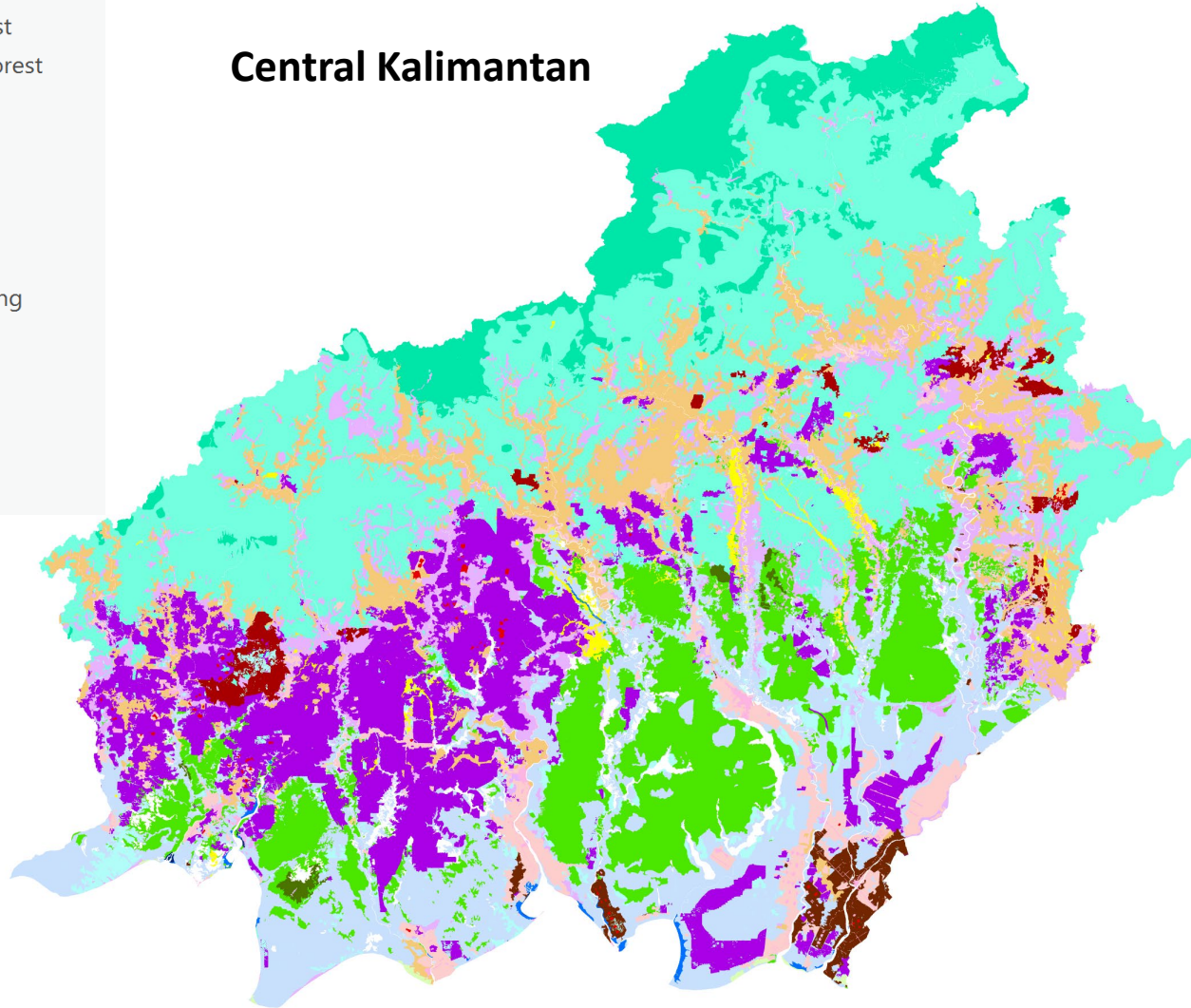
2019 land cover



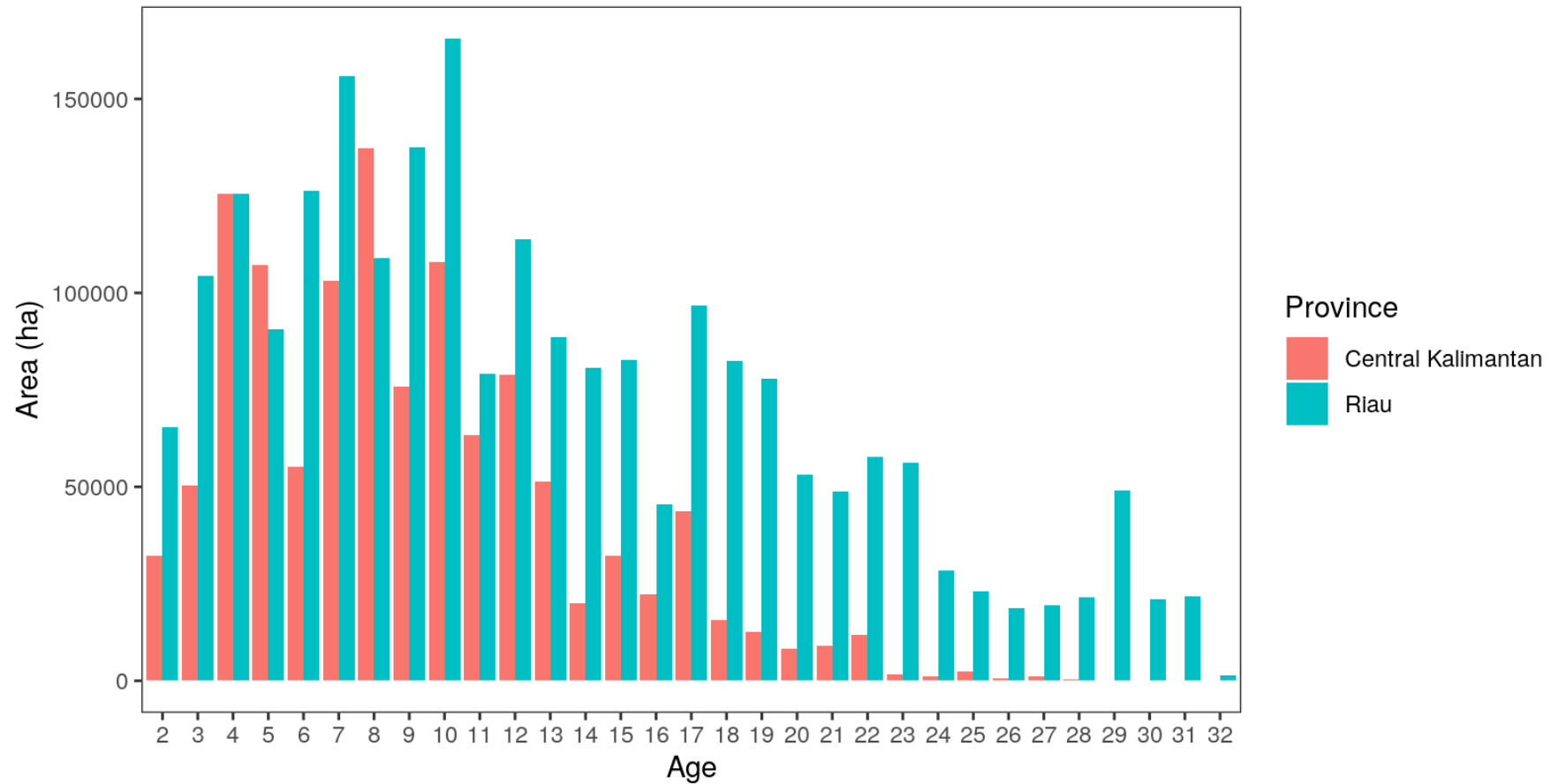
Riau



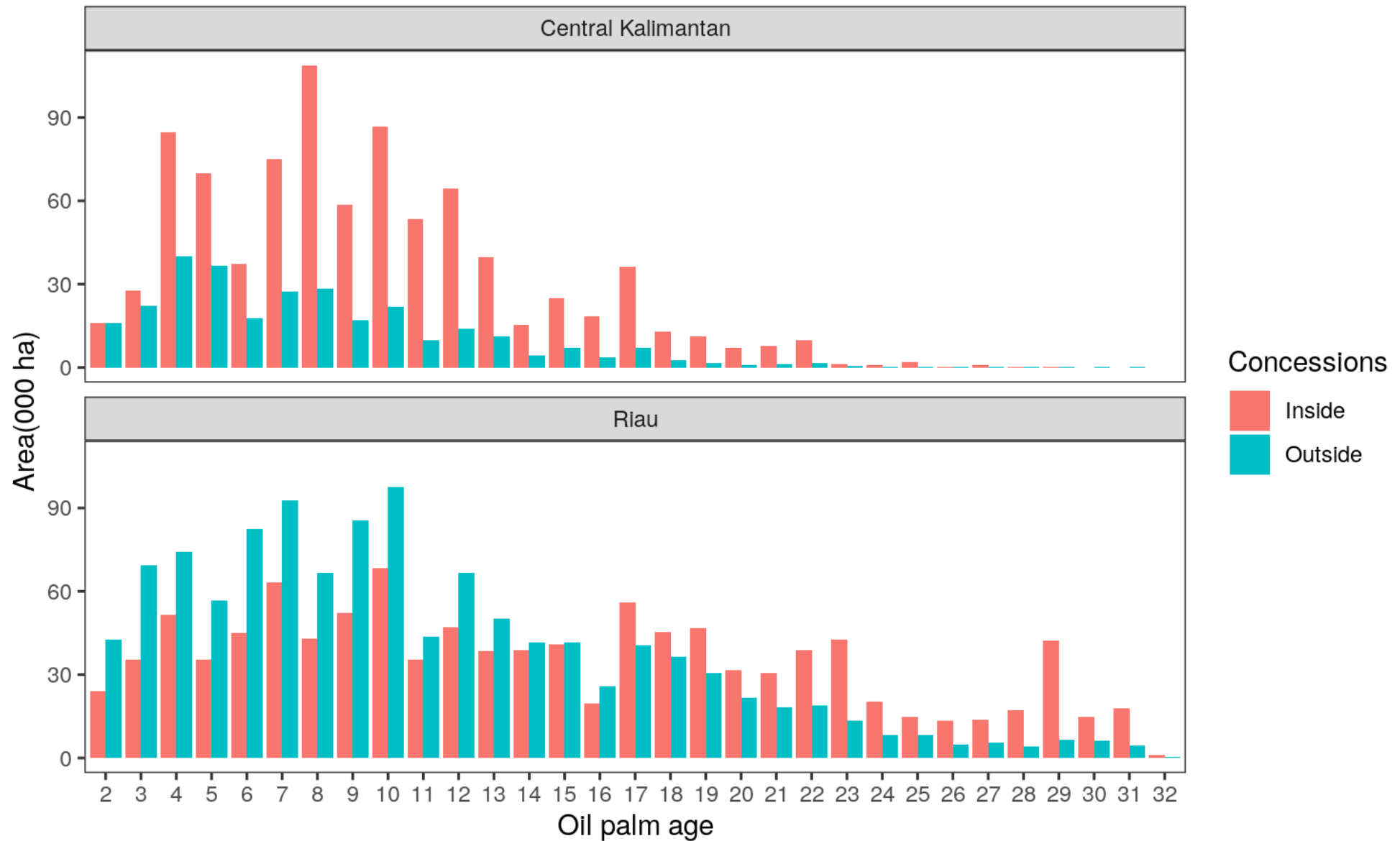
Central Kalimantan



Oil palm age distribution in Riau and Central Kalimantan



Age distribution inside and outside concession

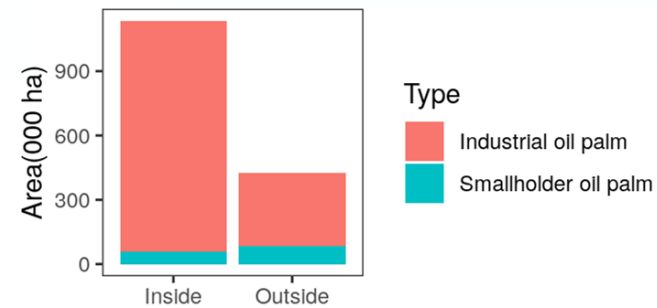
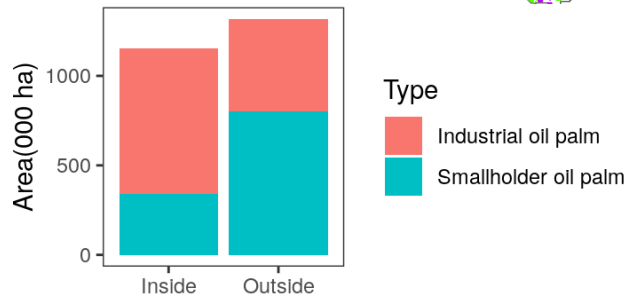
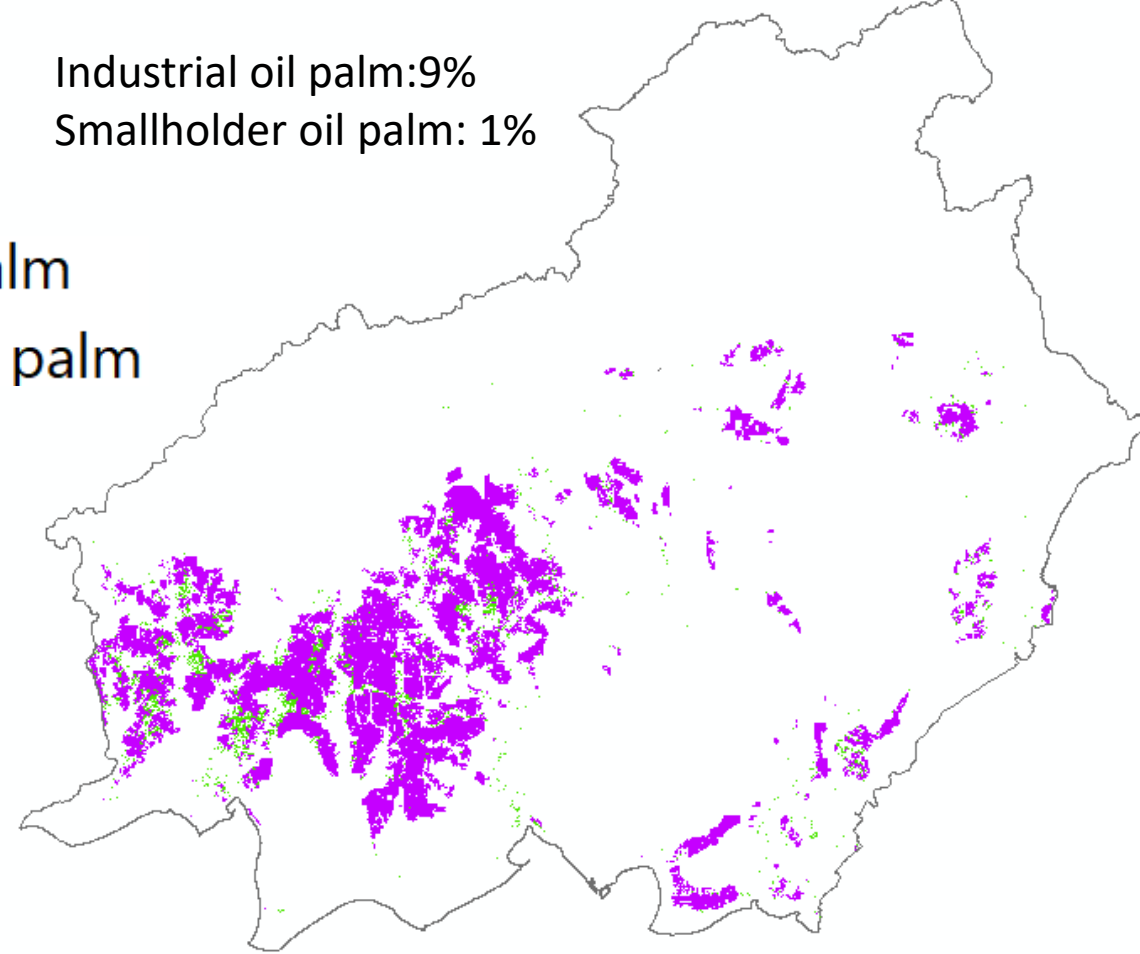
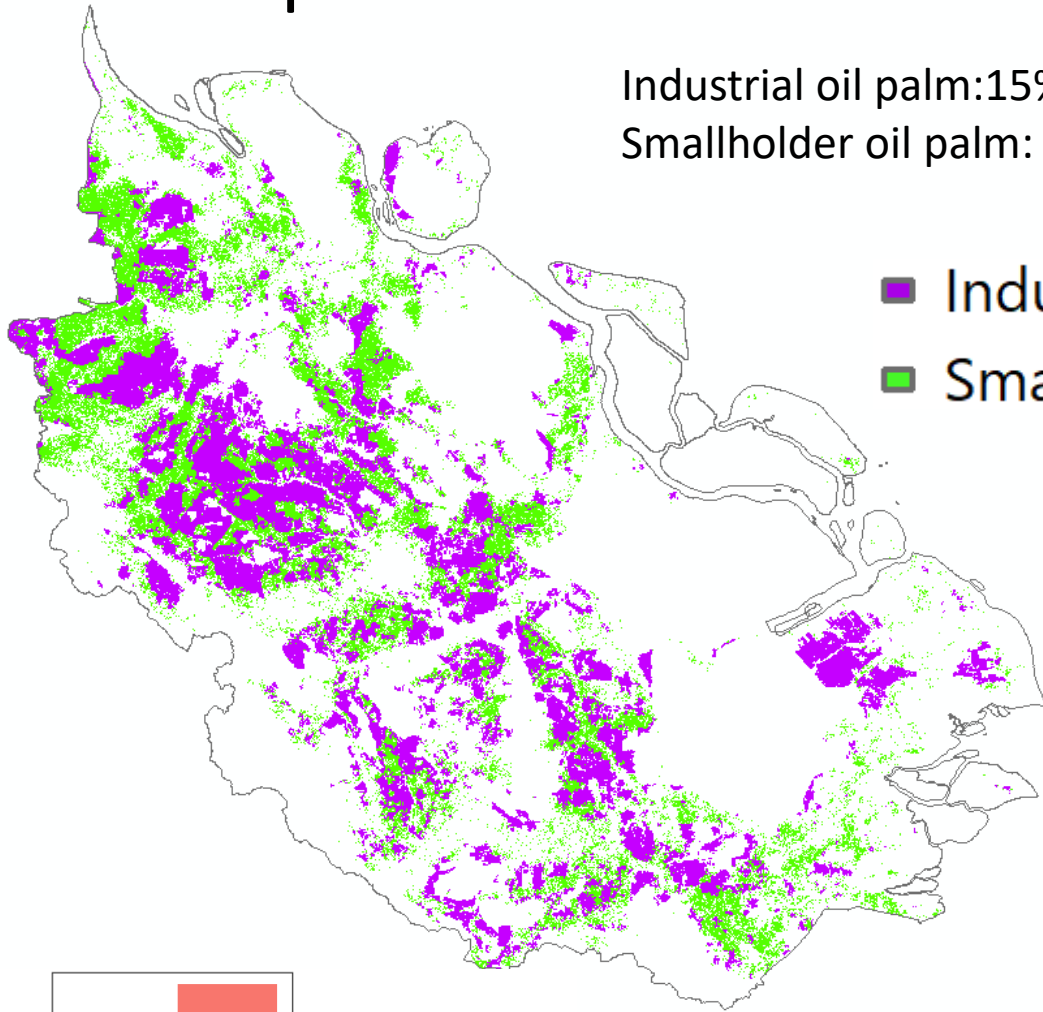


Oil palms in Riau and Central Kalimantan(2019)

Industrial oil palm:15%
Smallholder oil palm: 13%

Industrial oil palm:9%
Smallholder oil palm: 1%

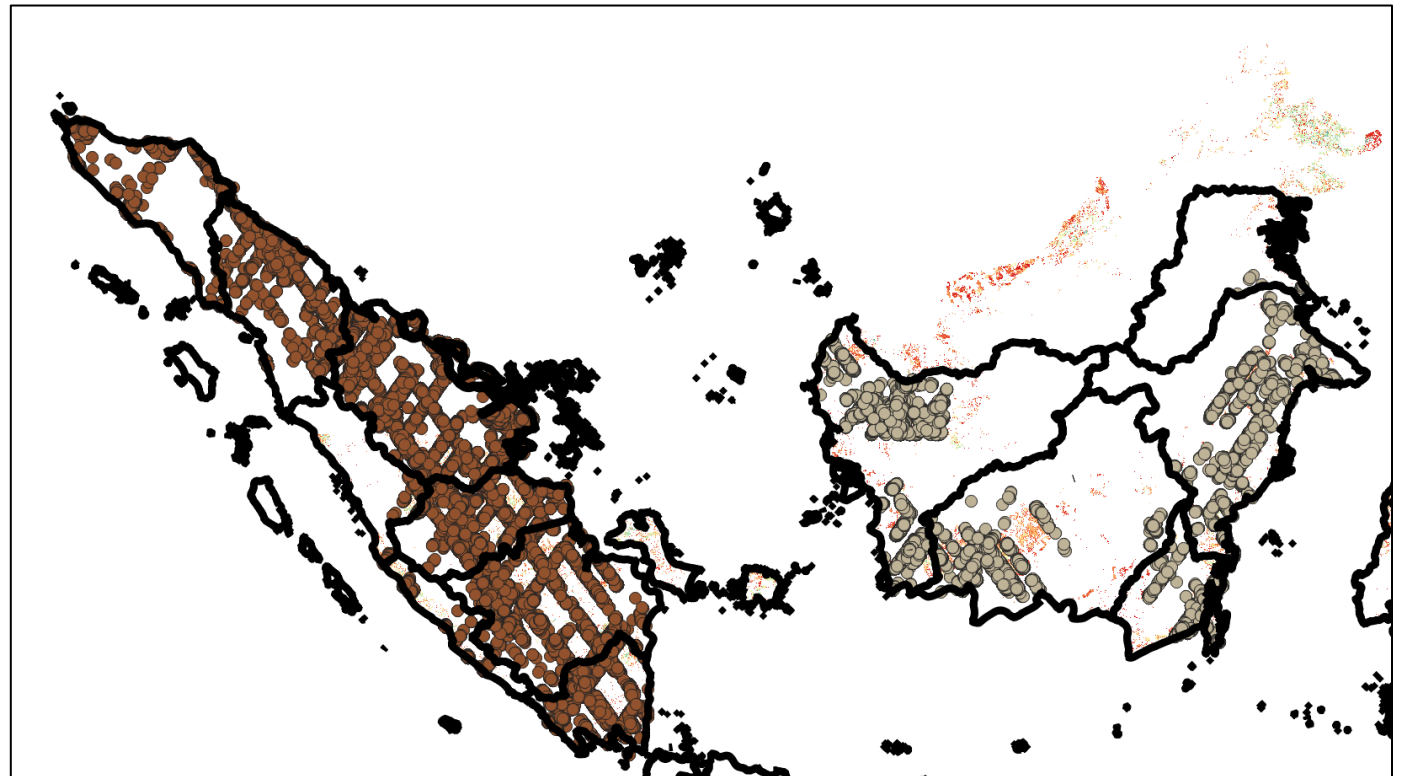
■ Industrial oil palm
■ Smallholder oil palm



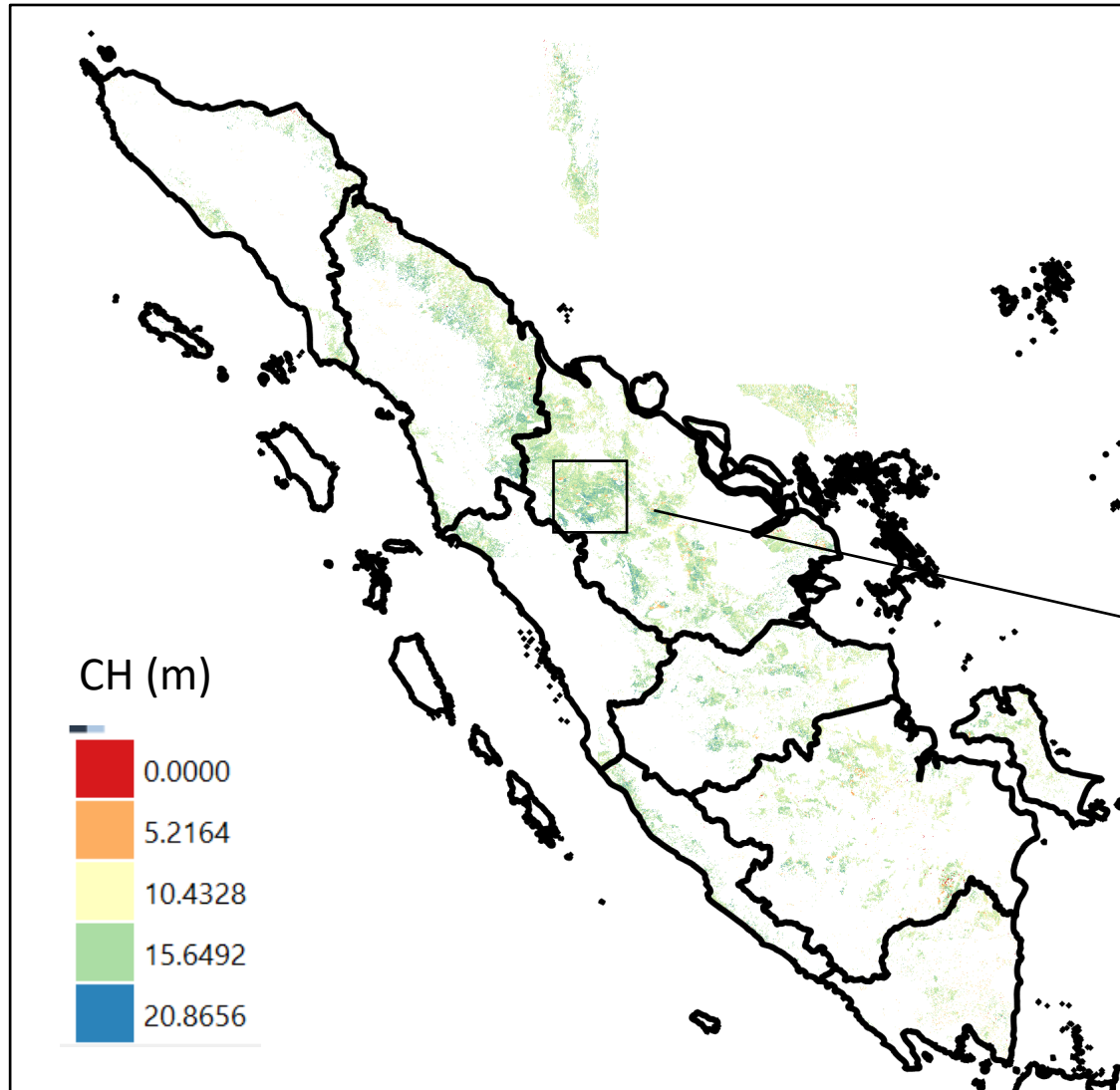
The 2019 GEDI L2A data over Sumatra and Kalimantan

GEDI L2A Version 2 data

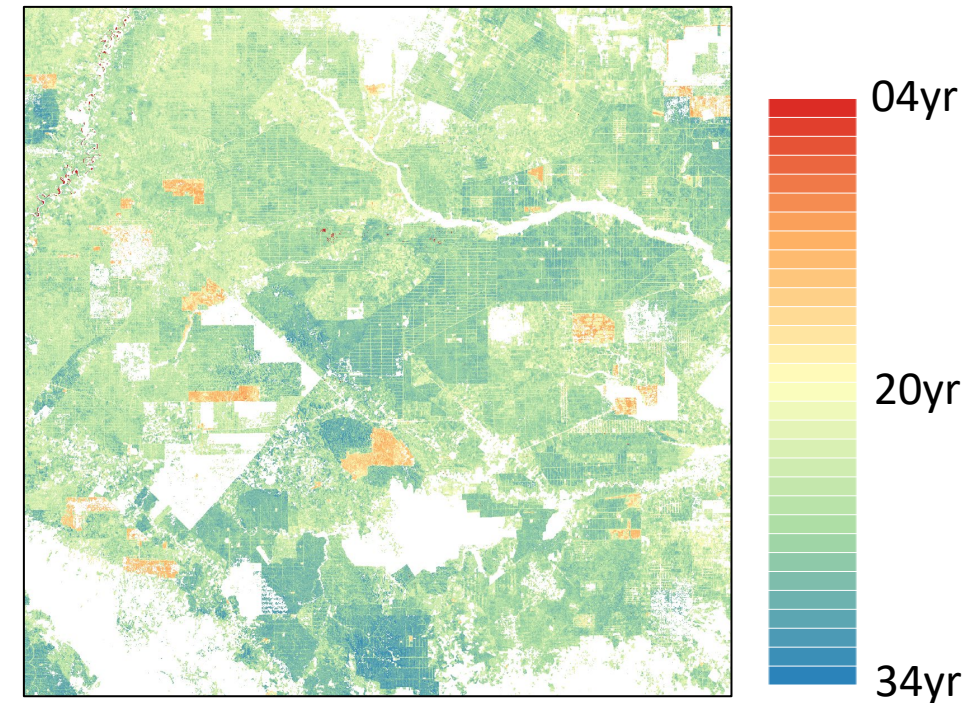
- 223,357 filtered GEDI footprints for Sumatra + 89,776 from Kalimantan
- Predictive variables
 - Landsat surface reflectance, vegetation indices
 - Oil palm age map (Danylo et al., 2021)
 - Elevation, Slope and Aspect
- Training data:
 - 16,753 points from Sumatra
 - 16,161 points from Kalimantan
- Validation data:
 - 5,585 points from Sumatra
 - 5,378 points from Kalimantan



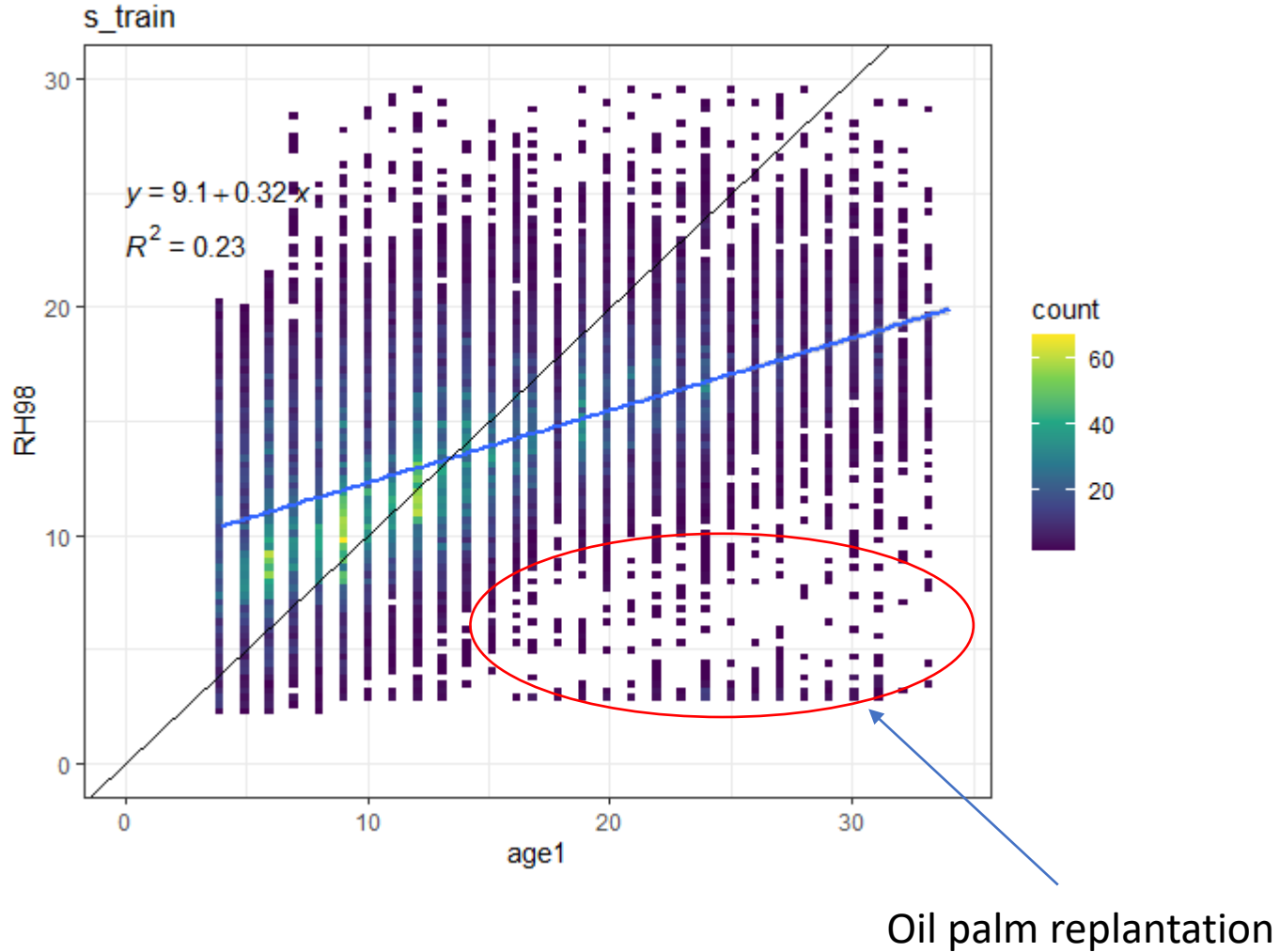
Oil palm canopy height map by a predictive model using GEDI



Oil palm age map (Danylo et al., 2021)



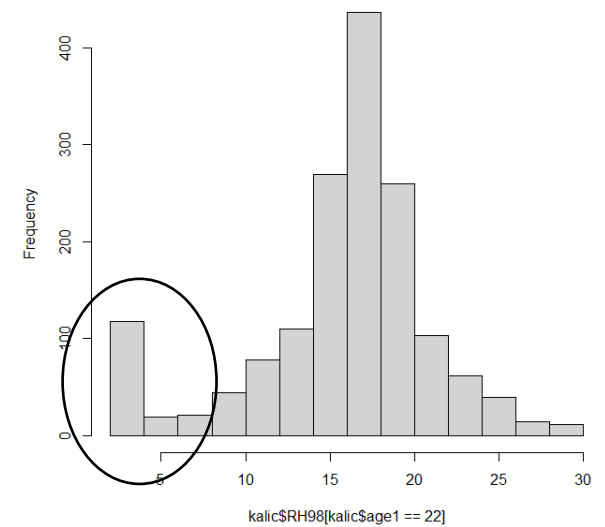
Data correction: Mismatch between GEDI and OP age map



22yr-old OP in 2019



Histogram of kalic\$RH98[kalic\$age1 == 22]



➤ GEDI performance analysis on canopy height estimation

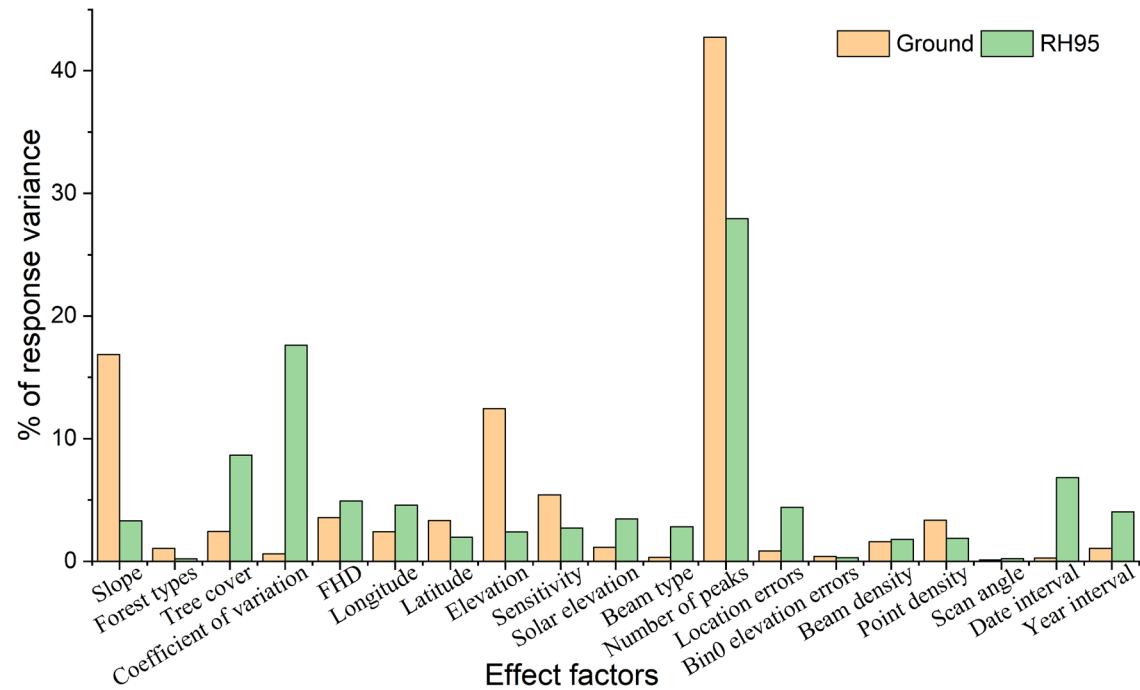


Figure 6. The importance of 19 factors for explaining the differences of ground elevation and RH measurements between GEDI and GEDI-simulated waveforms.

1. Factors have different effects on estimations of surface elevation and vegetation height.
2. Most of explanation variations from different factors can be interactive for GEDI waveform.
3. Waveform complex influence GEDI canopy height and ground elevation estimations mostly (Figure 6). This factor is heavily influenced by slope indicating by small effect on bias after removing slope effect (Figure 7).

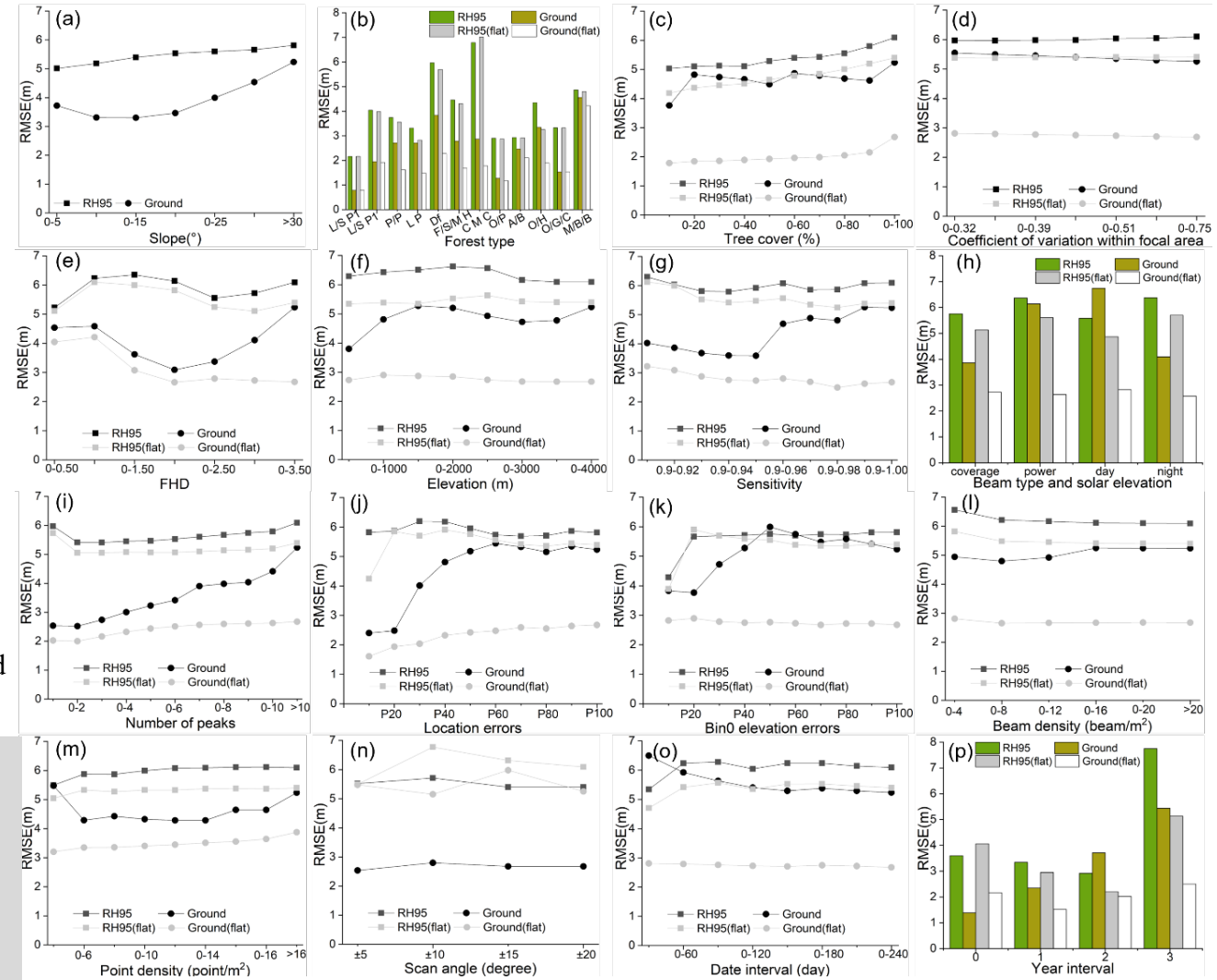


Figure 7. RMSE analysis of GEDI performance of ground elevation and RH95 estimations under different slope (a), forest type (b), tree cover (c), coefficient of variation (d), FHD (e), elevation (f), sensitivity (g), beam type, and solar elevation (h), number of peaks (i), beam density (j), point density (k), scan angle (l), date interval (m), and year interval (n), respectively. The RH95 (flat) and ground (flat) showed the RMSE of RH95 and ground elevation in flat areas with a slope lower than 15 degrees.

➤ Framework for canopy height mapping by integrating GEDI LiDAR (FPSF-CH)

➤ Method

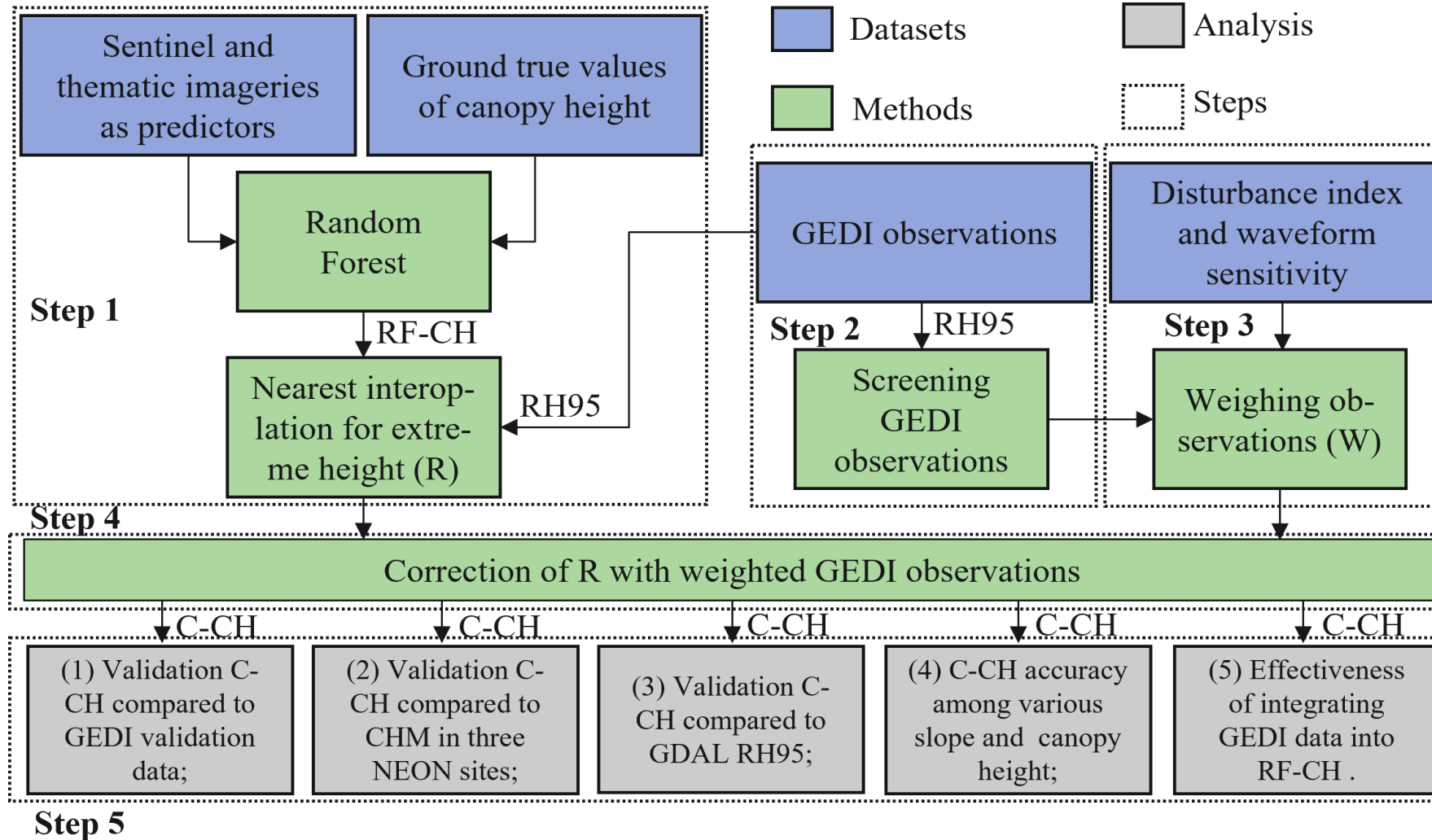


Figure 13. Flowchart of the FPSF-CH and its performance analysis. The RF-CH and C-CH are canopy heights derived from RF and the FPSF-CH. R and W are the nearest interpolation dataset and weight for each GEDI data, respectively. CHM is the canopy height model.

Acknowledgements NASA LCLUC team

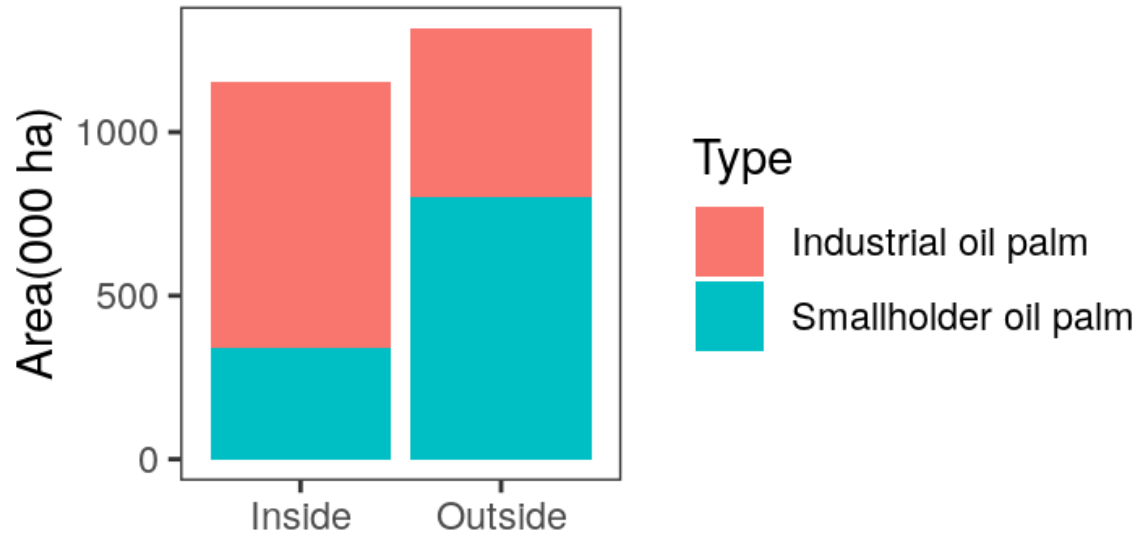
- **Bambang Hero Saharjo (IPB)**
- **Jing Zhao (UMCES)**
- **Izaya Numata (UMCES/SDSU)**
- **Xin Zhang (UMCES)**
- **Janice Lee (NTU)**
- **Andrew Elmore (UMCES)**
- **Cangjiao Wang (CUMT)**

Oil palm production trend in Riau

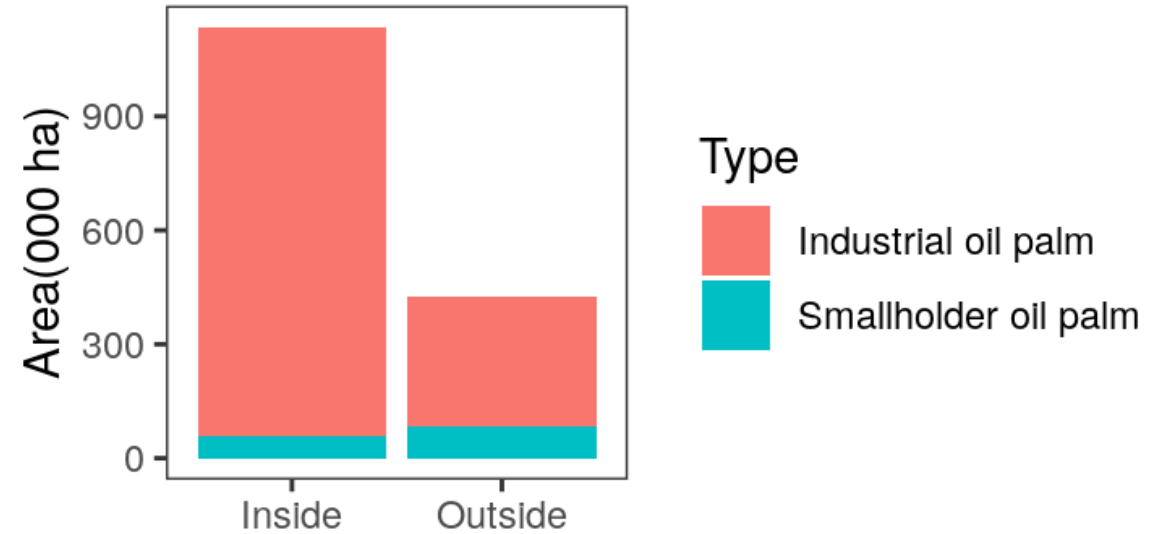
Based on current age composition and scenarios for yield improvement

Oil palm inside and outside oil palm concession

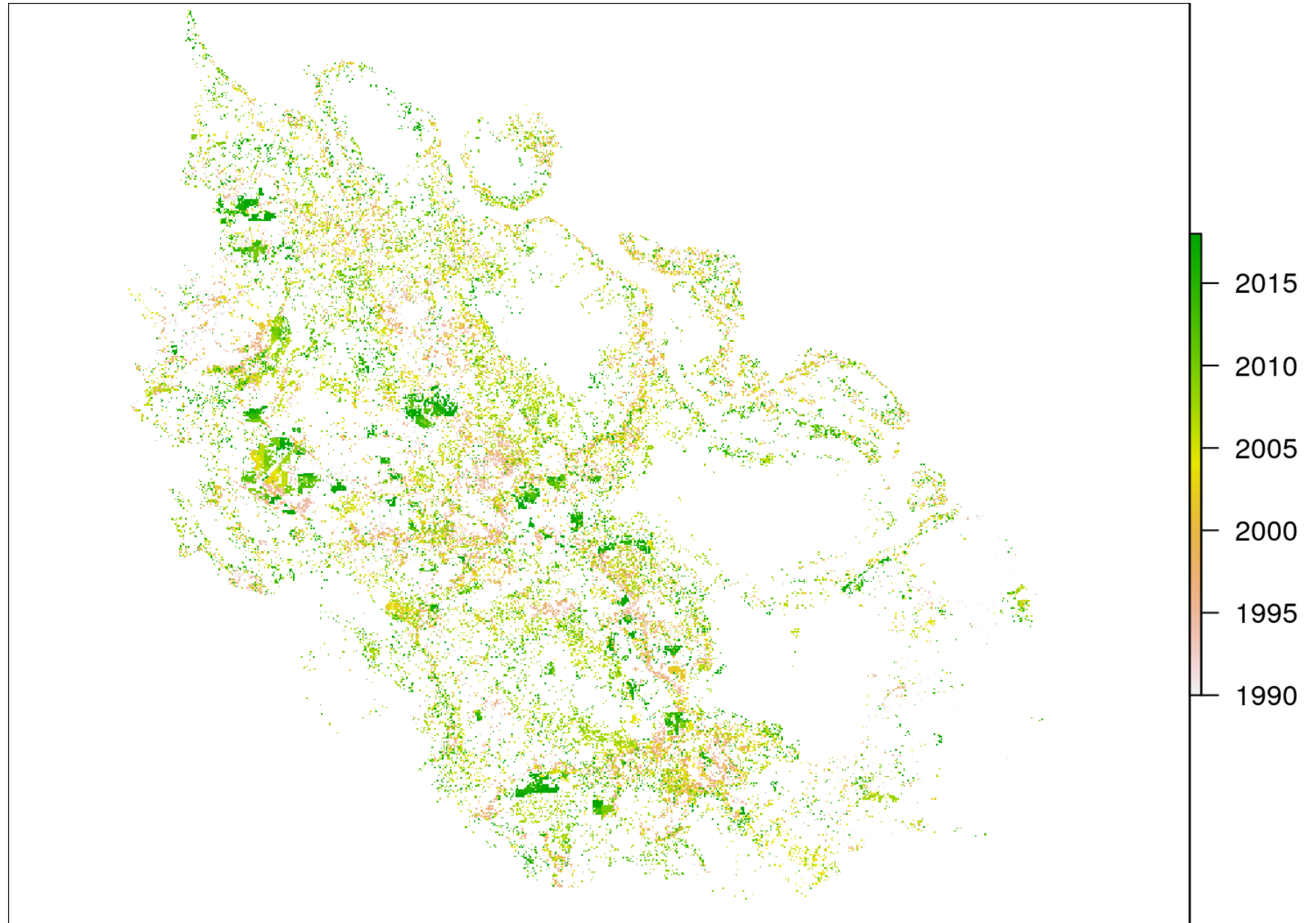
Riau



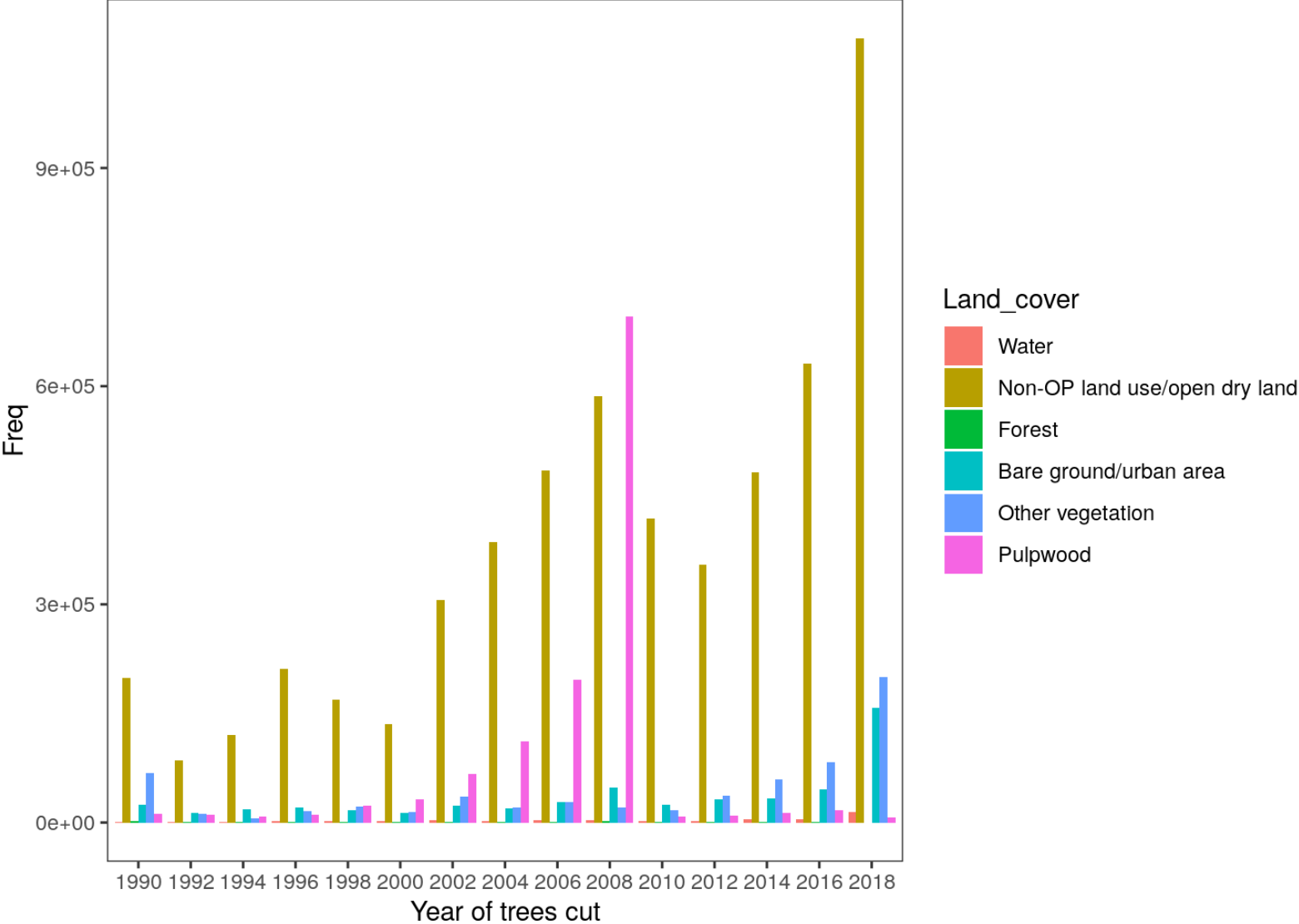
Central Kalimantan



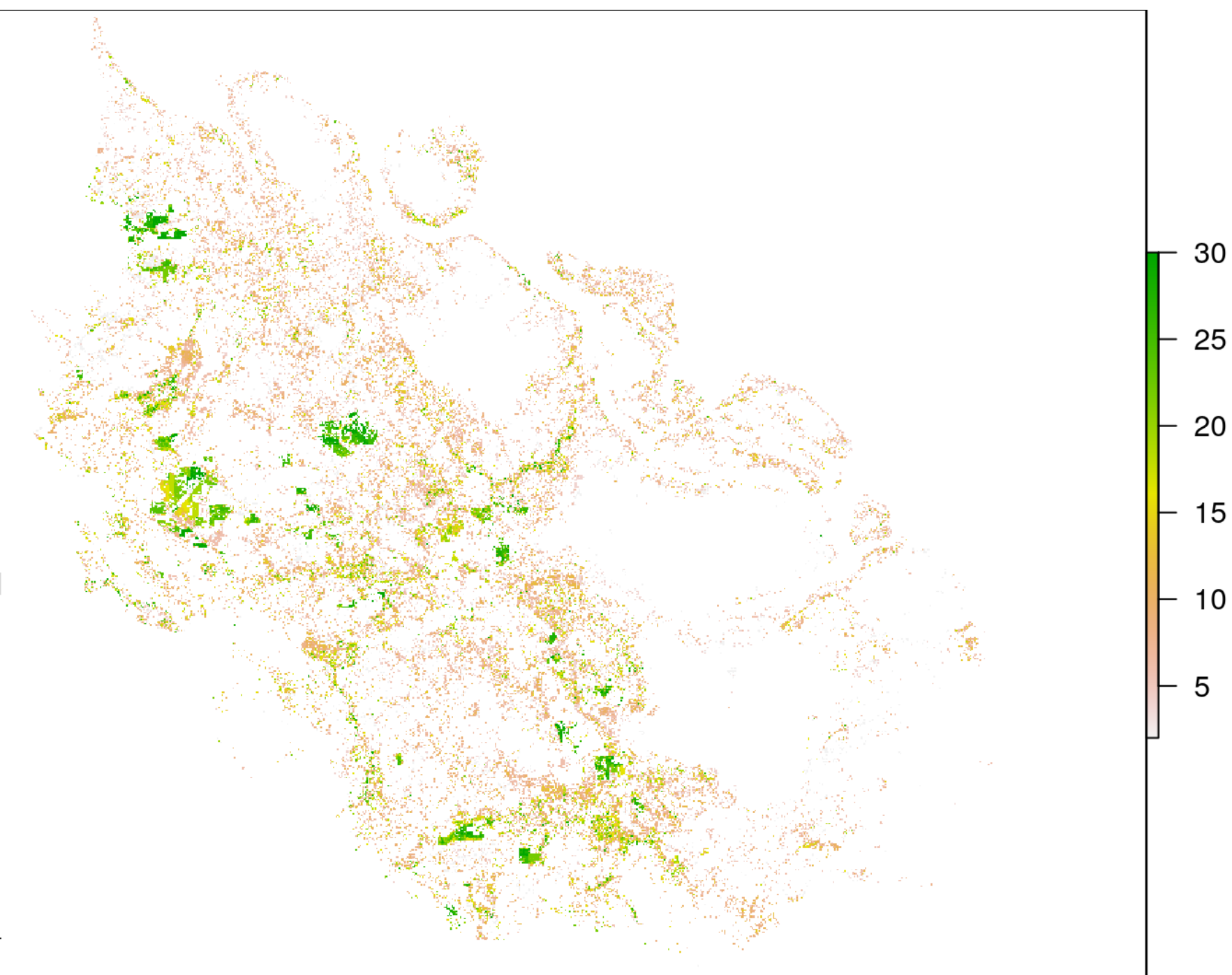
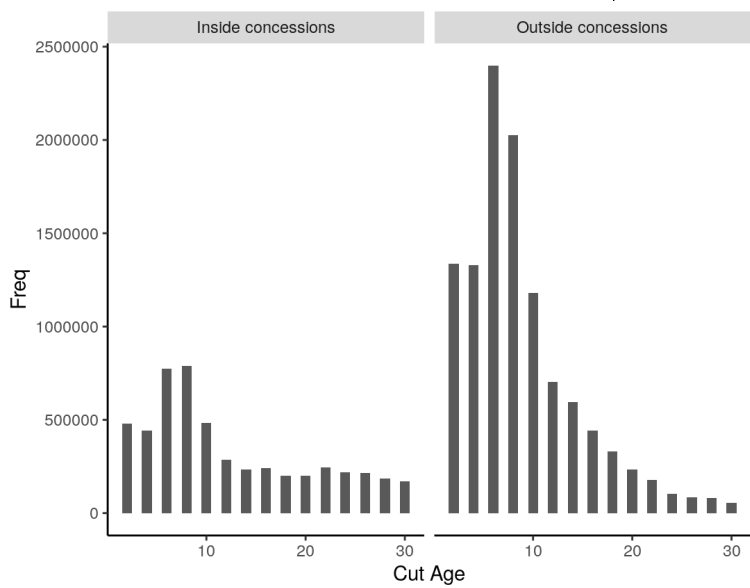
Cut year



Current land cover for cut but not replanted yet



Cut age



Compare Riau and Central Kalimantan

Cumulative production difference with 4%

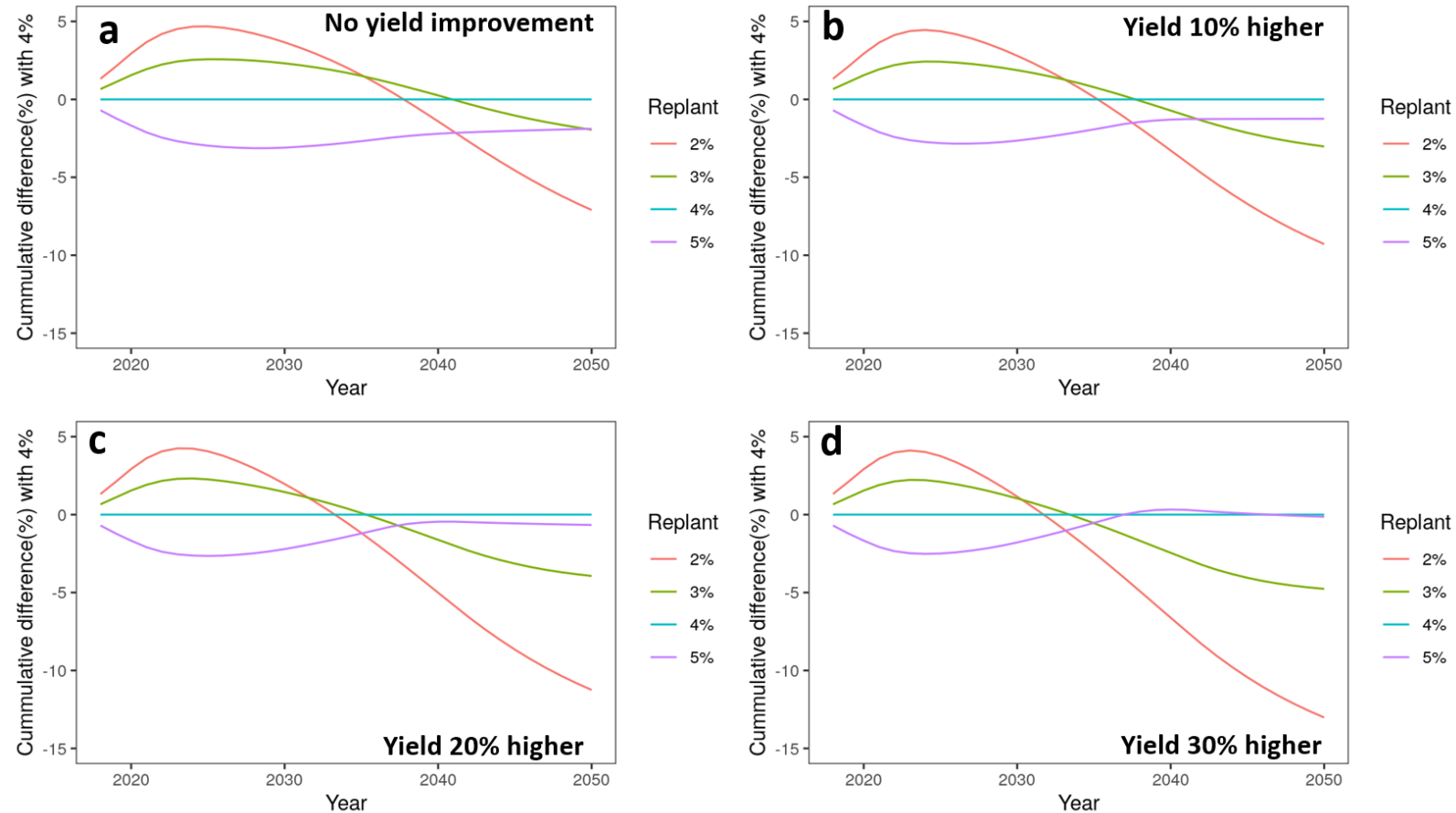
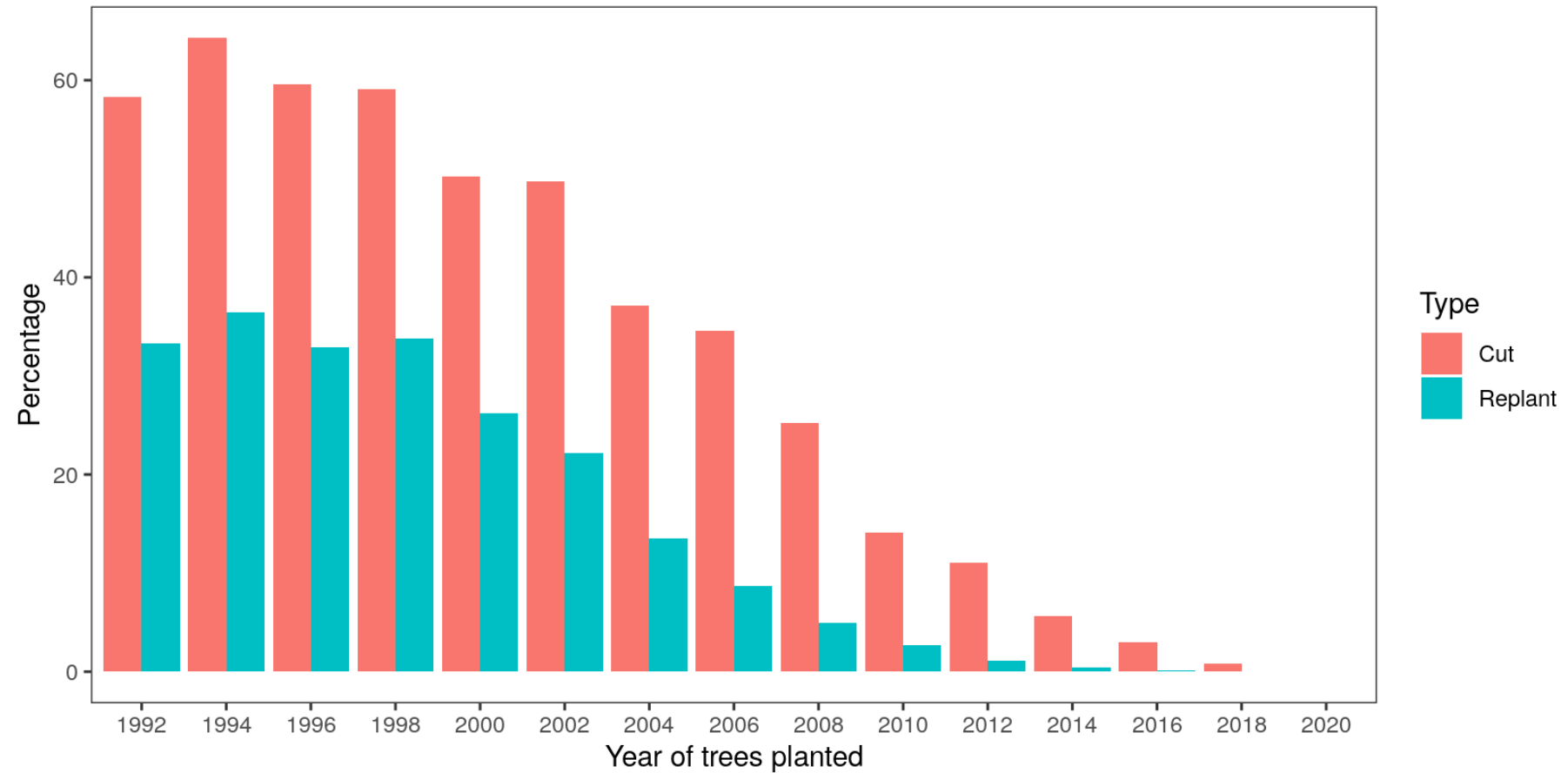


Figure 4. Cumulative difference (%) for FFB production compared to replanting by 4% per year. Panel a shows the trend under current yield with different replanting rate. Panel b shows the trend with 10% higher yield for replanted trees. Panel c shows the trend with 20% higher yield for replanted trees. Panel d shows the trend with 30% higher yield for replanted trees.

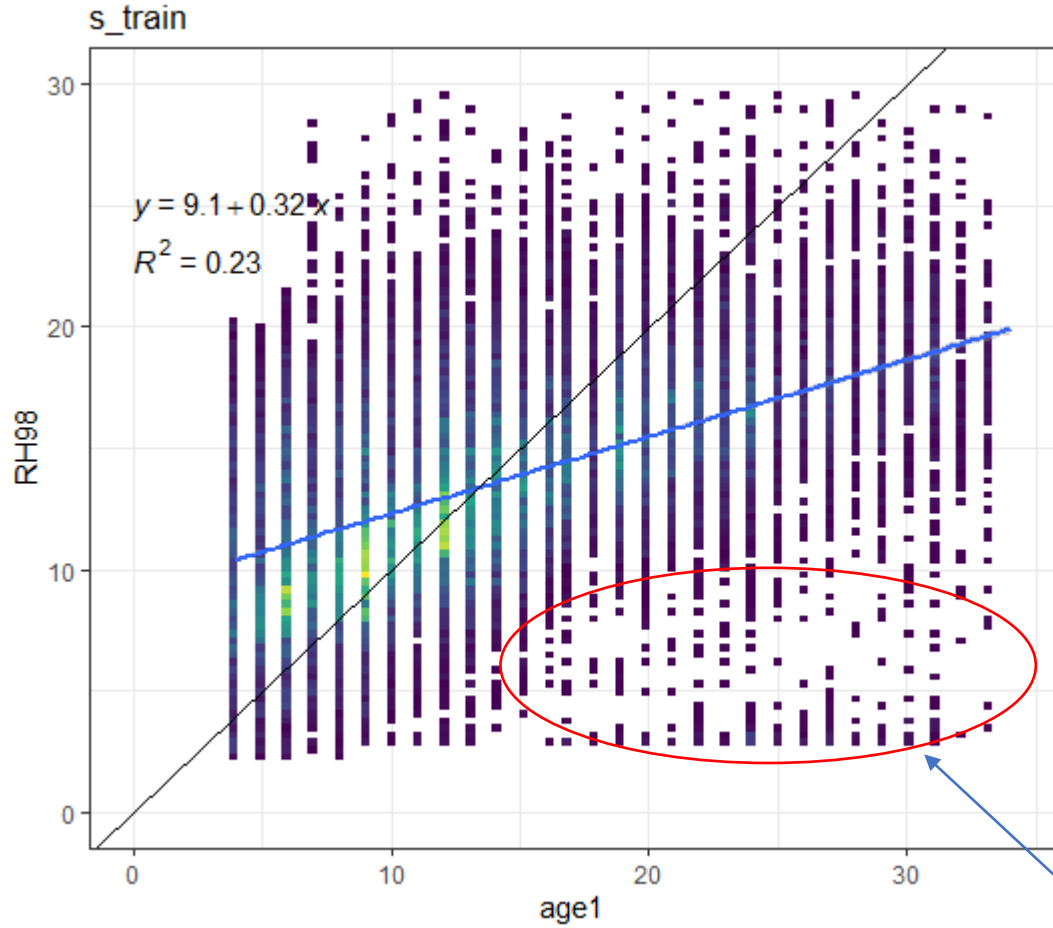
Percentage of cut and replant



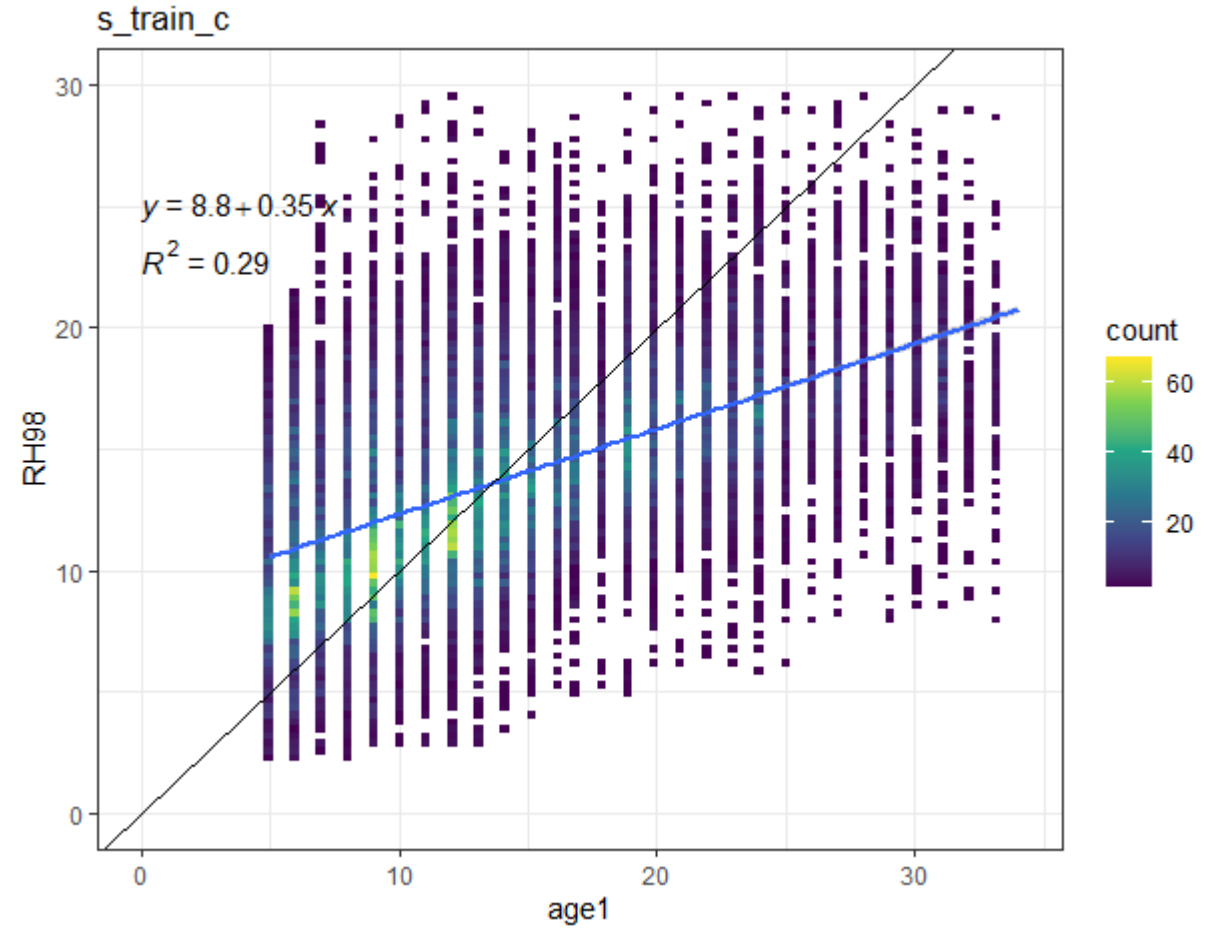
2019 land cover in Central Kalimantan.

Land cover type	FREQUENCY	Area(ha)	Percentage(%)
Airport/port	3	243	0.0
Scrub	4121	1159185	7.7
Swamp scrub	3613	2076177	13.8
Primary dryland forest	436	1069306	7.1
Secondary dryland forest	1820	4246493	28.3
Primary mangrove forest	12	1736	0.0
Secondary mangrove forest	64	22661	0.2
Primary swamp forest	23	32357	0.2
Secondary swamp forest	1186	1696606	11.3
Plantation forest	2073	169404	1.1
Settlement	845	72936	0.5
Plantation	6703	1922493	12.8
Mining	1107	128434	0.9
Dryland farming	853	460225	3.1
Mixed dryland farming	1673	1469897	9.8
Rice field	752	150337	1.0
Pond	25	11397	0.1
Open ground	8415	314573	2.1
Transmigration	96	17515	0.1

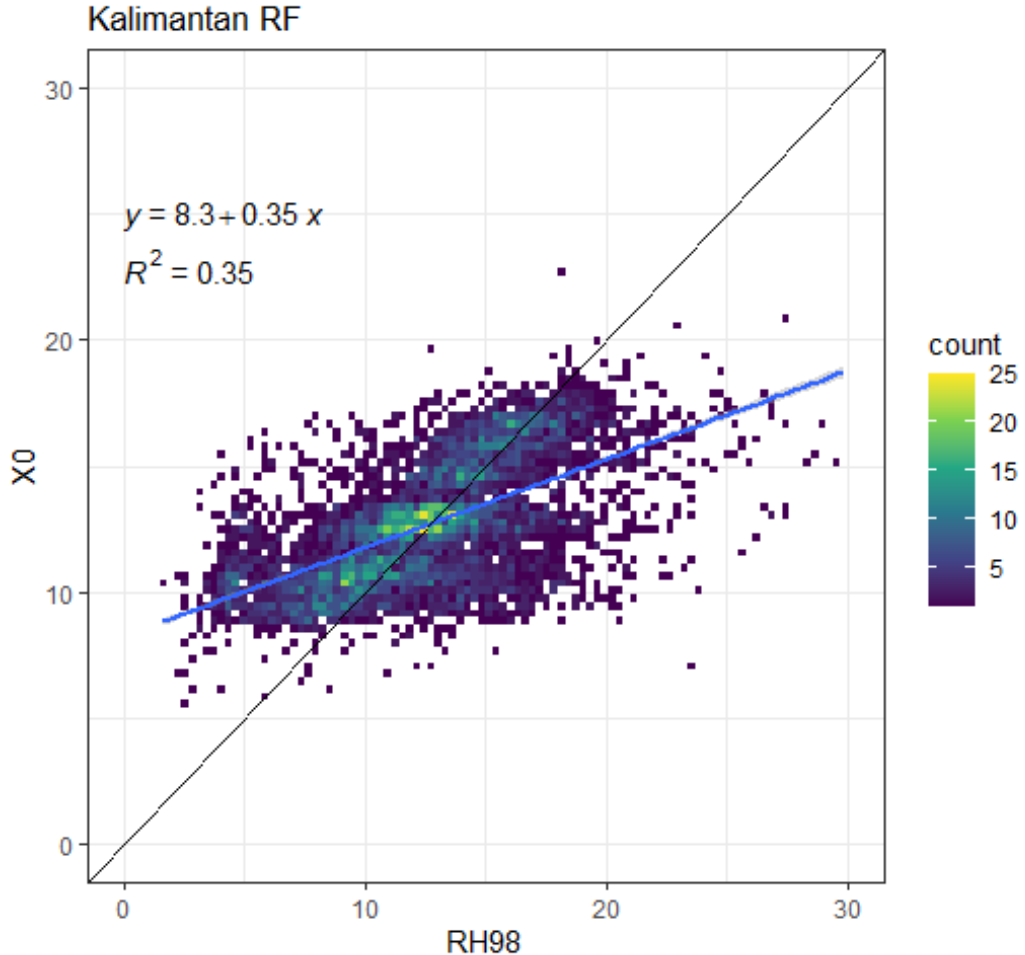
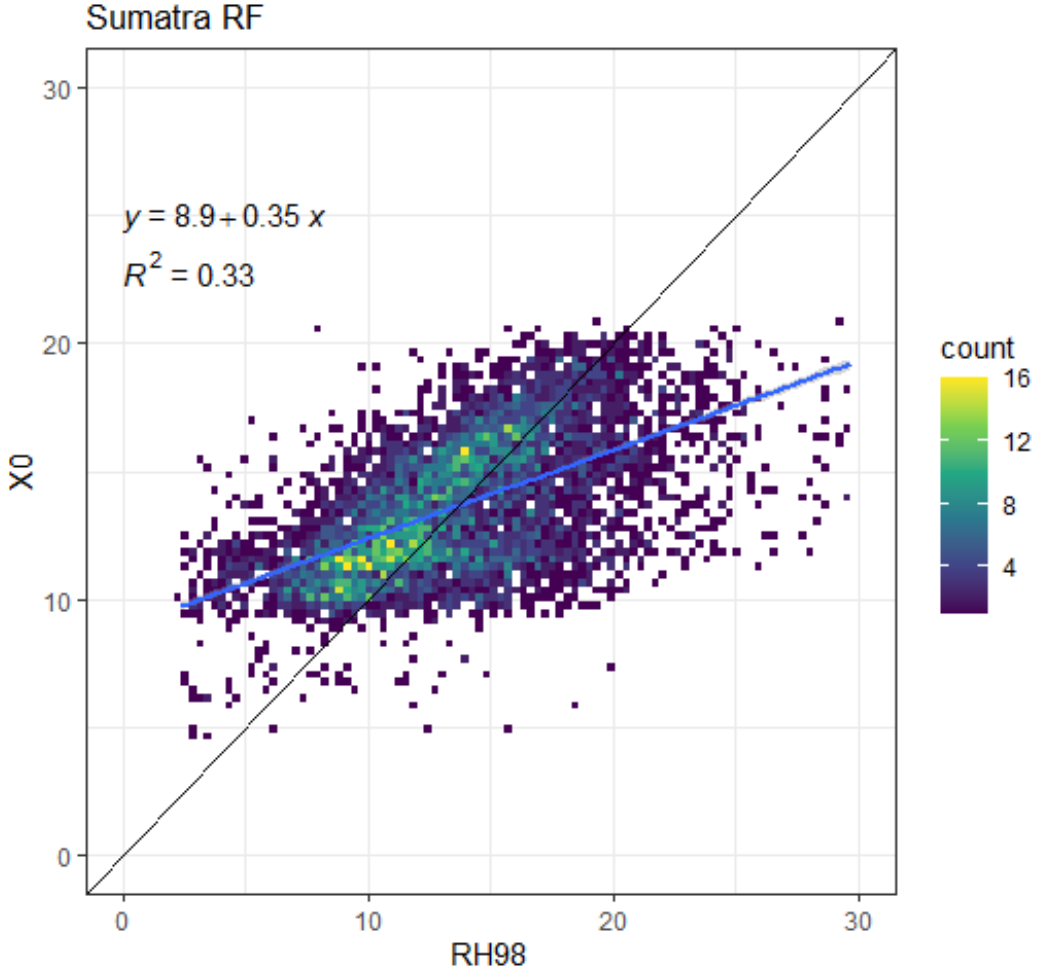
Data correction



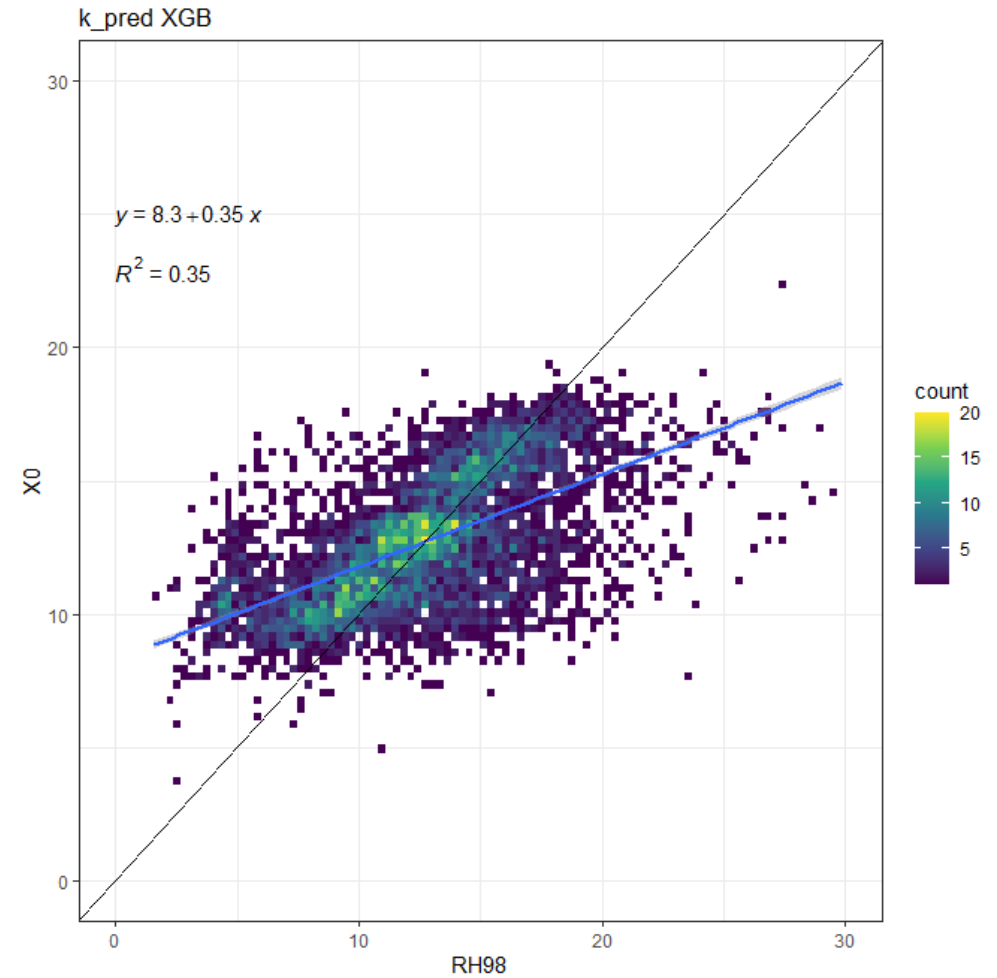
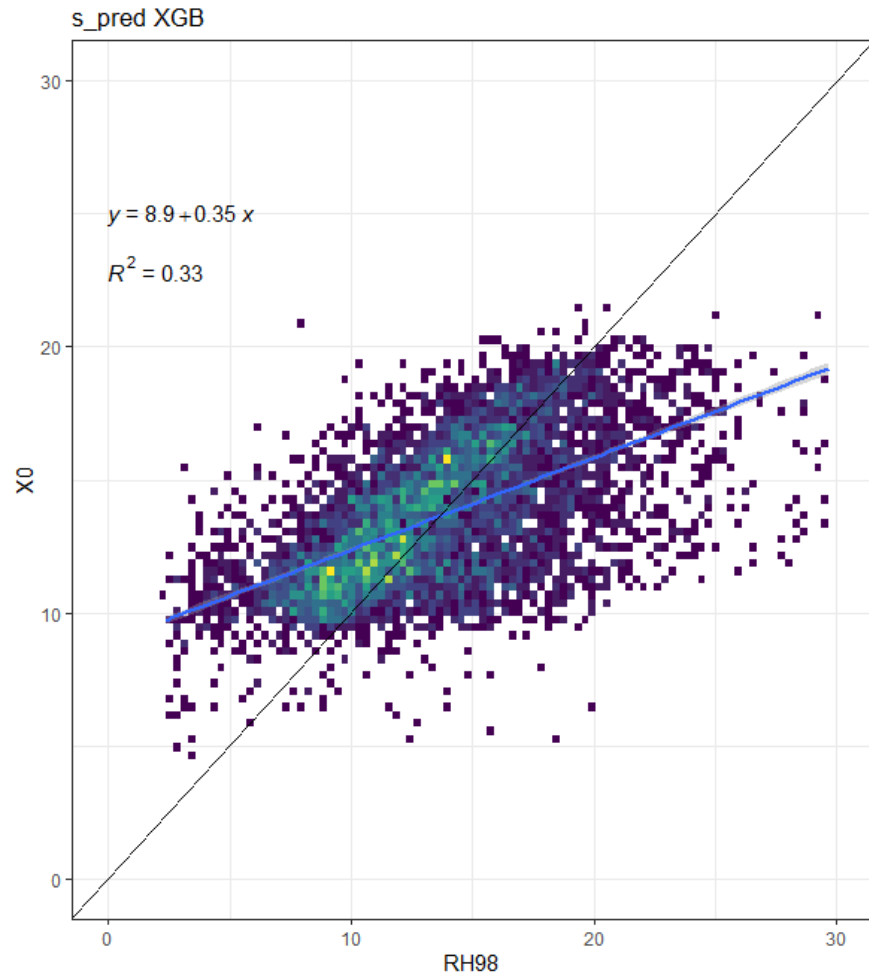
Oil palm replantation

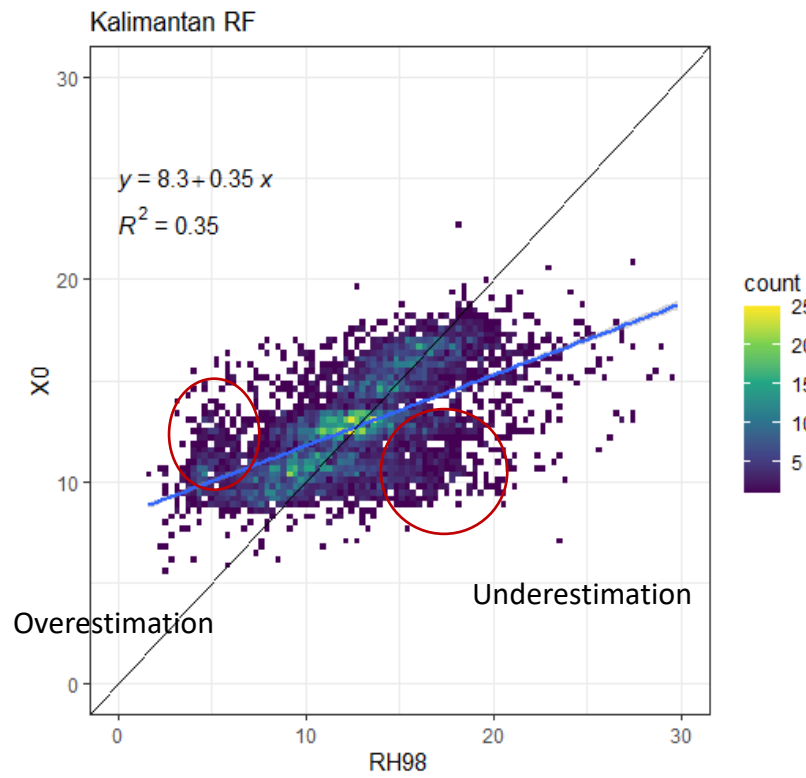


Random Forest Prediction

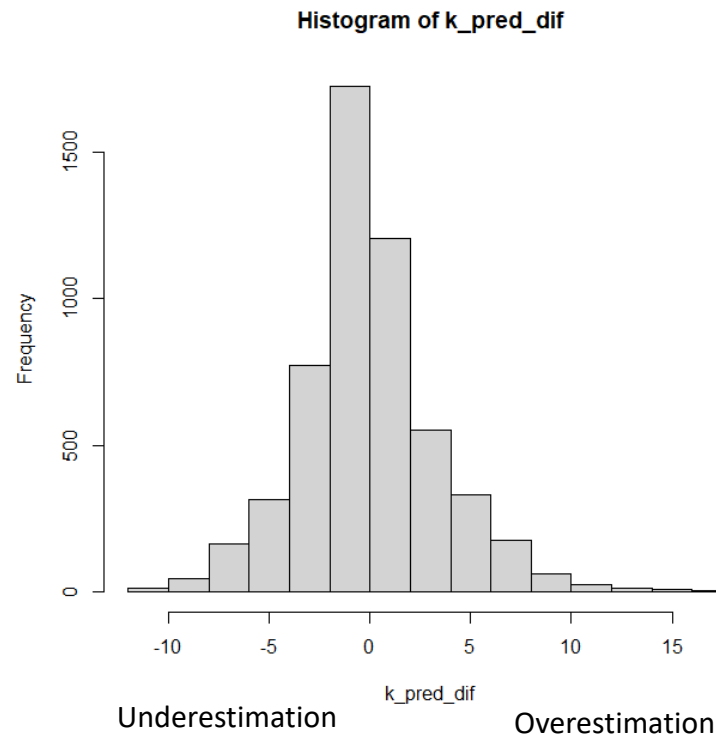


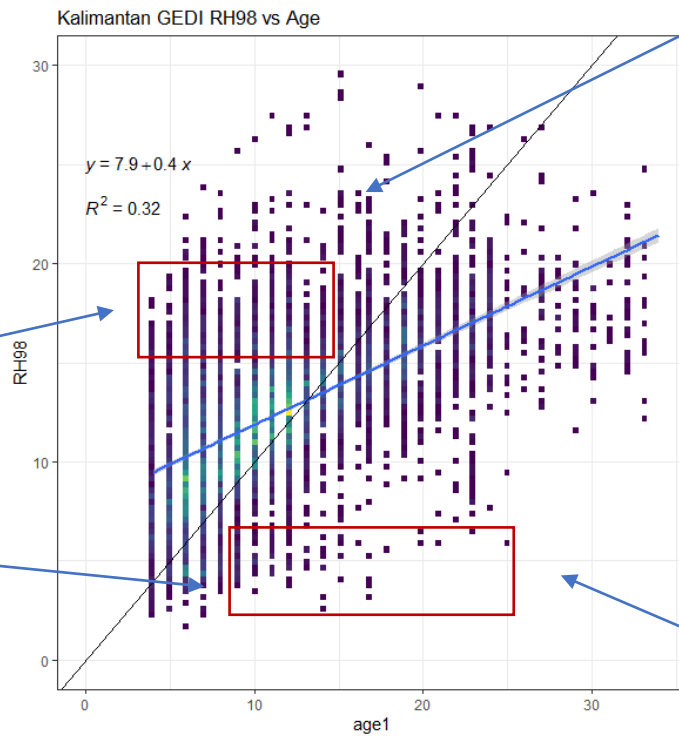
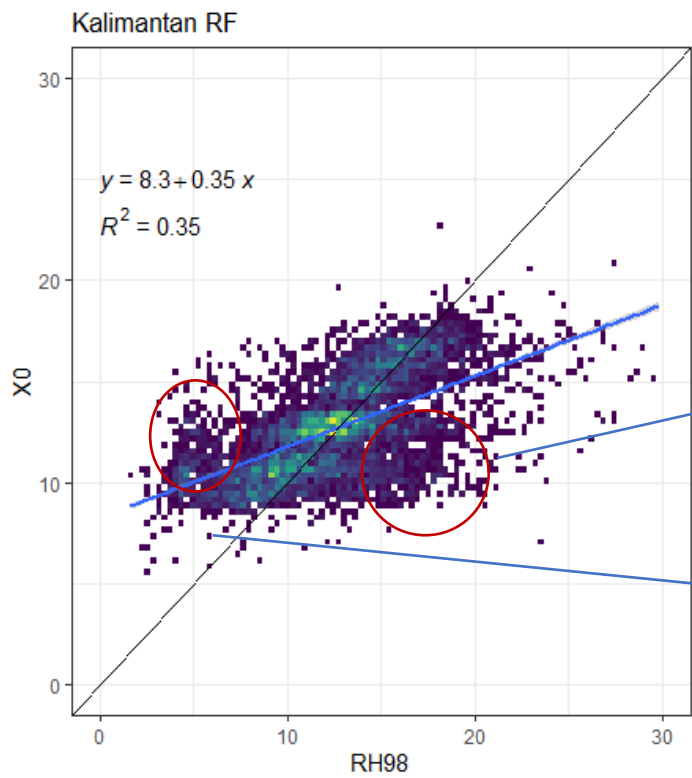
XGB Prediction



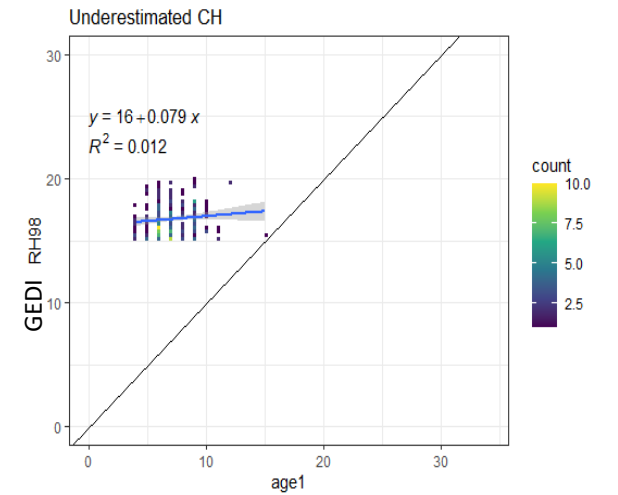


GEDI RH98 – RF Predicted RH98 (x)

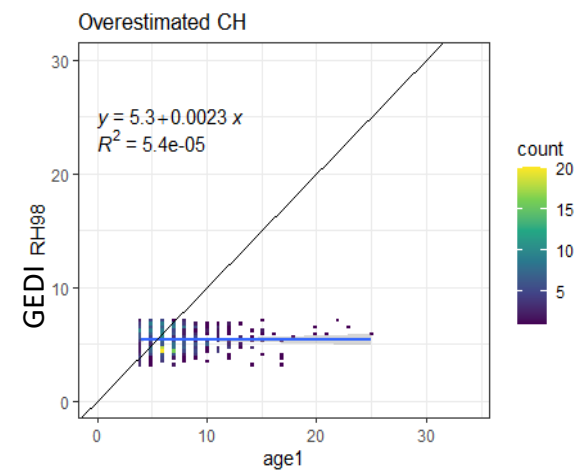




X0 9-13m vs GEDI RH98 15-20m



X0 10-15m vs GEDI RH98 3-7 m

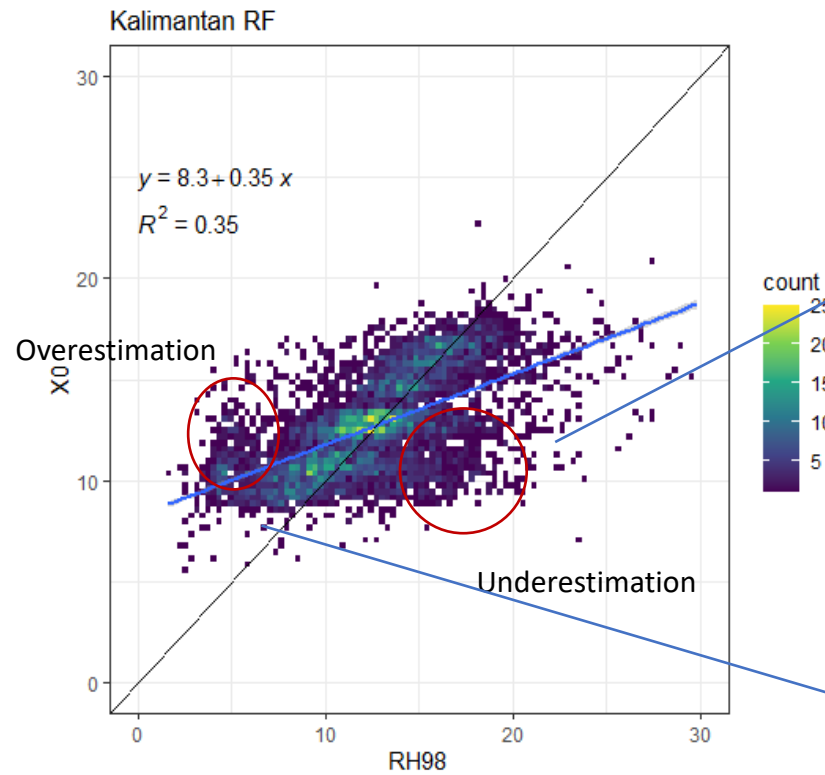


Problem with GEDI or OP age map?

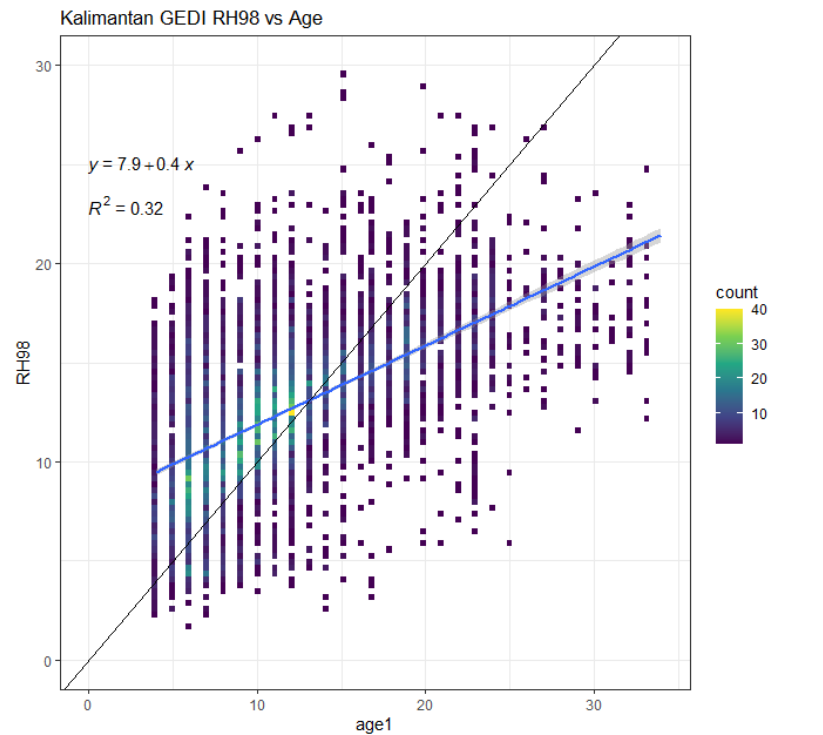
9yr-old OP with RH98 = 20m



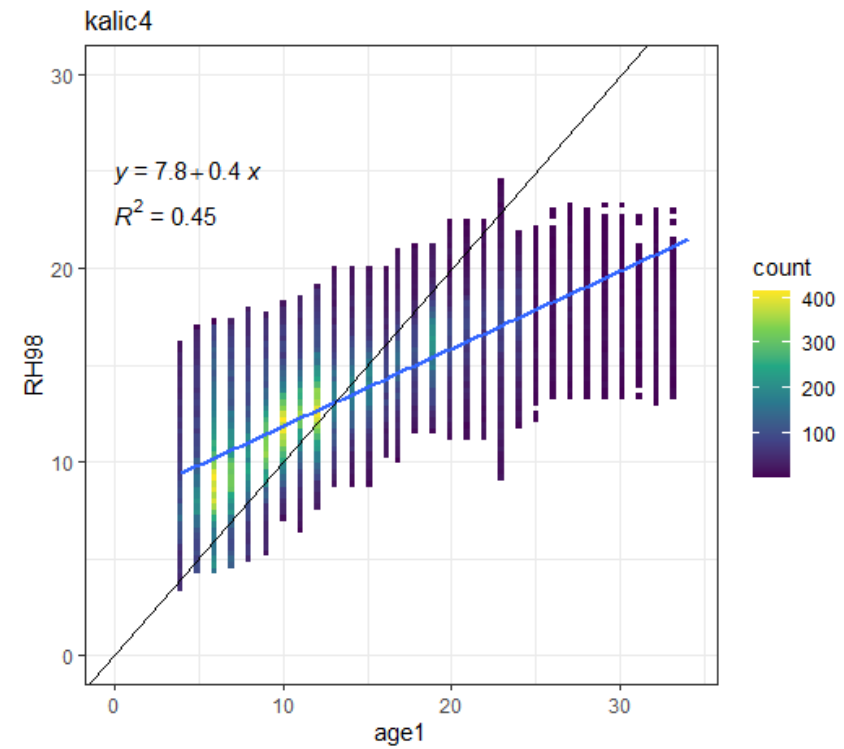
25yr-old with RH98 = 9.4m

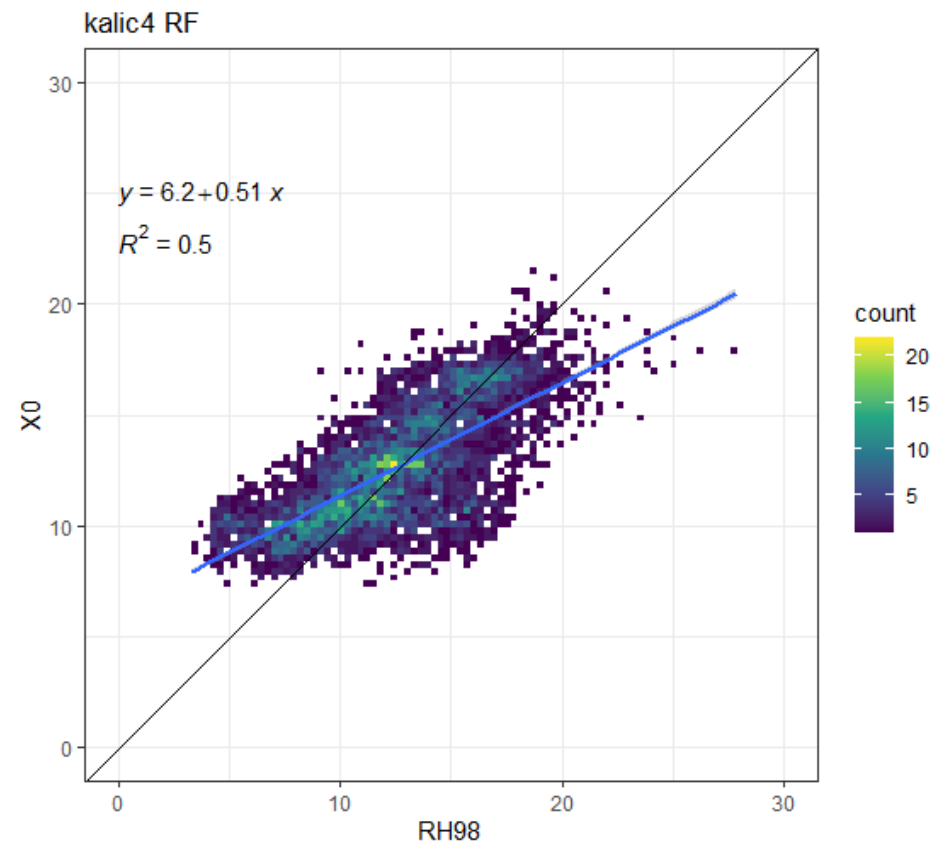
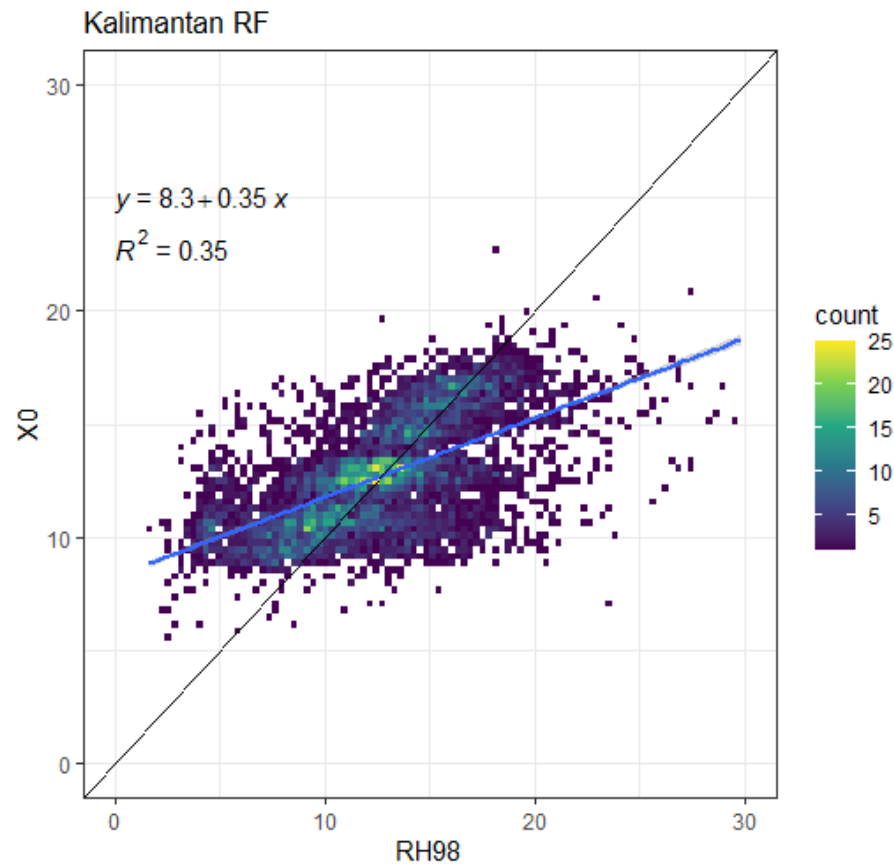
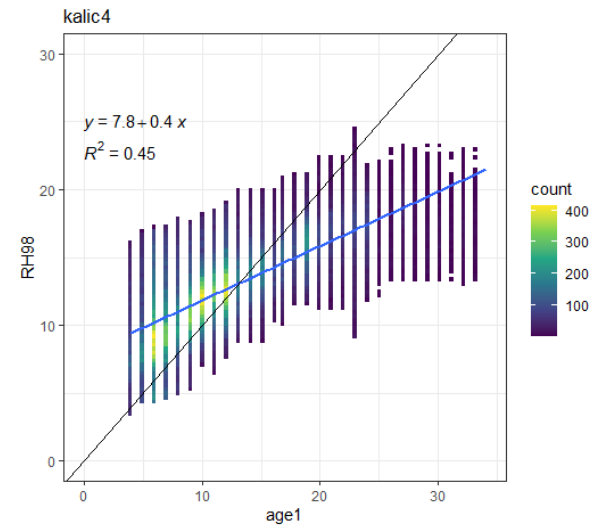
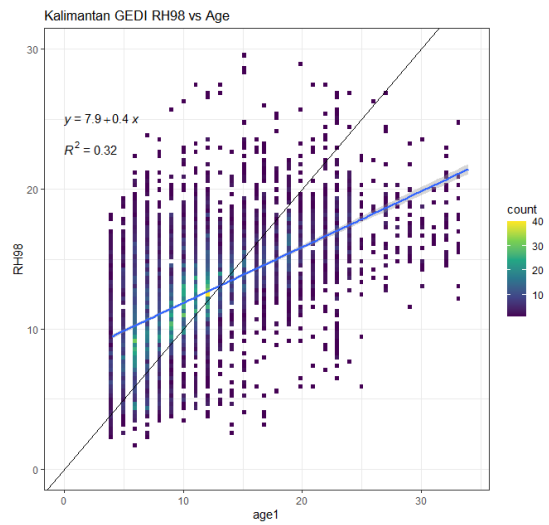


Before constraining training data

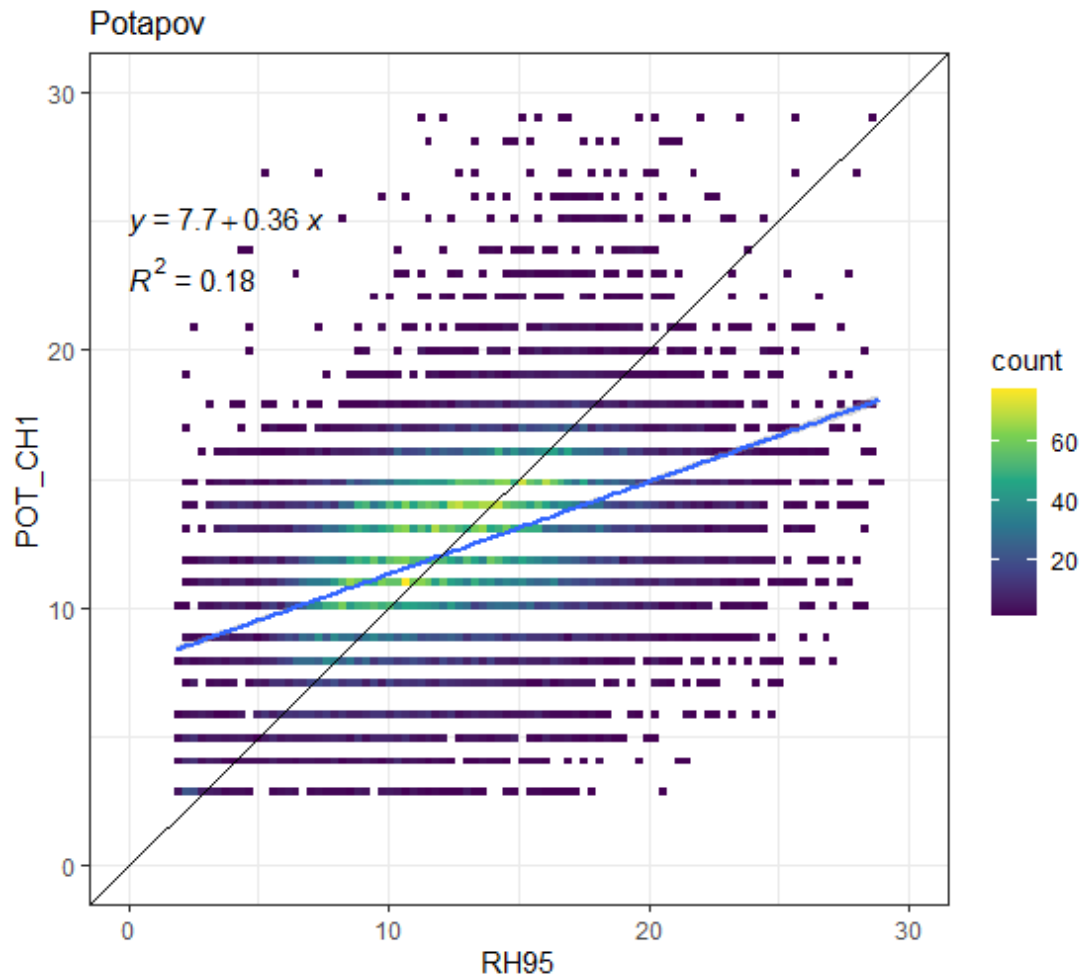


Training data was constrained with
RH98 > 0.5 percentile
RH98 < 0.95 percentile for each age

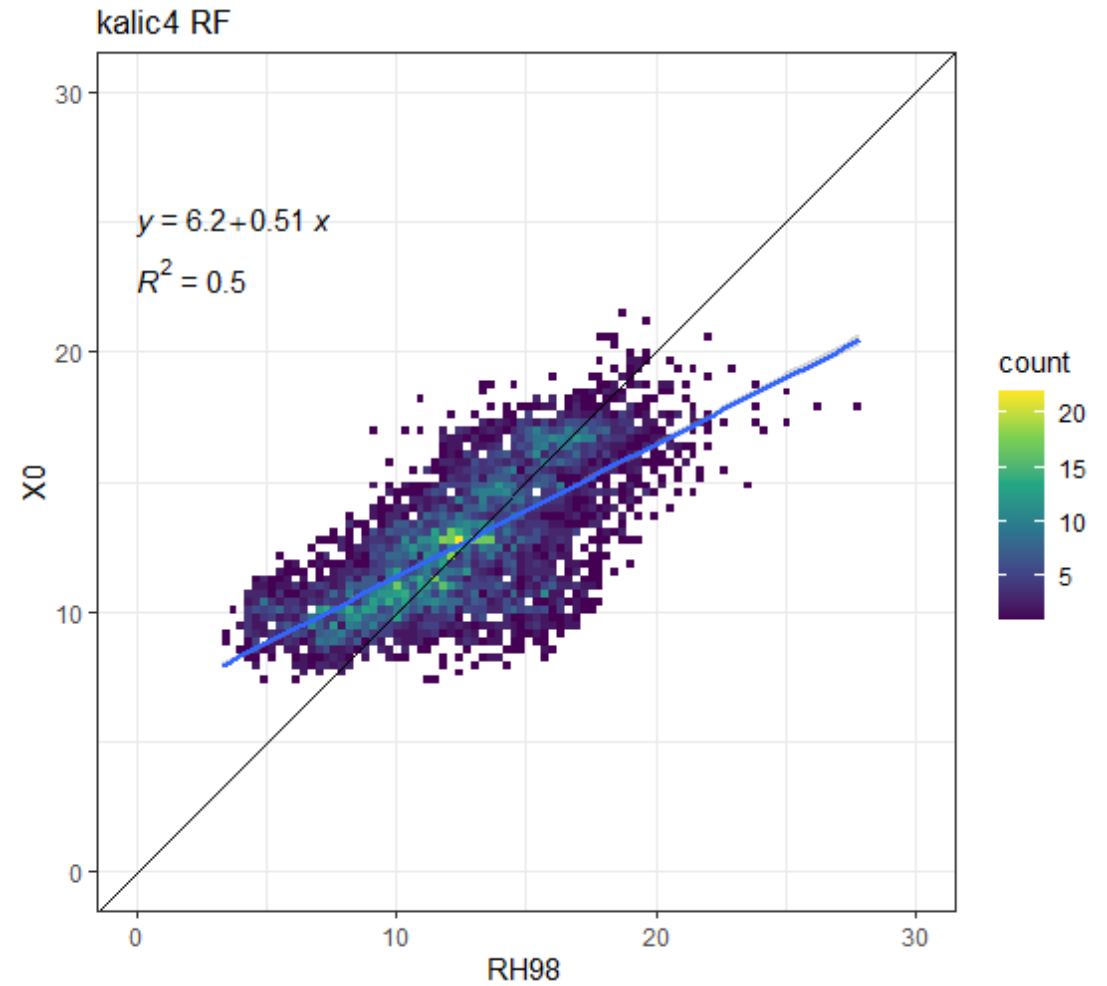




Other product also struggles... In the case of Potapov et al (2021) Oil palm CH: GEDI RH95 vs Predicted RH95



RMSE = 4.63m
MAE = 3.47m



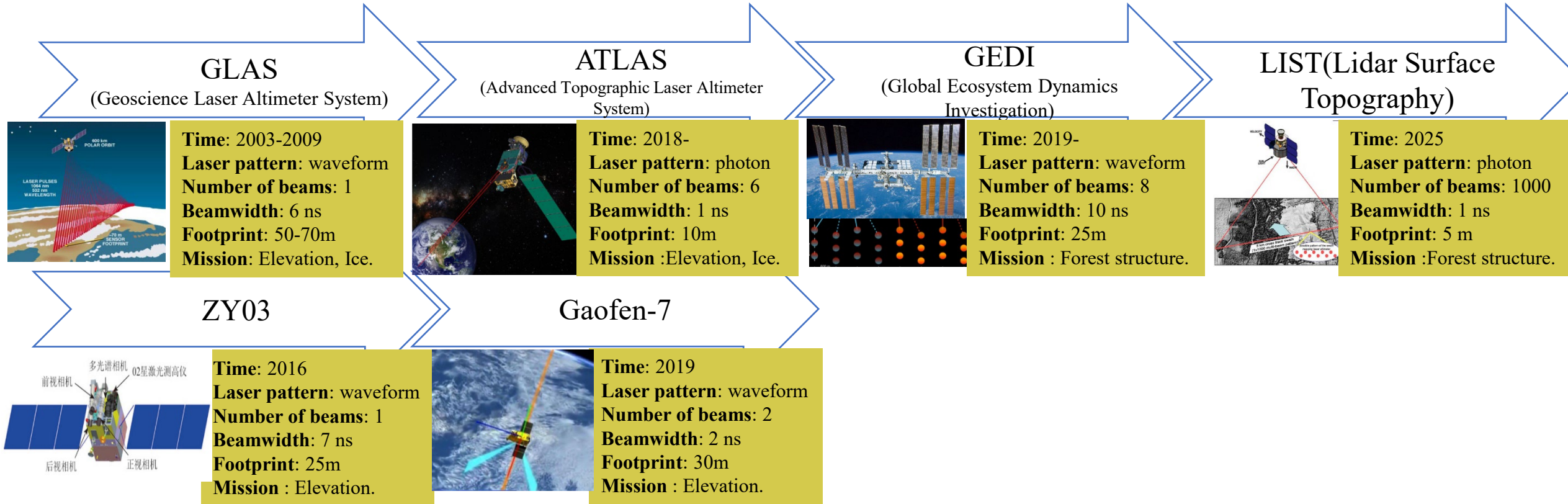
RMSE = 2.83m
MAE = 2.15m

Cangjiao Wang
mm:dd:yy: 07/18/2022

Contents

- Background
- GEDI performance analysis on canopy height estimation
- Framework for canopy height mapping based on integrating GEDI LiDAR (FPSF-CH)
- Limitations and Future Work

➤ Background



Aim 1:

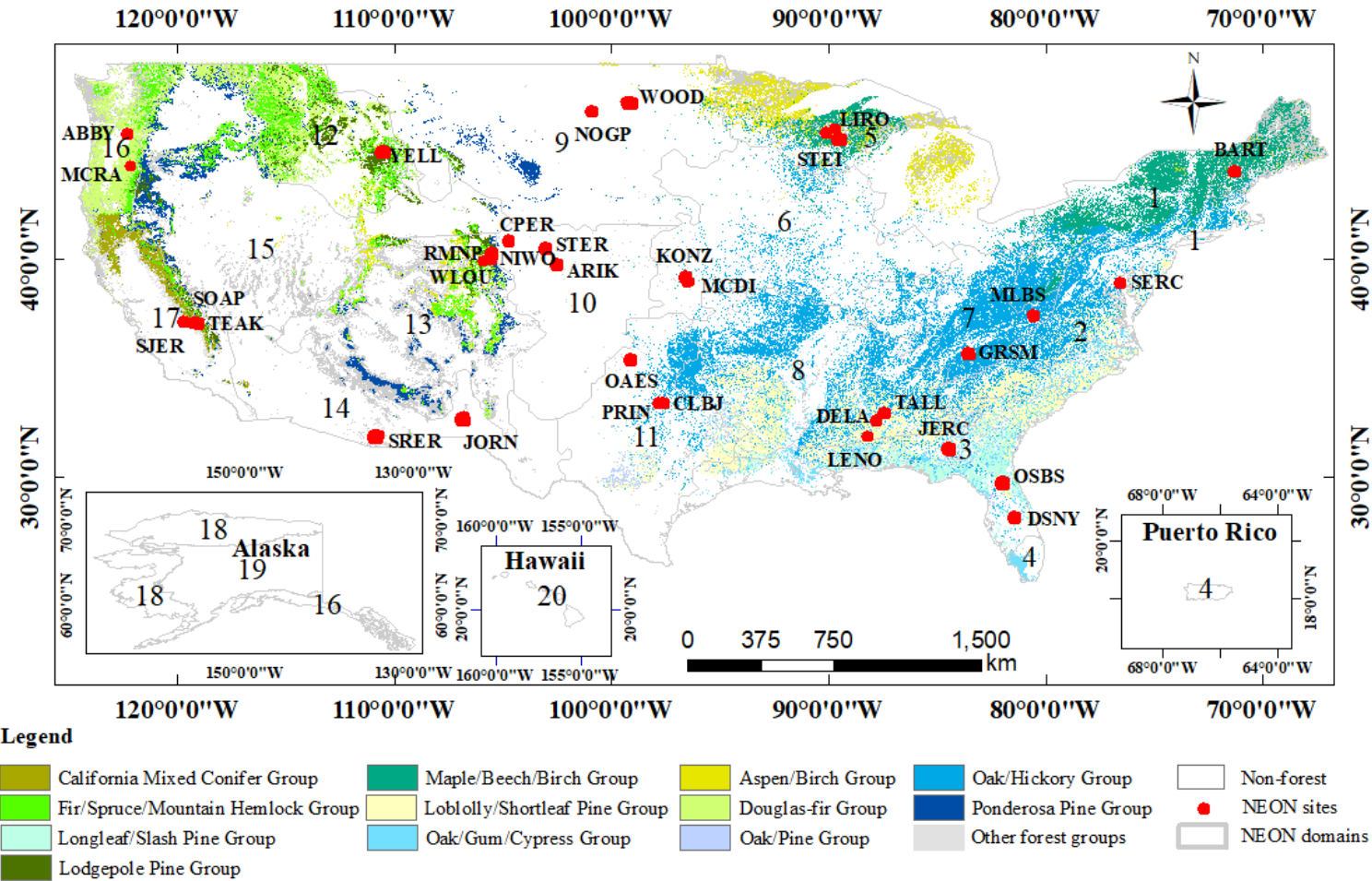
- ✓ What is the difference of vertical structure distribution between GEDI- and LiDAR?
- ✓ What is the most/best consistent canopy height index between the GEDI- and Lidar- products?
- ✓ What's the most important factor influencing the consistence between these two datasets?

Aim 2:

- ✓ How GEDI can be used for improving wall-to-wall canopy height mapping over large-scale region?

➤ GEDI performance analysis on canopy height estimation

➤ Study Area and Datasets



We have used 33 NEON discrete LiDAR datasets observed from 2017-2019 as reference datasets, and searched all available GEDI observation from 2019 to 2020.

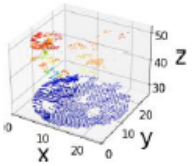
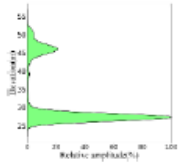
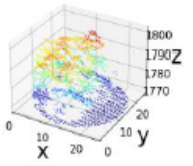
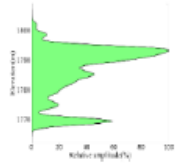
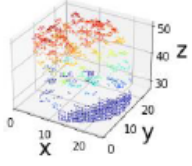
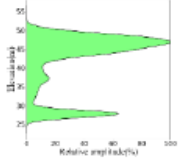
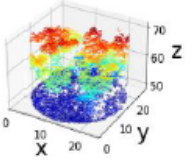
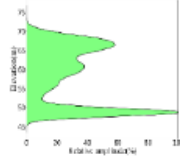
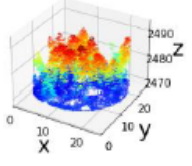
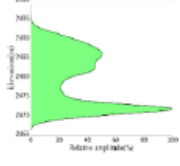
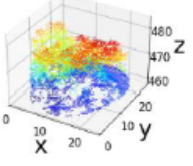
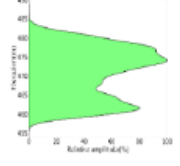
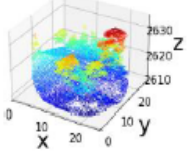
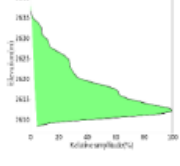
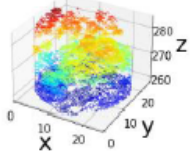
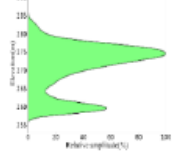
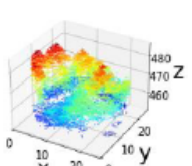
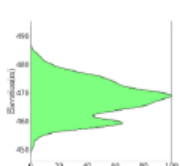
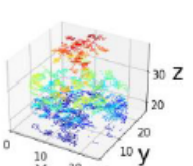
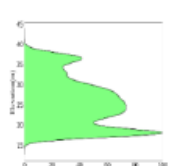
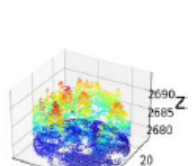
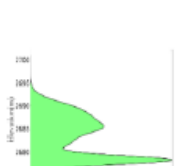
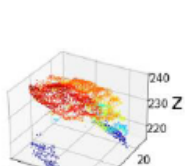
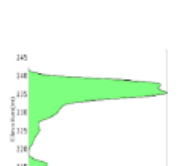
A total of 146,292 GEDI footprints within the NEON sites boundary box were extracted from the GEDI L2A product.

➤ GEDI performance analysis on canopy height estimation

➤ Study Area and Datasets

Over these 33 sites, forests include evergreen coniferous forest, mixed forest, and deciduous broadleaf forest. Among forest areas, twelve forest types with different tree species were selected to analyze GEDI performance among different forest types.

Table 3. The twelve forest types where the waveform is simulated from ALS based on rGEDI with 25m diameter footprint size.

Forest type	Discrete LiDAR	Waveform	Forest type	Discrete LiDAR	Waveform
Longleaf/ slash Pine Needled evergreen tree; Height (m): $19.20 \pm 5.81(5.13-40.27)$; Cover: $0.58 \pm 0.30(0.00-0.99)$; Slope: $4.44 \pm 2.90(0.00-28.07)$; Layers: $3 \pm 2(1-19)$;			California Mixed Conifer Needled tree; Height (m): $35.94 \pm 12.39(5.27- 70.66)$; Cover: $0.75 \pm 0.26(0.00-1.00)$; Slope: $15.91 \pm 8.81(0.62- 48.04)$; Layers: $5 \pm 4(1-20)$;		
Loblolly/shortleaf Pine Needled evergreen tree; Height (m): $25.89 \pm 7.19(5.04- 49.77)$; Cover: $0.73 \pm 0.26(0.00-1.00)$; Slope: $4.94 \pm 3.63(0.00-21.24)$; Layers: $4 \pm 3(1-18)$;			Oak/ Pine Mixed trees with understory; Height (m): $22.13 \pm 6.63(5.03- 59.21)$; Cover: $0.58 \pm 0.27(0.00-1.00)$; Slope: $4.54 \pm 3.97(0.62- 44.62)$; Layers: $5 \pm 4(1-20)$;		
Ponderosa Pine Needled evergreen tree; Height (m): $24.45 \pm 9.99(5.53- 70.33)$; Cover: $0.70 \pm 0.26(0.00-1.00)$; Slope: $17.61 \pm 10.80(0.00-54.10)$; Layers: $3 \pm 3(1-19)$;			Aspen/ Birch Deciduous broadleaf tree; Height (m): $20.90 \pm 7.23(5.03- 43.80)$; Cover: $0.74 \pm 0.26(0.00-1.00)$; Slope: $10.59 \pm 10.61(0.00-50.85)$; Layers: $3 \pm 2(1-11)$;		
Lodgepole Pine Needled tree; Height (m): $23.30 \pm 9.22(5.06- 71.30)$; Cover: $0.70 \pm 0.27(0.00-1.00)$; Slope: $17.24 \pm 10.07(0.00-62.67)$; Layers: $3 \pm 3(1-18)$;			Oak/ Hickory Deciduous broadleaf tree with sparse understory; Height (m): $25.95 \pm 12.59(5.02-66.40)$; Cover: $0.77 \pm 0.28(0.00-1.00)$; Slope: $11.67 \pm 10.68(0.00-52.99)$; Layers: $4 \pm 3(1-19)$;		
Douglas-fir Needled deciduous tree; Height (m): $37.24 \pm 17.42(5.03- 82.96)$; Cover: $0.82 \pm 0.25(0.00-1.00)$; Slope: $22.59 \pm 12.14(0.43- 61.61)$; Layers: $3 \pm 3(1-18)$;			Oak/ Gum/ Cypress Deciduous broadleaf tree with understory; Height (m): $21.39 \pm 6.74(5.06- 40.66)$; Cover: $0.71 \pm 0.29(0.00-1.00)$; Slope: $4.06 \pm 2.63(0.43- 19.31)$; Layers: $4 \pm 2(1-15)$;		
Fir/spruce/ Mountain Hemlock Needled evergreen tree. Height (m): $29.44 \pm 13.07(5.11- 80.27)$; Cover: $0.74 \pm 0.24(0.00-1.00)$; Slope: $18.66 \pm 10.06(0.62- 53.92)$; Layers: $4 \pm 3(1-20)$;			Maple/ Beech/ Birch Deciduous broadleaf tree; Height (m): $26.13 \pm 6.24(5.11-56.47)$; Cover: $0.85 \pm 0.23(0.00-1.00)$; Slope: $14.93 \pm 12.13(0.00- 62.05)$; Layers: $4 \pm 2(1-15)$;		

➤ GEDI performance analysis on canopy height estimation

➤ Results

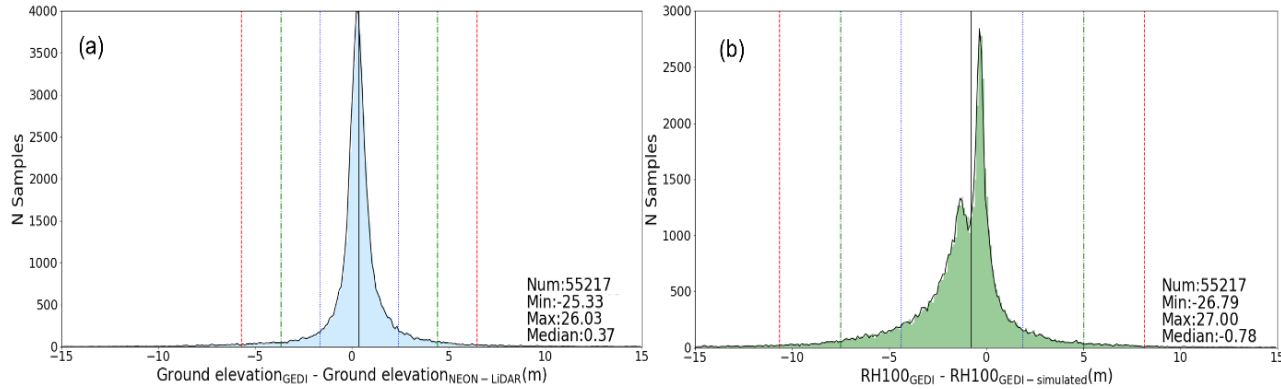


Figure 2. Histogram of ground elevation (A) and RH100 (B) differences between GEDI and NEON LiDAR, where the red, green, and blue dashed lines represent 3σ , 2σ , and 1σ , respectively.

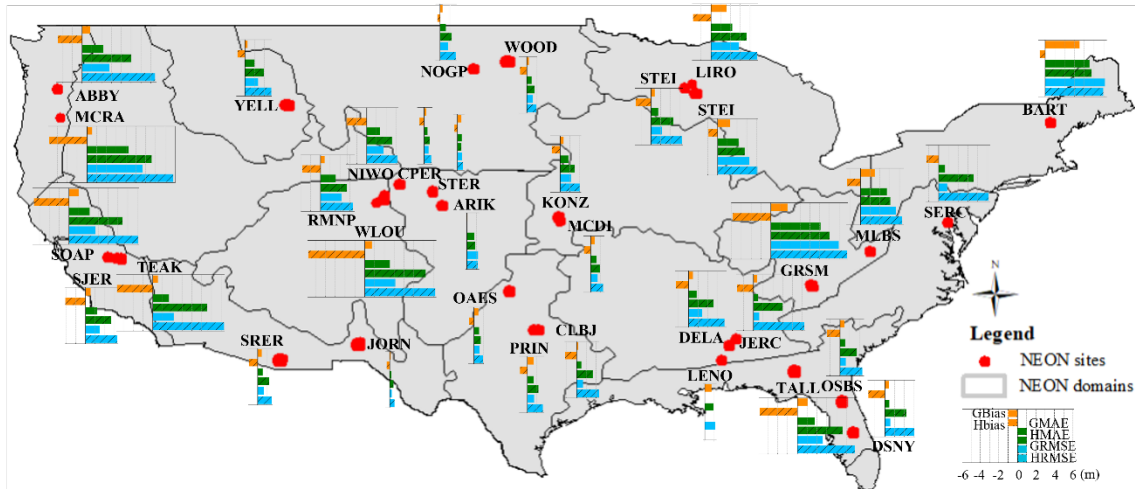


Figure 3. GEDI performance of ground elevation and RH100 estimations compared to NEON LiDAR, where GBias and Hbias, GMAE and HMAE, and GRMSE and HRMSE represent Bias, MAE, and RMSE for ground elevation and RH100 estimations, respectively. All the bars have the same scale.

Figure 4. Comparison of GEDI and GEDI-simulated RHs changing from RH05 to RH100. The %Bias and %RMSE were rescaled by dividing 100%.

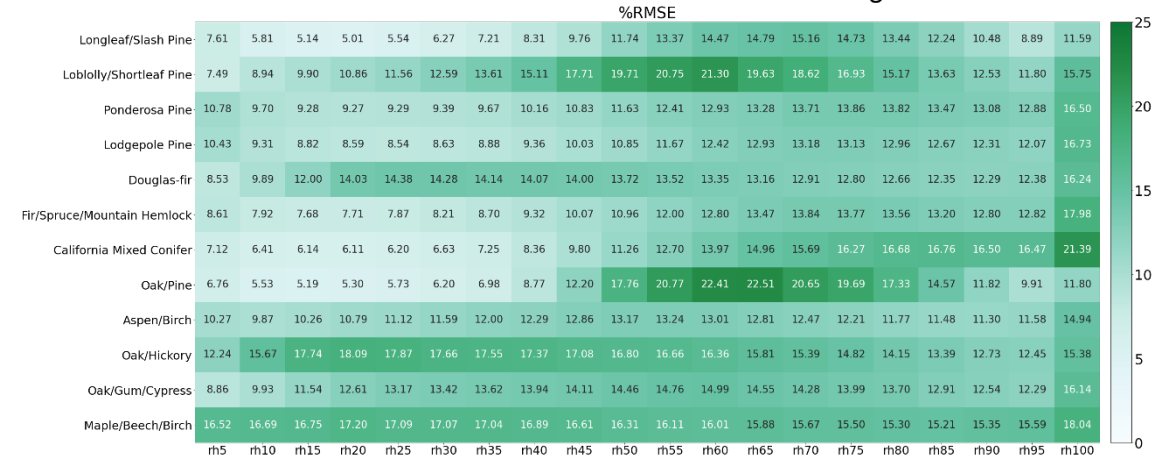
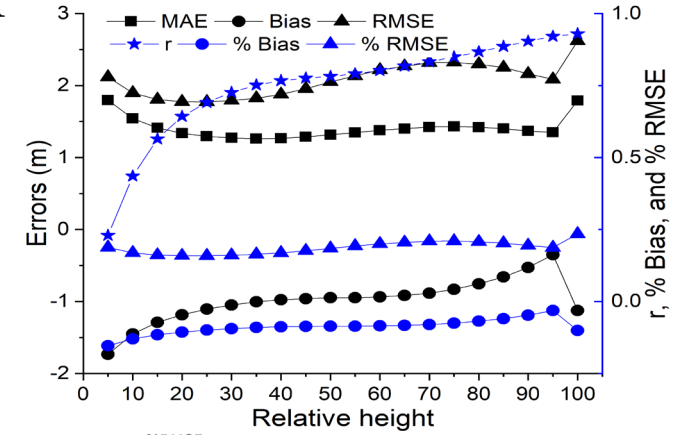


Figure 5. %RMSE as a function of RH among forest types. Color darkens with increasing %RMSE.

1. GEDI data generally is accurate for canopy height mapping, but it is sensitive to abnormal observations (Figure 2);
2. GEDI data performed variously over space (Figure 3), different canopy height (Figure 4), and forest types (Figure 5).

➤ GEDI performance analysis on canopy height estimation

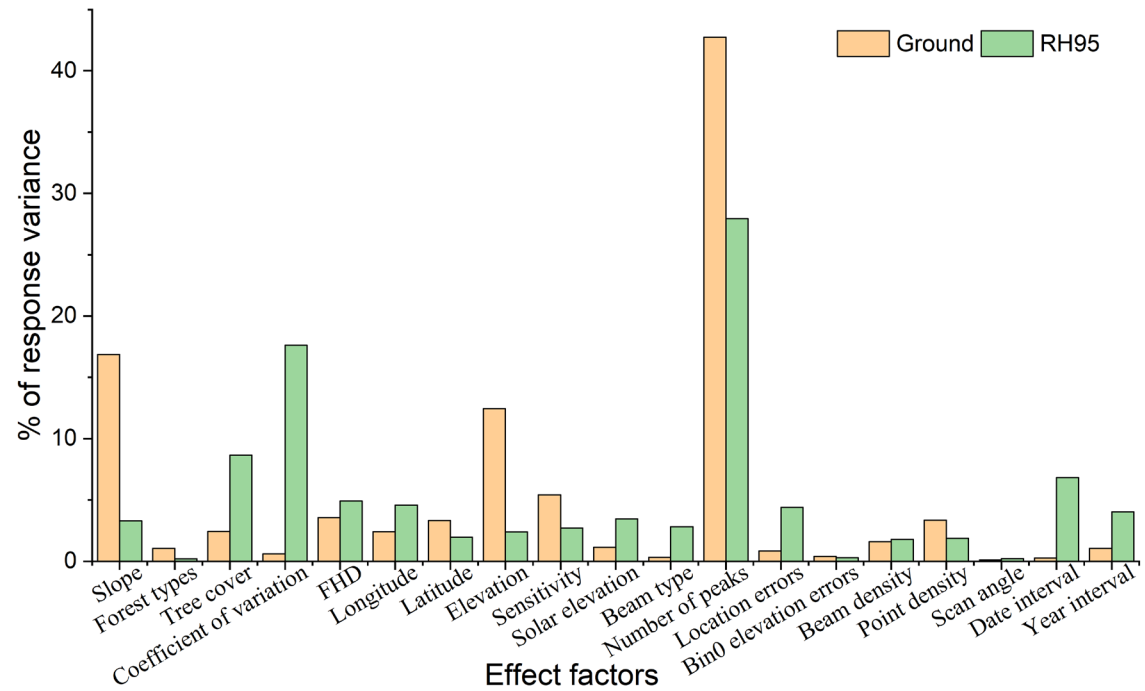


Figure 6. The importance of 19 factors for explaining the differences of ground elevation and RH measurements between GEDI and GEDI-simulated waveforms.

1. Factors have different effects on estimations of surface elevation and vegetation height.
2. Most of explanation variations from different factors can be interactive for GEDI waveform.
3. Waveform complex influence GEDI canopy height and ground elevation estimations mostly (Figure 6). This factor is heavily influenced by slope indicating by small effect on bias after removing slope effect (Figure 7).

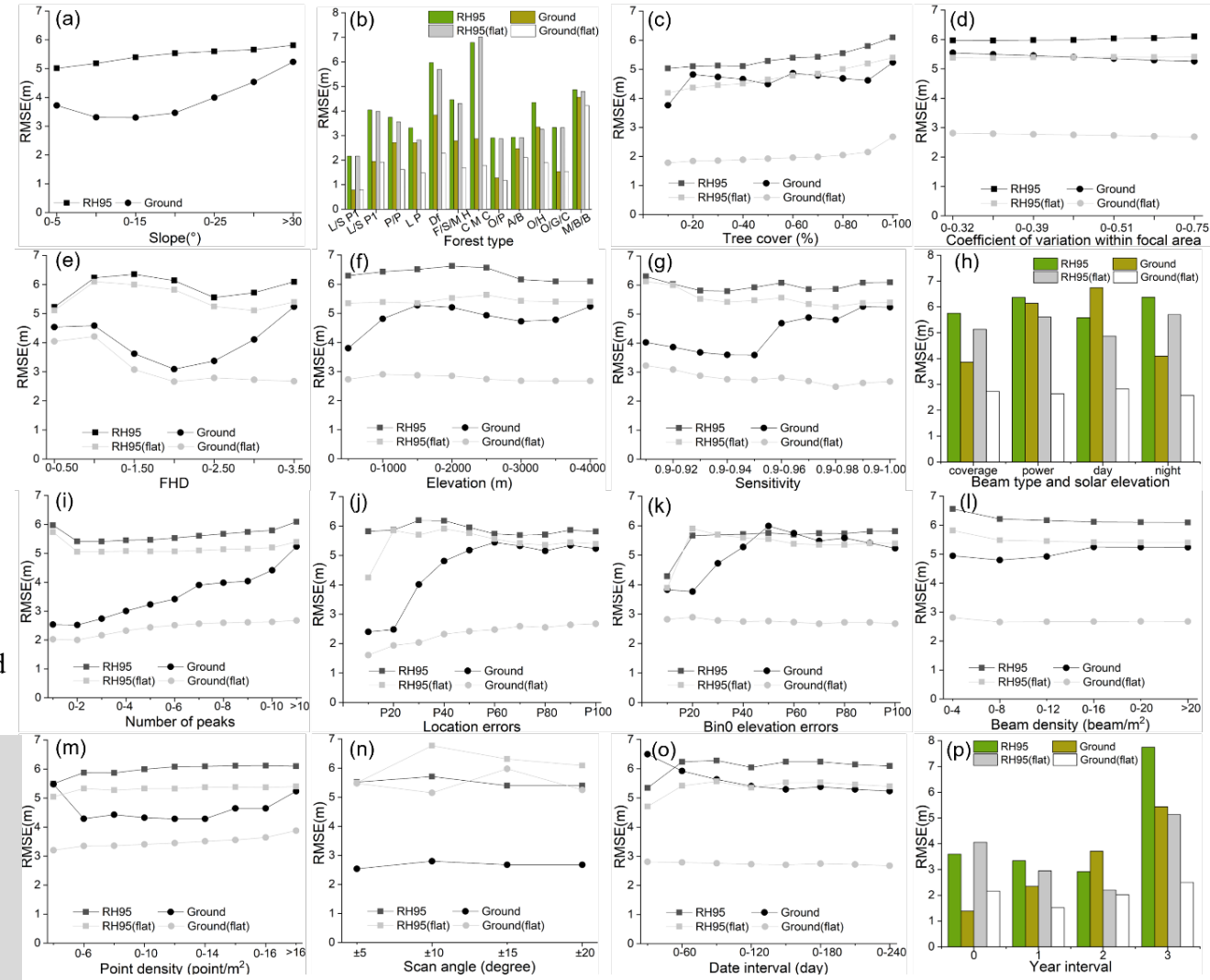


Figure 7. RMSE analysis of GEDI performance of ground elevation and RH95 estimations under different slope (a), forest type (b), tree cover (c), coefficient of variation (d), FHD (e), elevation (f), sensitivity (g), beam type, and solar elevation (h), number of peaks (i), beam density (j), point density (k), scan angle (l), date interval (m), and year interval (n), respectively. The RH95 (flat) and ground (flat) showed the RMSE of RH95 and ground elevation in flat areas with a slope lower than 15 degrees.

➤ GEDI performance analysis on canopy height estimation

➤ Results

1. Biases of GEDI ground elevation and canopy height estimations have a negative relationship (Figure 8).
2. For needle leaf or mixed forests, this negative relationship was apparent to varying degrees in some forest types (Longleaf/Slash pine, Loblolly/Shortleaf pine, Oak/Pine, and Oak/Gum/Cypress) but minimal or not existent in others (Lodgepole pine, Douglas Fir, Fire/Spruce/Mountain Hemlock, California Mixed Conifer).
3. Finding true ground is a particular challenge in broadleaf forest types with high tree cover.

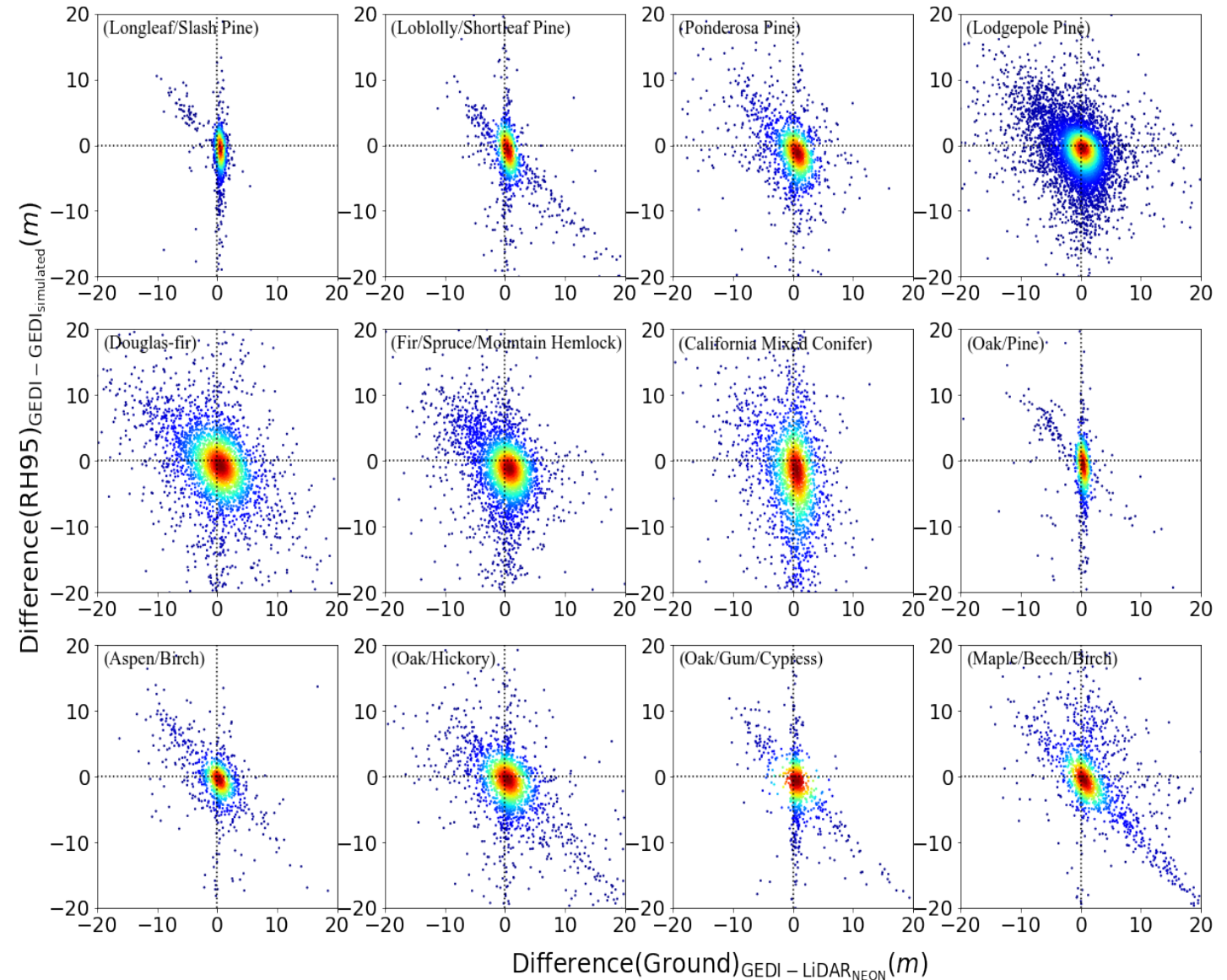


Figure 8. The relationships of ground elevation and RH95 differences between GEDI and GEDI-simulated waveforms of different forest types.

➤ GEDI performance analysis on canopy height estimation

➤ Results

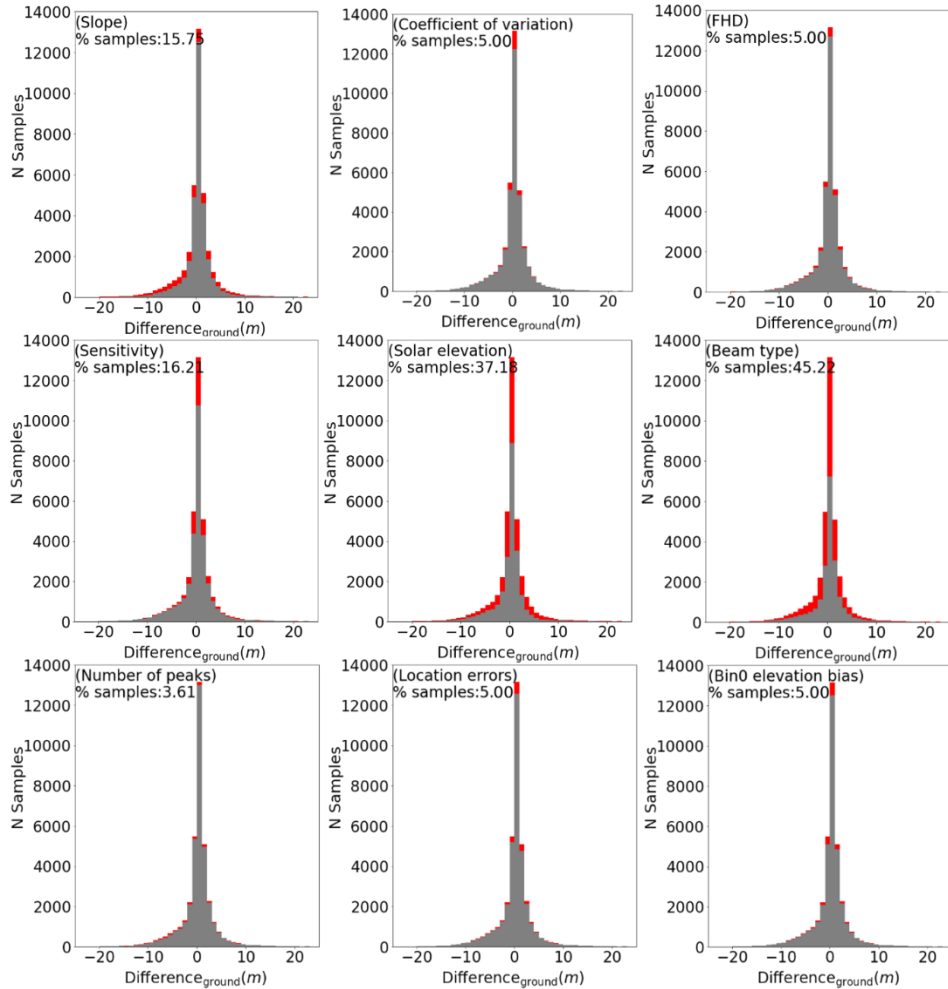


Figure 9. Filtering GEDI observations using different factors, where y-axes are samples and x-axes is differences of ground elevation between GEDI and NEON-LiDAR. Red and gray histograms were filtered out and retained observations, respectively. % samples indicate the percentage of filtered out samples from gray to the red histogram.

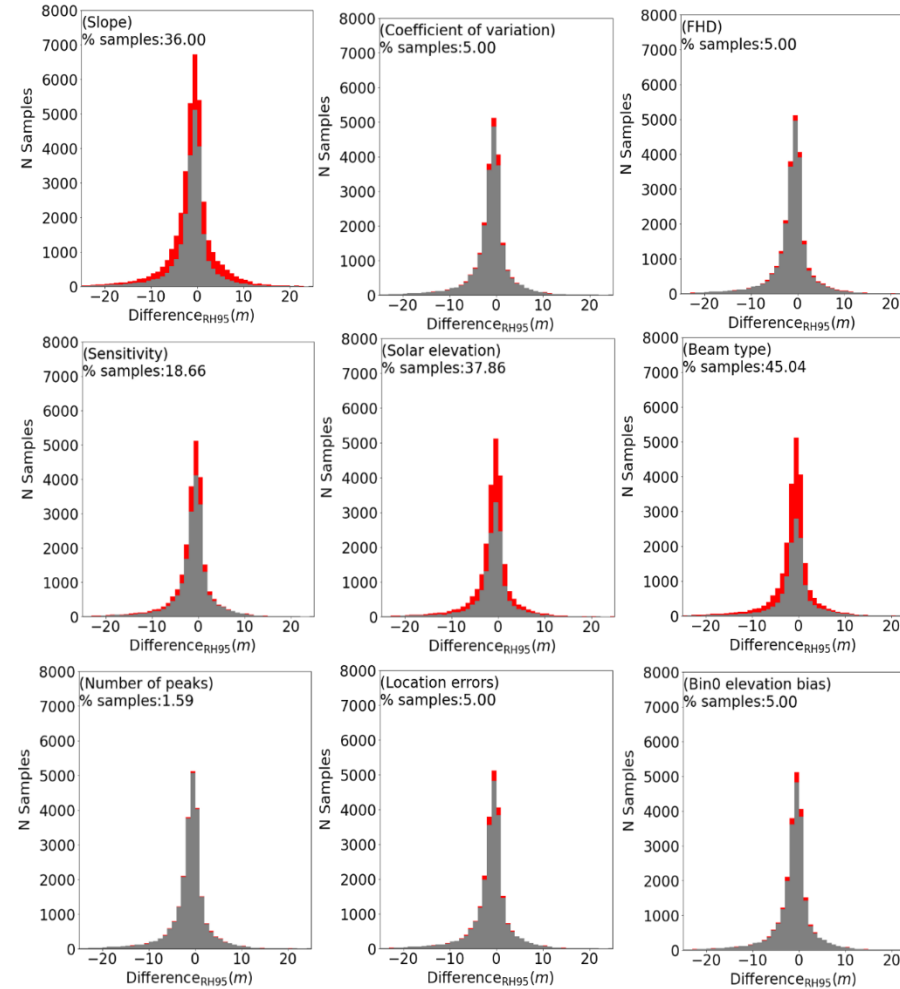


Figure 10. Filtering GEDI observations using different factors, where y-axes are samples and x-axes is differences of RH95 between GEDI and NEON-LiDAR. Red and gray histograms were filtered out and retained observations, respectively. % samples indicate the percentage of filtered out peaks samples from gray to the red histogram.

1. Screening GEDI data by factors other than GEDI quality_flag sometimes provides only a marginal improvements for GEDI accuracy metrics for canopy height estimation, but does result in the removal of a large amount of good-quality GEDI data with small bias. (Figure 9 and Figure 10).

➤ GEDI performance analysis on canopy height estimation

➤ Results

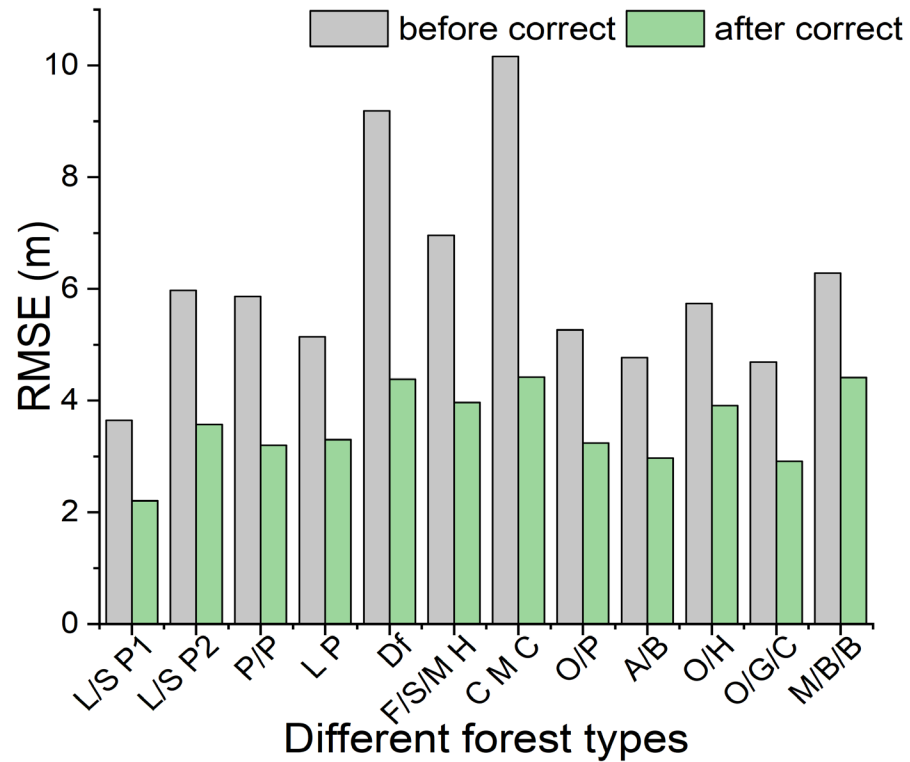


Figure 14. The RMSE of GEDI RH100 estimation among forest types before and after geolocation correction. The L/S P1, L/S P2, P/P, L P, Df, F/S/M H, C M C, O/P, A/B, O/H, O/G/C, and M/B/B represent Loblolly/Shortleaf pine, Longleaf/Slash pine, Ponderosa pine, Lodgepole pine, Douglas-fir, Fir/Spruce/Mountain Hemlock, California mixed conifer, Oak/Pine, Aspen/Birch, Oak/Hickory, Oak/Gum/Cypress, and Maple/Beech/Birch, respectively.

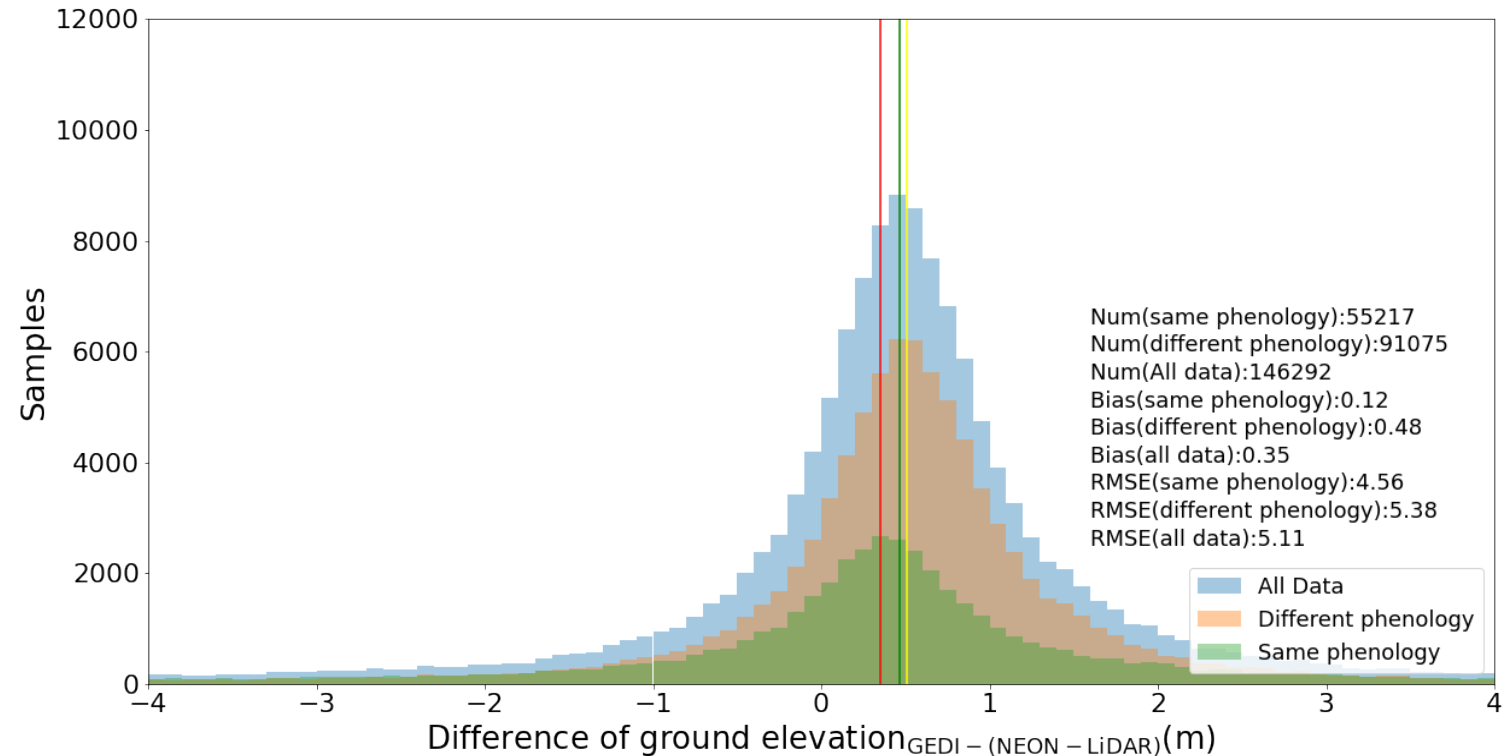


Figure 11. Comparison of GEDI performance in ground elevation estimation using the same and different phenology periods of observations between GEDI and NEON LiDAR.

1. Geolocation uncertainties affect GEDI performance of canopy height estimation, which vary from forest types.
2. GEDI data probably will be affected by different phenology of observations.

➤ Framework for canopy height mapping by integrating GEDI LiDAR (FPSF-CH)

➤ Study Area and Datasets

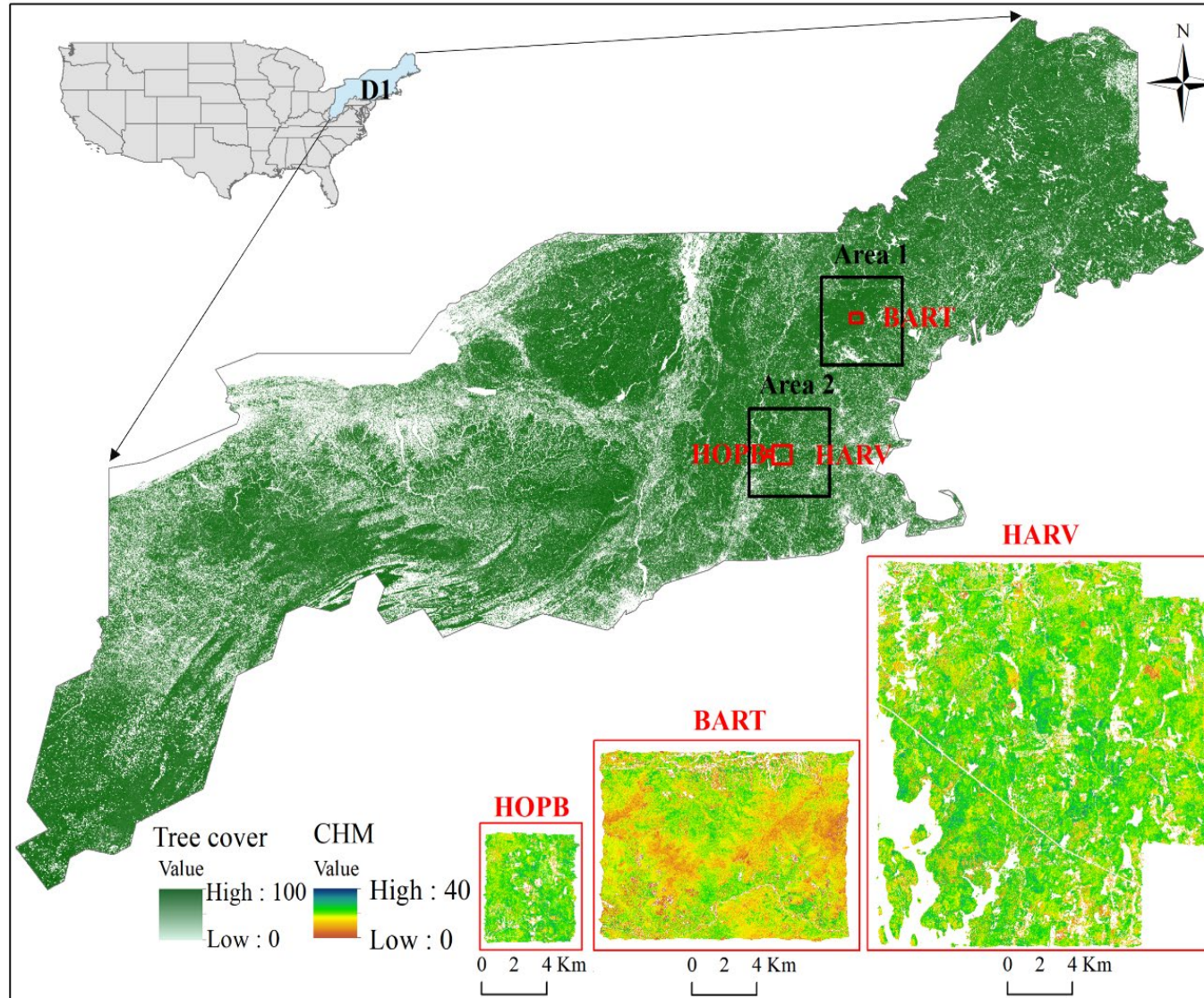


Figure 12. Locations of study areas. The black rectangles showed the locations of Area 1 and Area 2 with $1^\circ \times 1^\circ$ tiles in the ecoregion domain of North American Eastern Forests. Three red rectangles are the locations of three NEON sites including the BART, HOPB, and HARV. The tree cover map was downloaded from the Global Land Analysis and Discovery website (<https://glad.umd.edu/dataset>). The canopy height models (CHMs) in BART, HOPB, and HARV were at the same scale with data ranging from 0 to 40 m.

➤ Framework for canopy height mapping by integrating GEDI LiDAR (FPSF-CH)

➤ Method

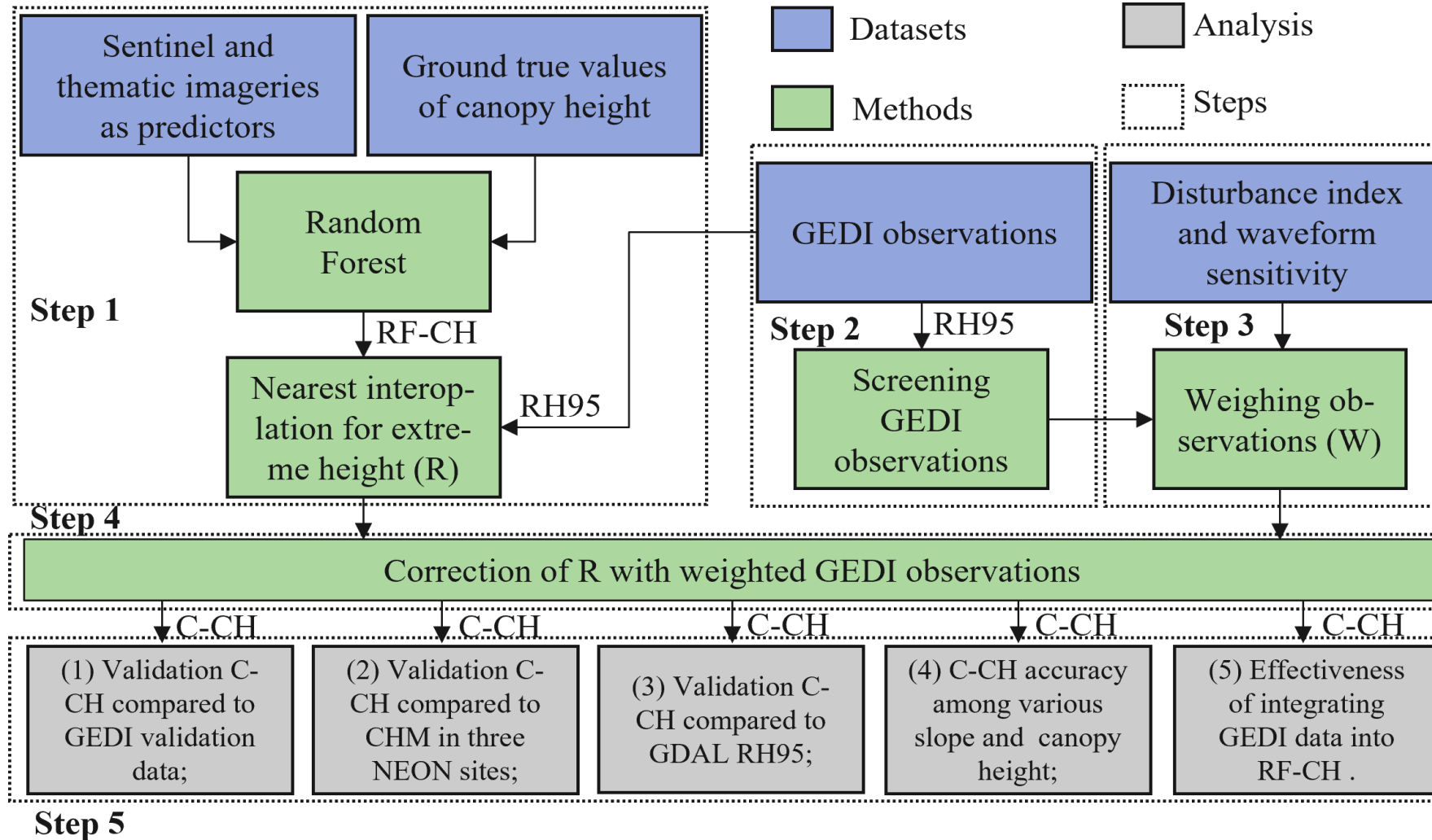


Figure 13. Flowchart of the FPSF-CH and its performance analysis. The RF-CH and C-CH are canopy heights derived from RF and the FPSF-CH. R and W are the nearest interpolation dataset and weight for each GEDI data, respectively. CHM is the canopy height model.

➤ Framework for canopy height mapping by integrating GEDI LiDAR (FPSF-CH)

➤ Result

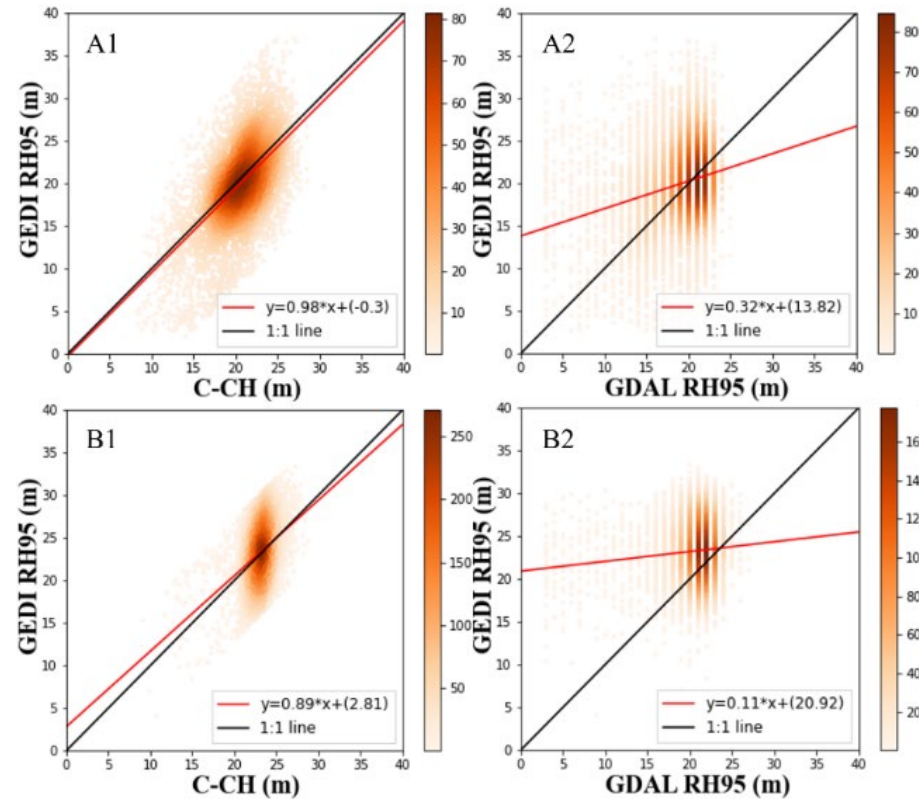


Figure 14. The relationship of canopy heights of C-CH (A1 and B1) and GDAL RH95 (A2 and B2) compared to high-quality GEDI validation data in Area 1 (A) and Area 2 (B), respectively.

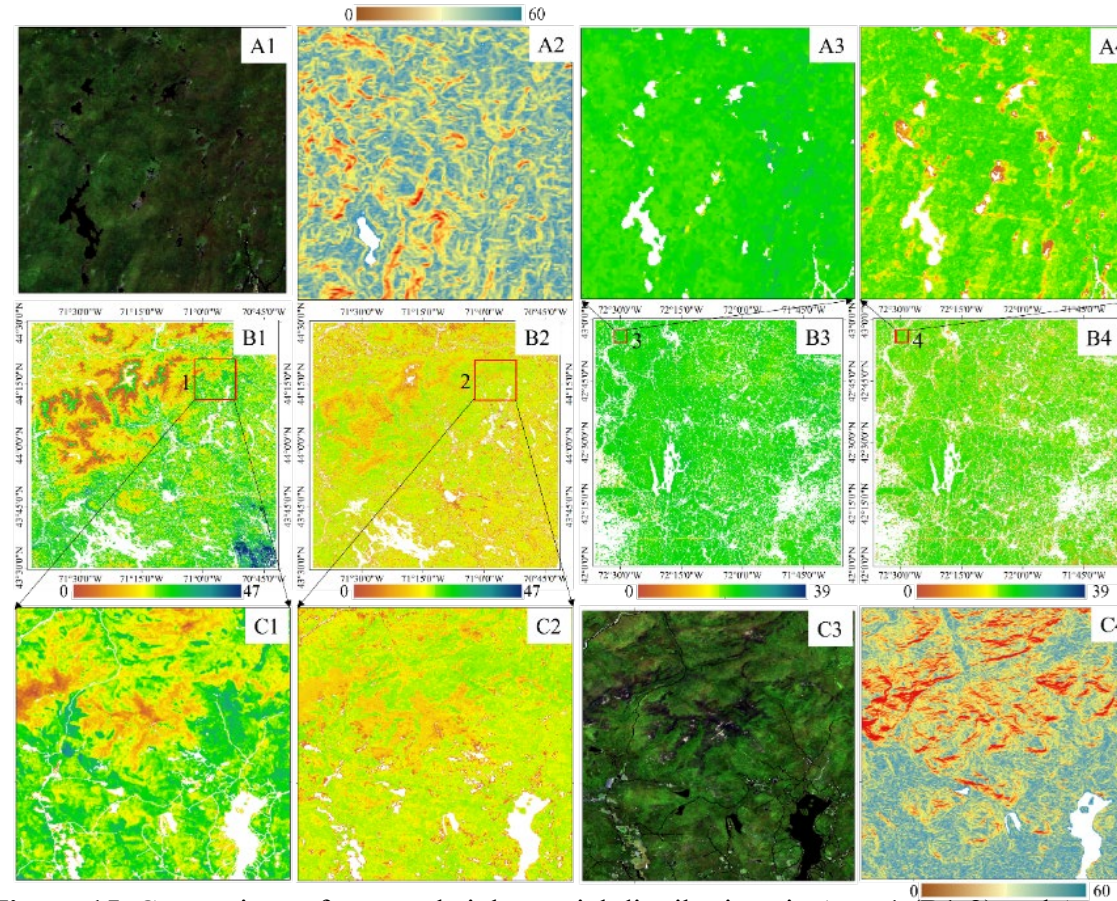


Figure 15. Comparison of canopy height spatial distributions in Area 1 (B1-2) and Area 2 (B3-4). The A1 and C3 are true color images while A2 and C4 are the topographic slope of the enlarged rectangle in Area 1 (B1-2) and Area 2 (B3-4), respectively. The B1 and B2, and B3 and B4 are C-CH, GDAL RH95 in Area 1 and Area 2, respectively. The true color images are composited by blue, green, and red bands of Sentinel-2. Masked areas are displayed in white.

1. The proposed framework (FPSF-CH) has better performance in canopy height mapping than GDAL RH95 (global canopy height potpov et al., 2019) (Figure 14);
2. The FPSF can reveal canopy height from short to high (Figure 15).
3. The GDAL RH95 over-represent short vegetation.

➤ Framework for canopy height mapping by integrating GEDI LiDAR (FPSF-CH)

➤ Result

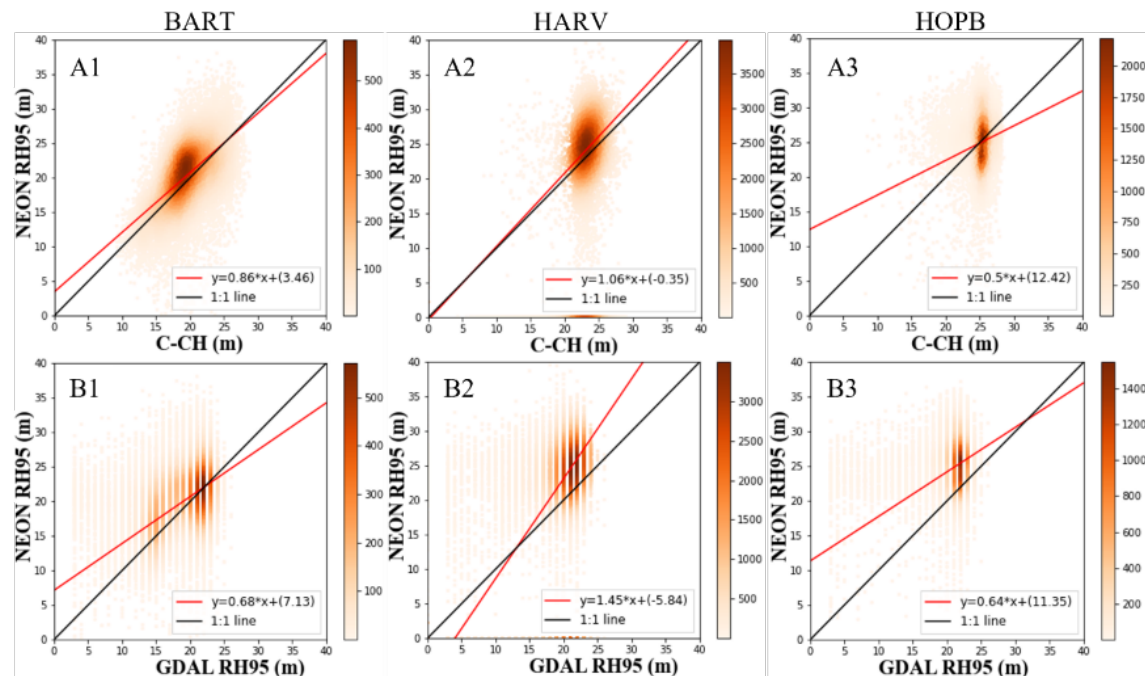


Figure 16. The relationship of canopy heights of C-CH (A1 and B1) and GDAL RH95 (A2 and B2) compared to NEON RH95 in Area 1 (A) and Area 2 (B), respectively.

Compared to NEON LiDAR, the FPSF-CH performed better than GDAL RH95 both in accuracy (Figure 16) and space (Figure 17).

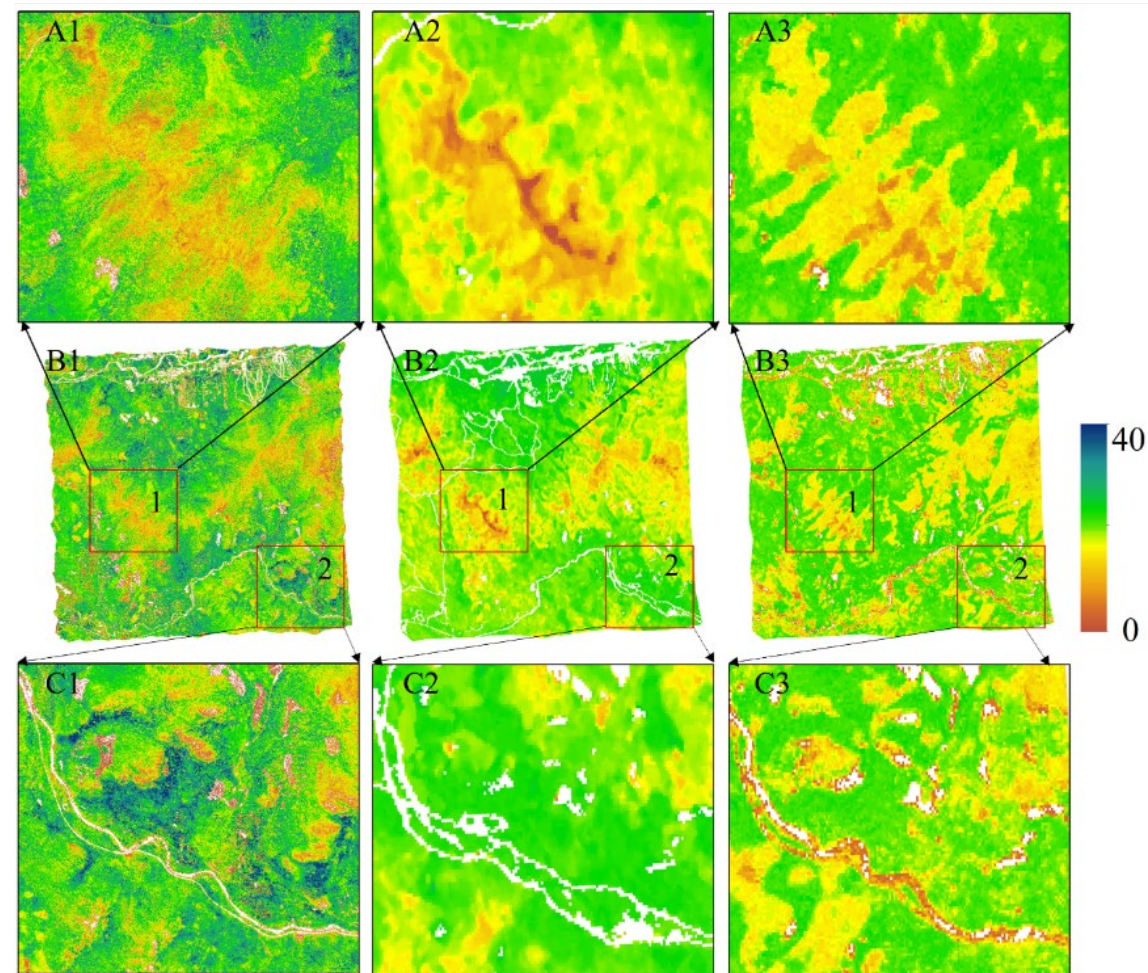


Figure 17. Comparison of canopy height spatial distributions among NEON CHM, C-CH, and GDAL RH95. The A1-3 and C1-3 are the subregions of '1' and '2' rectangles in B1-3, in B1, B2, and B3 represented the NEON CHM, C-CH, and GDAL RH95, respectively. To be comparative the canopy heights have the same scale ranging from 0 to 40. Masked areas are displayed in white.

➤ Framework for canopy height mapping by integrating GEDI LiDAR (FPSF-CH)

➤ Result

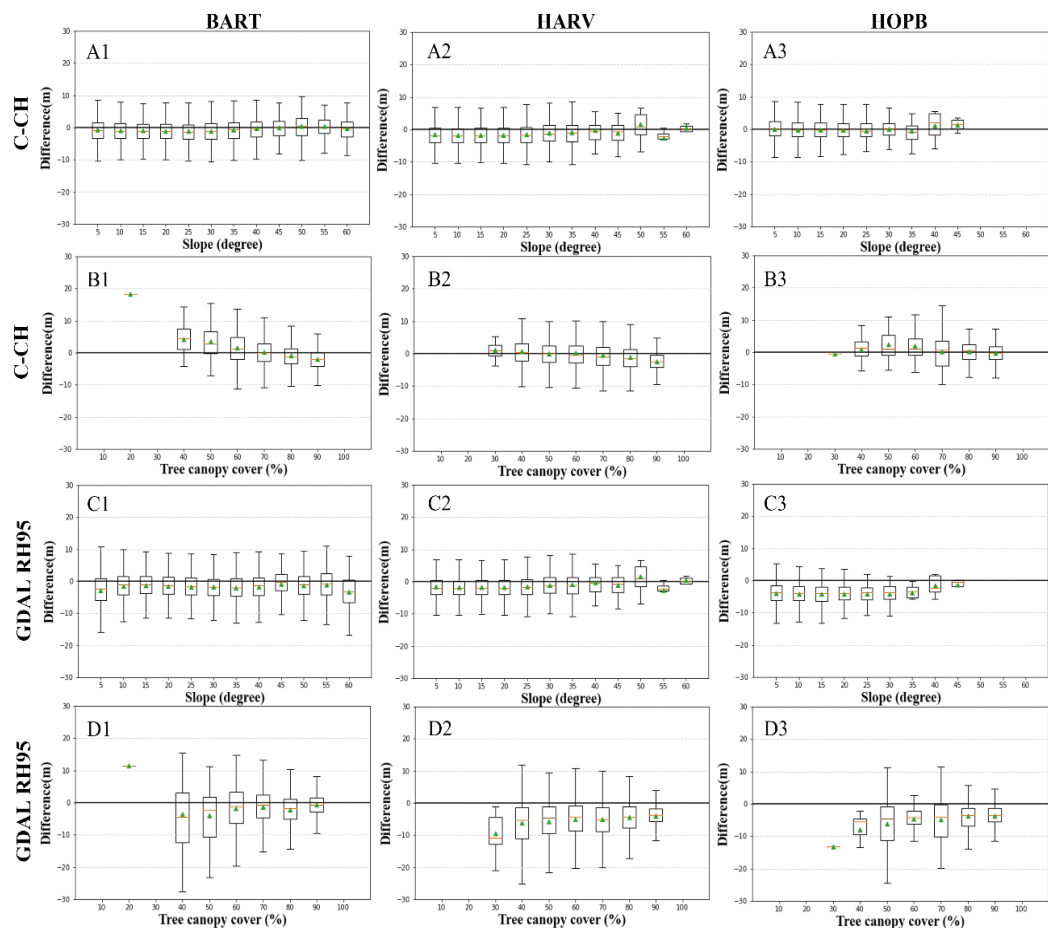


Figure 18. Canopy height residuals of C-CH (A and B) and GDAL RH95 (C and D) plotted as a function of slope (A1-A3 and C1-C3), tree canopy cover (B1-B3 and D1-D3) in BART, HARV, and HOPB. To be readable, the median and average of residuals are shown by the orange line and green triangle in the box, respectively. The negative median and average values indicate underestimation and vice versa. The upper and lower quartiles were indicated by the end of lines.

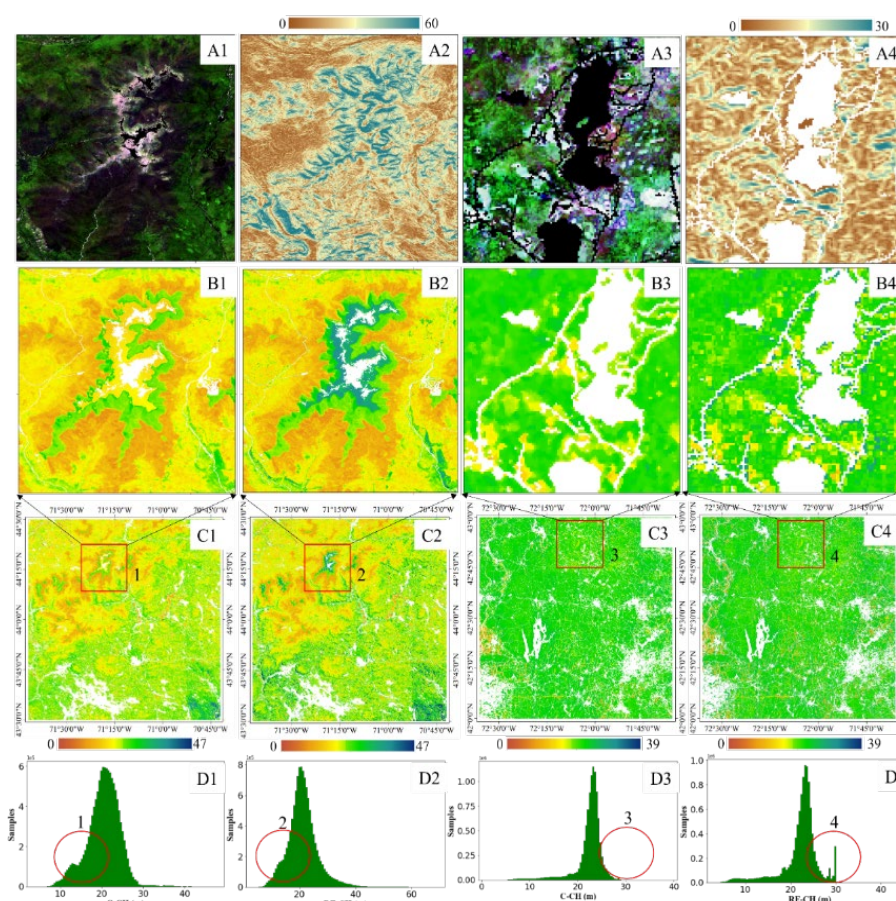


Figure 19. Comparison of distributions between C-CH (C1 and C3) and RF-CH (C2 and C4) over space and height histograms. A1 and A3 are true color images while A2 and A4 are topographic slopes for the enlarged rectangle in Area 1 (B1-2) and Area 2 (B3-4). D1-4 represents histograms of canopy height of C-CH (D1 and D3) and RF-CH (D2 and D4) in Area 1 (D1-2) and area 2 (D3-4), respectively. The red circles in D1-4 show the obvious difference between canopy heights of RF-CH and C-CH. The true color images are composited by blue, green, and red bands of Sentinel-2. Masked areas are displayed in white.

1. The FPSF-CH is robust to different land surface with various slope and tree cover (Figure 18).
2. Compared to without integrating GEDI LiDAR, the FPSF-CH can calibrate abnormal short and high vegetation canopy height (Figure 19).

➤ Framework for canopy height mapping by integrating GEDI LiDAR

➤ Result

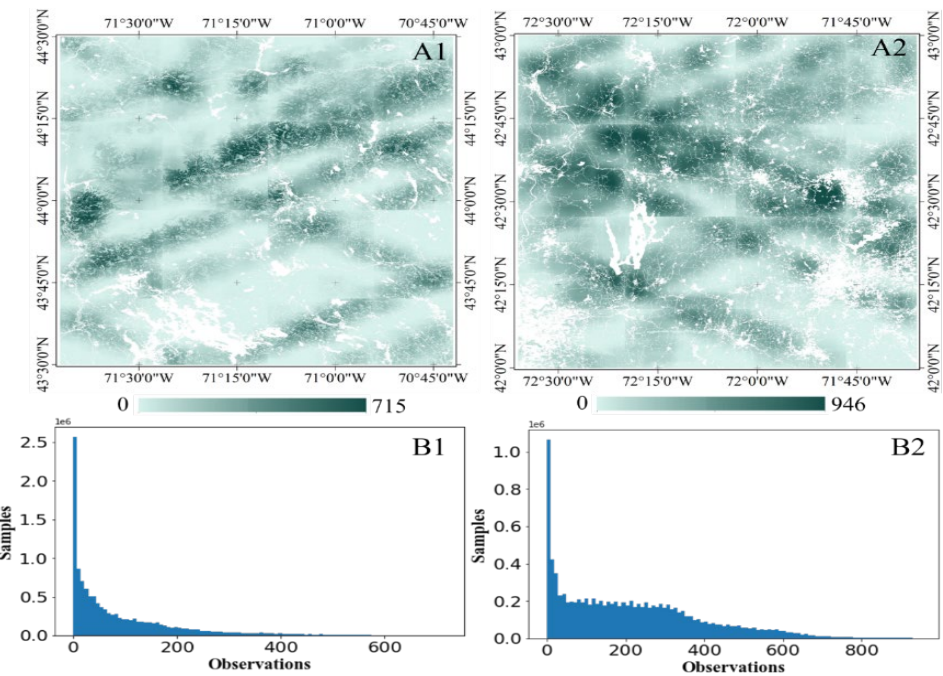


Figure 20. Densities of GEDI observations over space (A1 and A2) and amounts (B1 and B2) within a 6 km width window for each object pixel in RF-CH in Area 1 and Area 2, respectively. Masked areas in A1-2 are displayed in white.

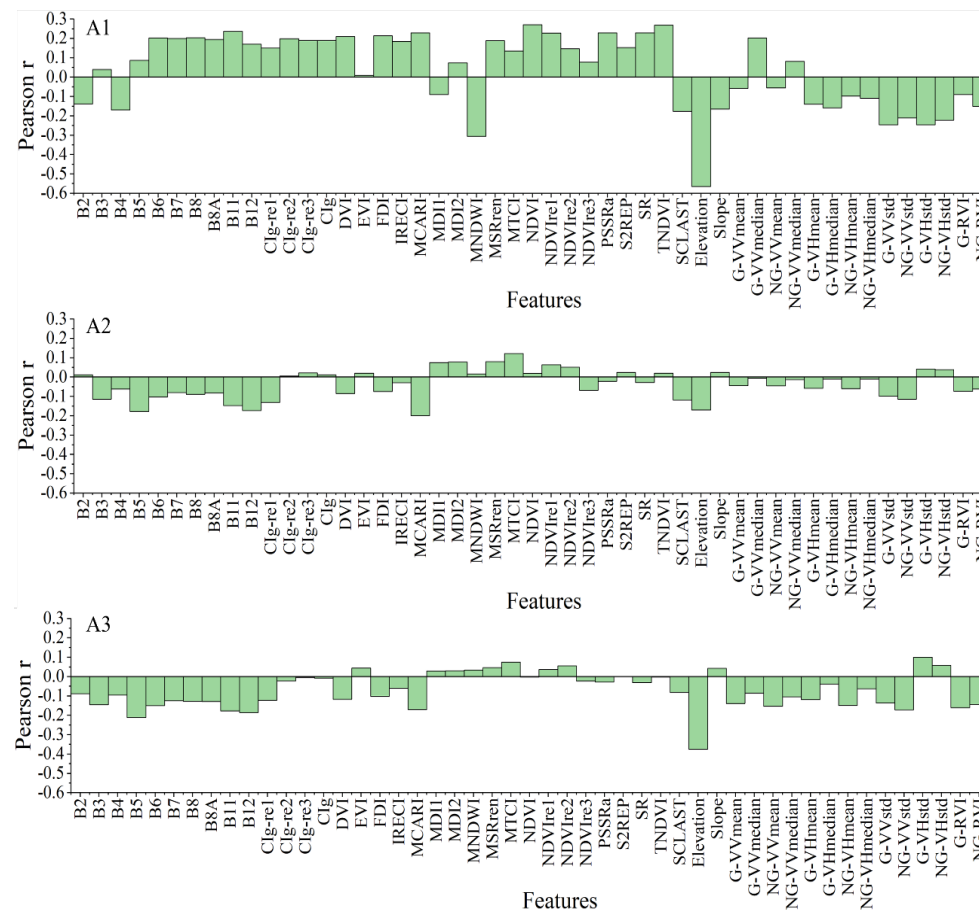


Figure 22. Correlations between canopy height and features derived from ancillary images in BART (A1), HARV (A2), and HOPB (A3). Explanations of each feature can be found in Table 4.

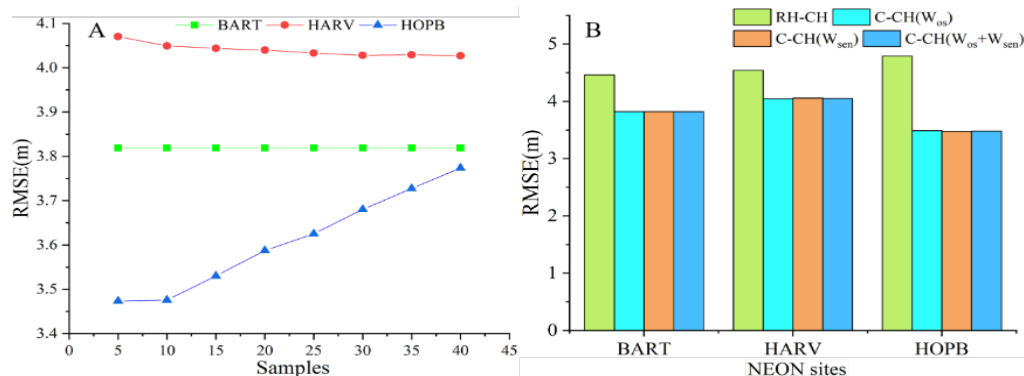


Figure 21. Correlations between canopy height and features derived from ancillary images in BART (A1), HARV (A2), and HOPB (A3). Explanations of each feature can be found in Table 4.

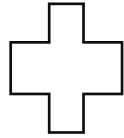
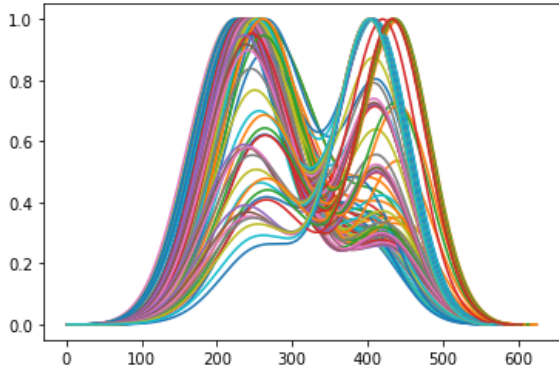
1. The FPSF-CH is comprehensively affected by the availability of GEDI data around corresponding pixel to be corrected (Figure 20-21) and the relationship between canopy height and ancillary imageries for the initial canopy height mapping for calibration (Figure 22).

➤ Limitations and Future Work

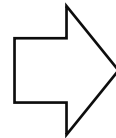
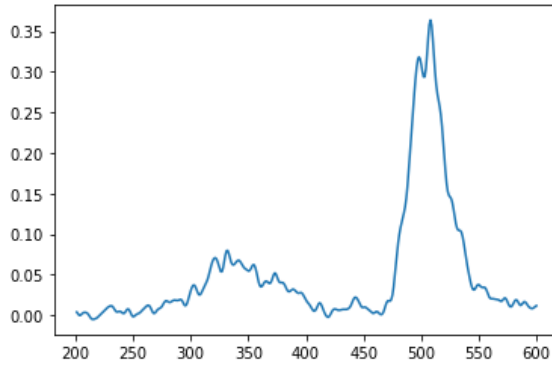
- For GEDI data application, geolocation is an randomly errors which is dependent on the heterogeneity of landscape.
- At present, there is lack of mitigation errors from GEDI geolocation uncertainty.
- Slope effect on GEDI canopy height estimation should be considered especially for mountainous areas.
- For canopy height mapping calibration, we proposed the FPSF-CH which allows one to integrate spatially scattered good-quality GEDI observations and a spatially continuous antecedent canopy height mapping.

➤ Colocation correction for GEDI waveform.

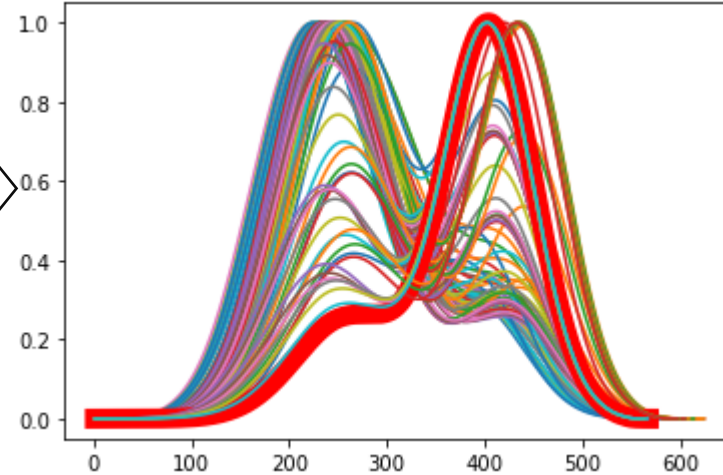
100 simulated waveforms



GEDI waveform



The most correlated simulated waveform



What's the shifts of the optimal simulated waveform?



Comparison of Bias, MAE and RMSE before and after shift simulated waveform location;

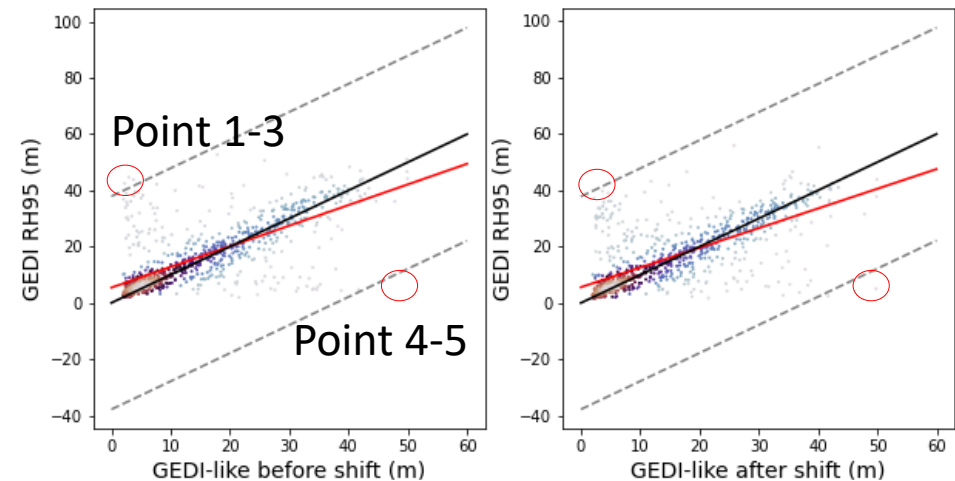


RH95 distributions of before and after location shifts of simulated waveform.



	-10	-8	-6	-4	-2	0	2	4	6	8	10
-10	5.05	1.01	1.1	1.11	1.6	0	1.8	1	1.8	1.21	4.39
-8	0.96	0.76	0.4	0.4	0.9	0	0.5	0.2	0.4	0.51	1.41
-6	1.46	0.51	0.2	0.51	0.5	0	0.6	0.6	0.4	0.3	1.01
-4	0.91	0.51	0.7	0.35	0.4	0	0.4	0.3	0.5	0.4	1.31
-2	1.21	0.4	0.5	0.45	0.5	0	0.7	0.2	0.5	0.61	1.36
0	0	0	0	0	0	12	0	0	0	0	0
2	0.91	0.35	0.6	0.45	0.1	0	0.5	0.4	0.3	0.51	0.96
4	1.16	0.76	0.4	0.25	0.5	0	0.3	0.4	0.6	0.4	1.21
6	1.06	0.3	0.6	0.25	0.5	0	0.6	0.3	0.5	0.45	1.72
8	1.67	0.35	0.3	0.56	0.7	0	1	0.4	0.3	0.51	1.11
10	3.74	1.16	0.6	1.06	1.8	0	2	1.7	1.2	1.67	5.2

	Samples	Bias	AAD	RMSE
Before shift	845	-1.49	5.16	9.05
After shift	845	-1.16	5.23	8.98
Difference	0	0.33	-0.07	0.07

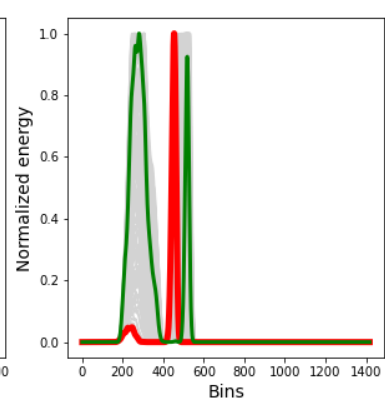
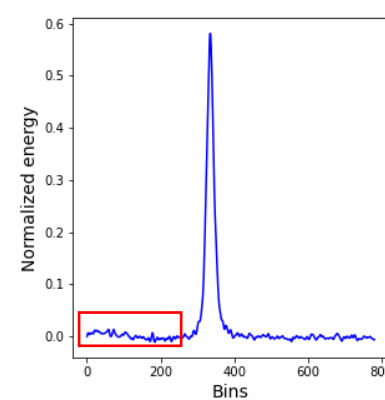
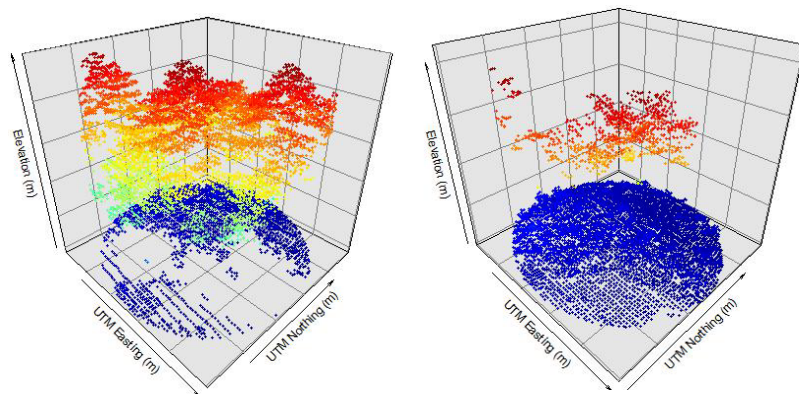


➤ Colocation correction for GEDI waveform.

S54050800200156415

X-shift: -10m

Y-shift: 10m

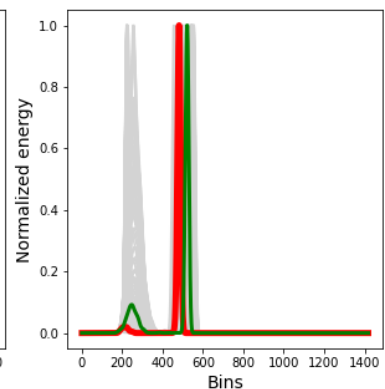
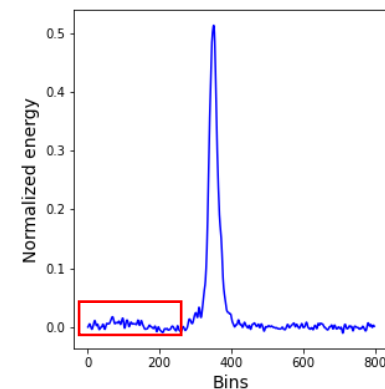
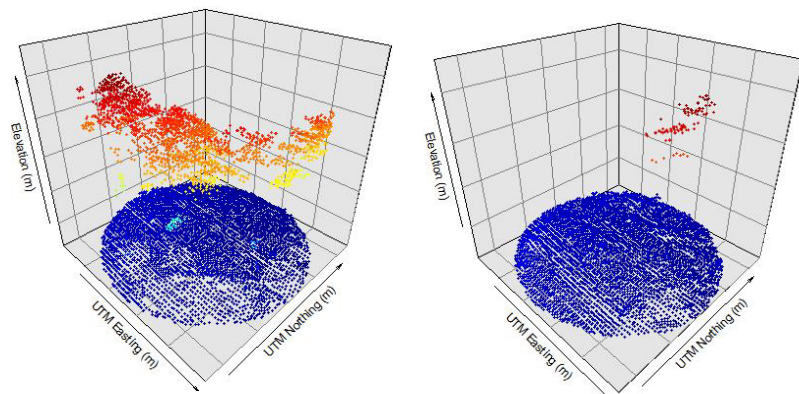


Waveforms
— GEDI
— After shift
— Before shift

S54050800200156416

X-shift: 2m

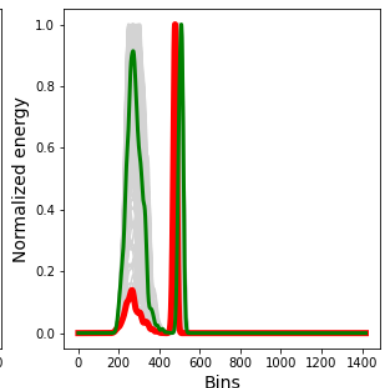
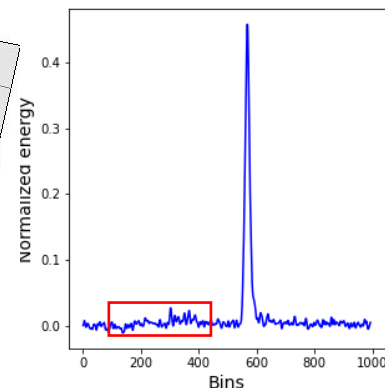
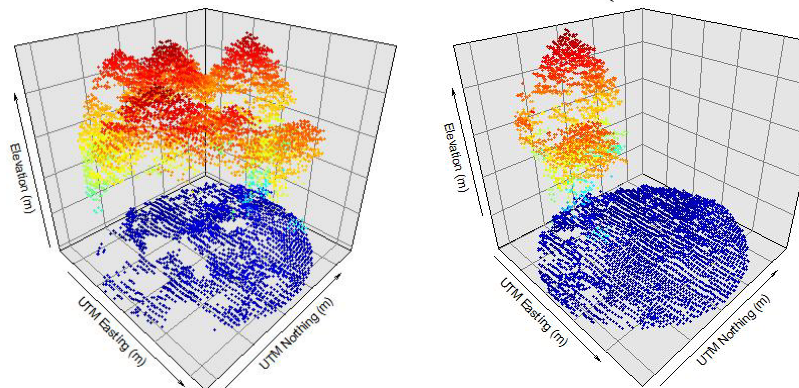
Y-shift: 10m



S54050800200156432

X-shift: 2m

Y-shift: 10m



Sensitivity would obviously affect GEDI waveform shape especially for sparse forest area in which top of canopy tend to be overwhelmed.

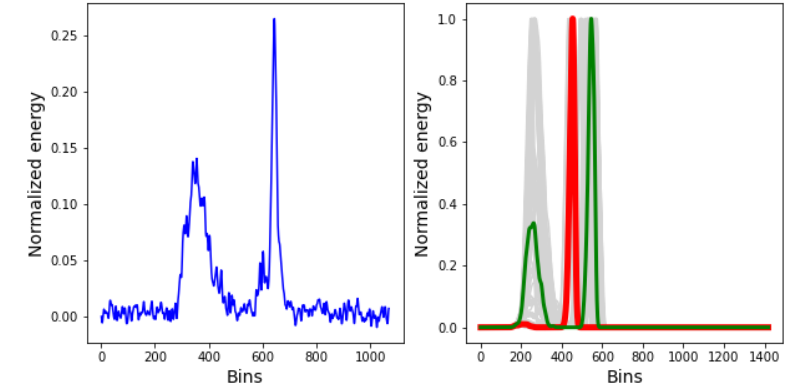
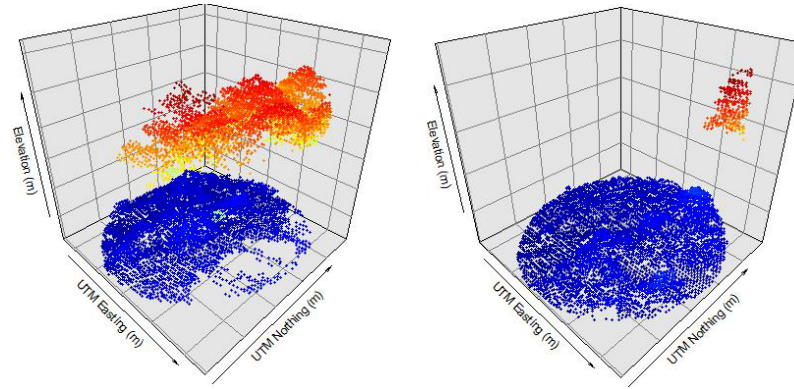
➤ Colocation correction for GEDI waveform.

Errors from waveform colocation;

S49930300200151410

X-shift: -10m

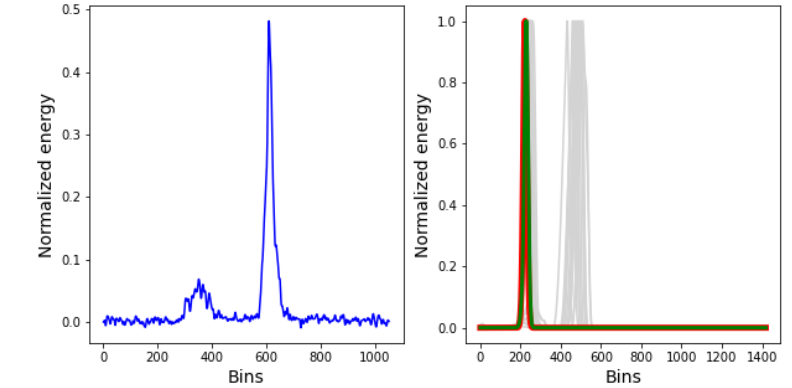
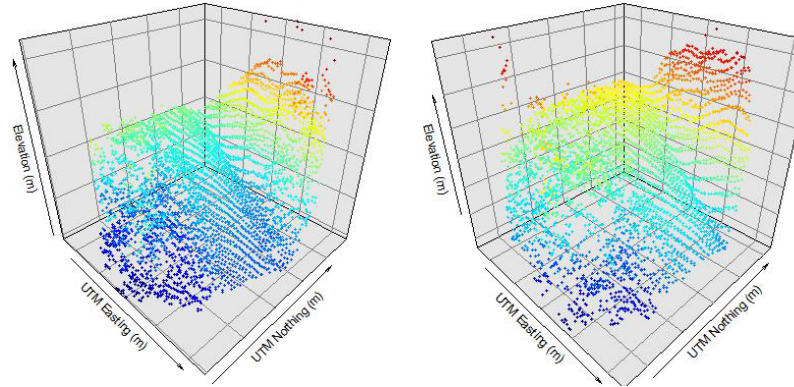
Y-shift: 10m



S54051100200151286

X-shift: -10m

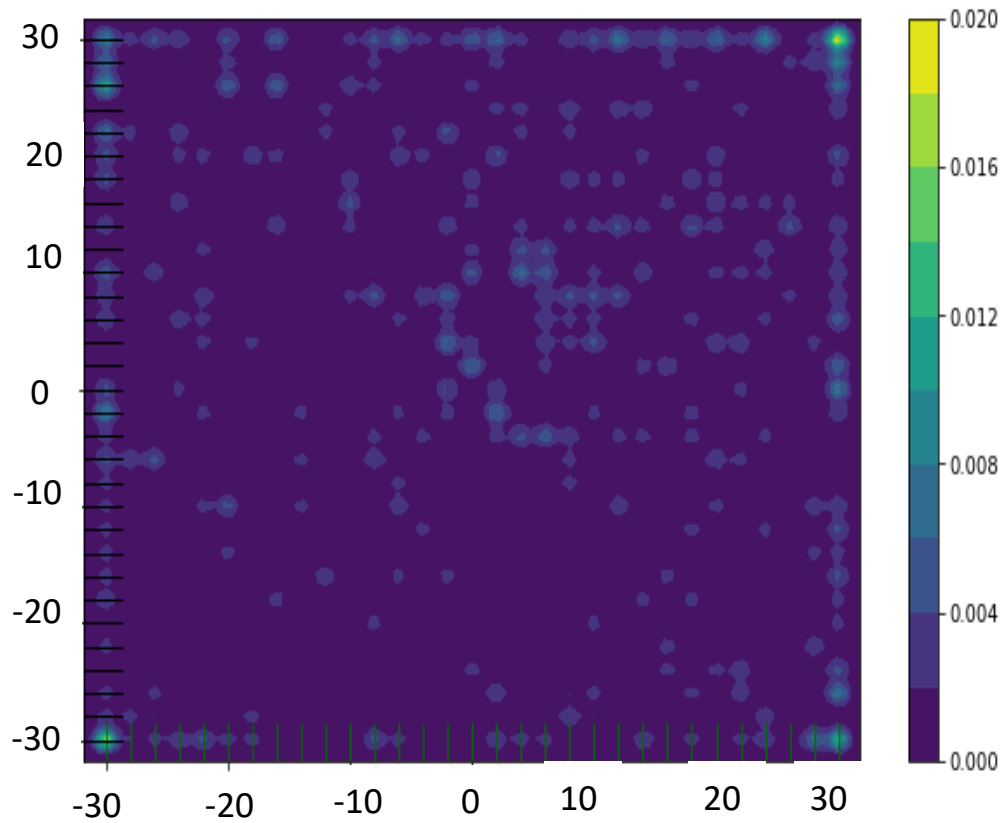
Y-shift: 2m



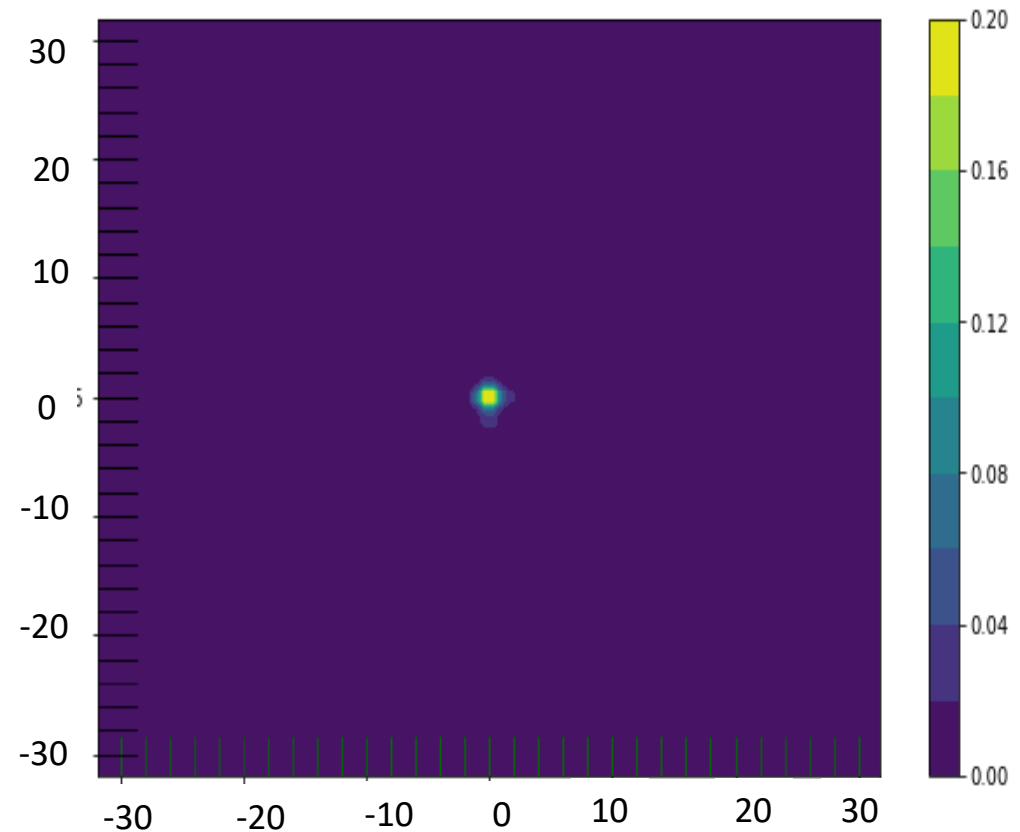
Waveform alignment?

Multiple scatter?

➤ Colocation correction for GEDI waveform.



Without using threshold for optimal simulated waveform selection;



With using threshold for optimal simulated waveform selection;

Thanks!

Spatial map of oil palm age in 2017

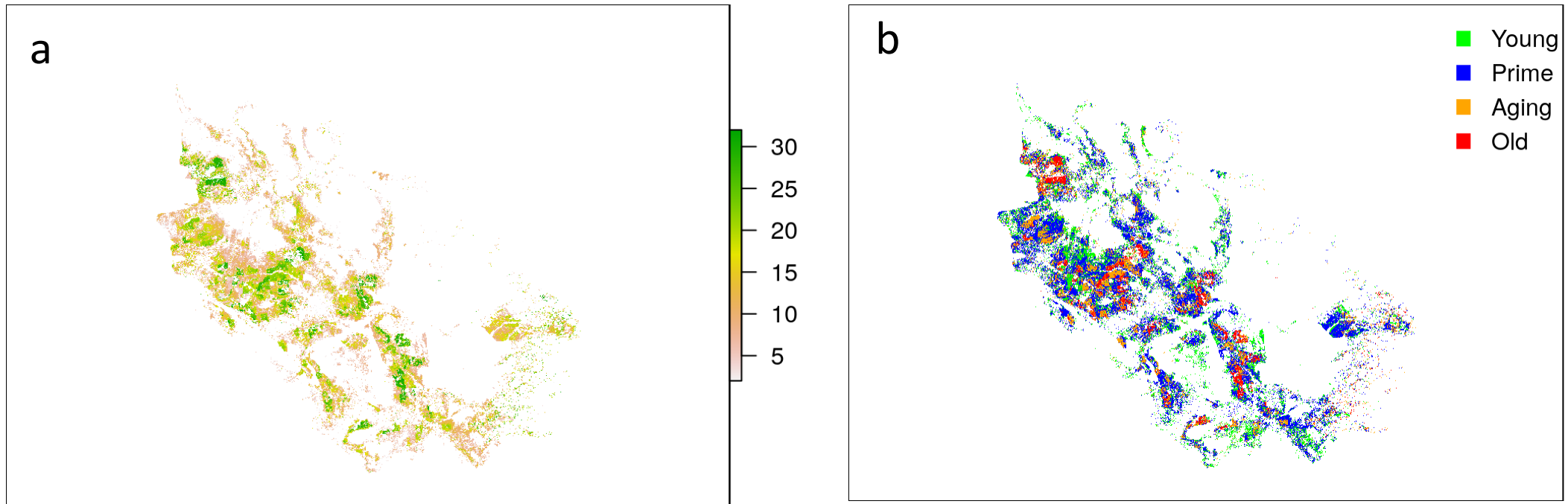
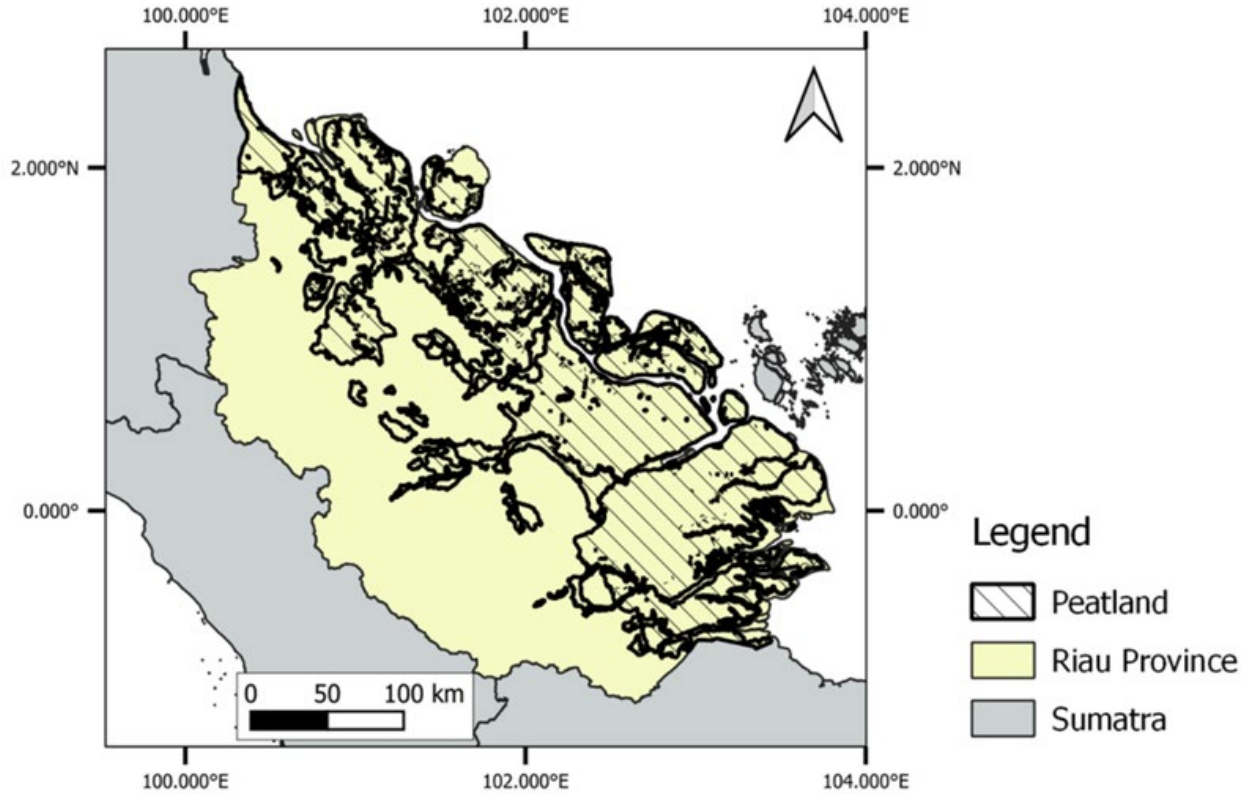


Figure 3. Spatial distribution of oil palm age in Riau in 2017. Panel a shows the age map of oil palm in Riau. Panel b shows the stage of oil palm in Riau. Young stands for age <8 , Prime for age <19 , Aging for age <25 , and Old means age from 25.

Riau province in Indonesia



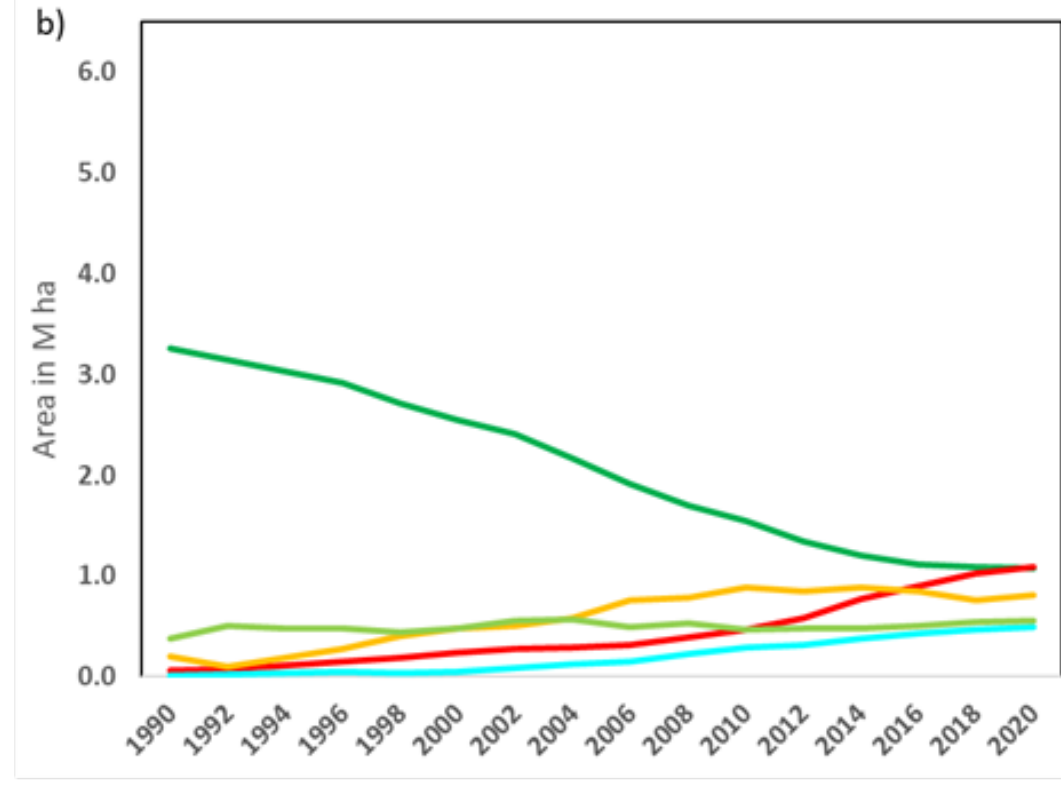
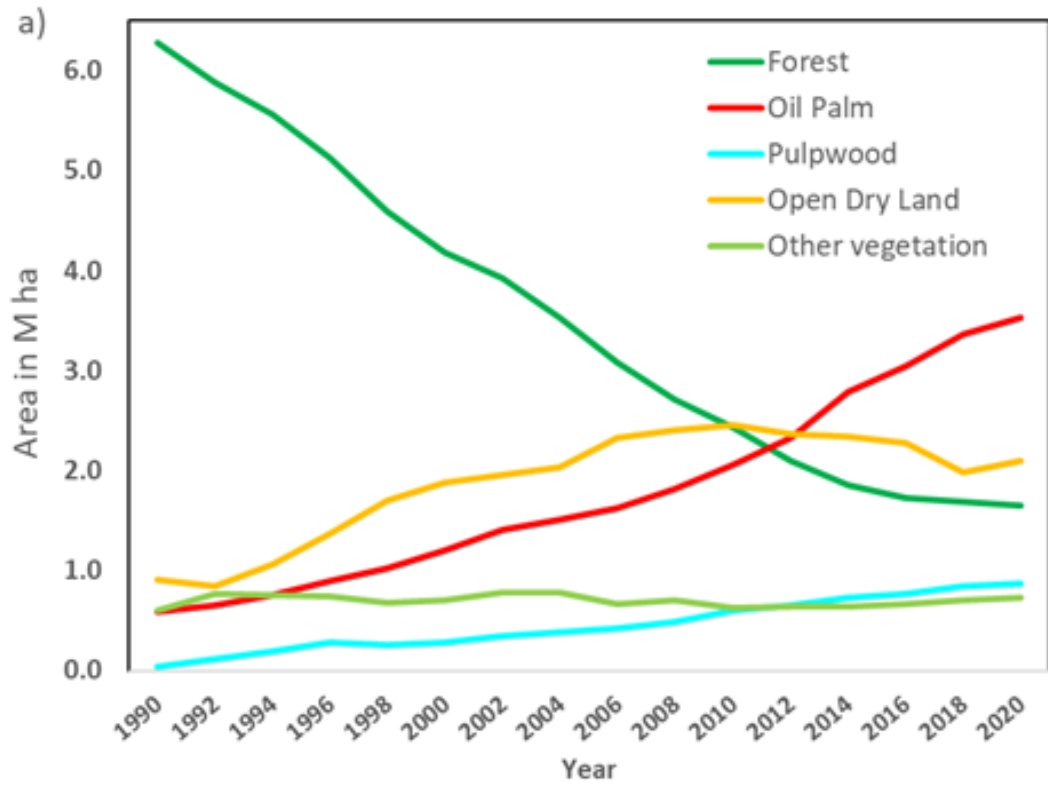


Figure 5. Total area of land cover classes: forest, oil palm, open dry land, pulpwood and other vegetation in Riau (a) and within Riau's peatland (b) during 1990-2020.

Land cover classes in Riau

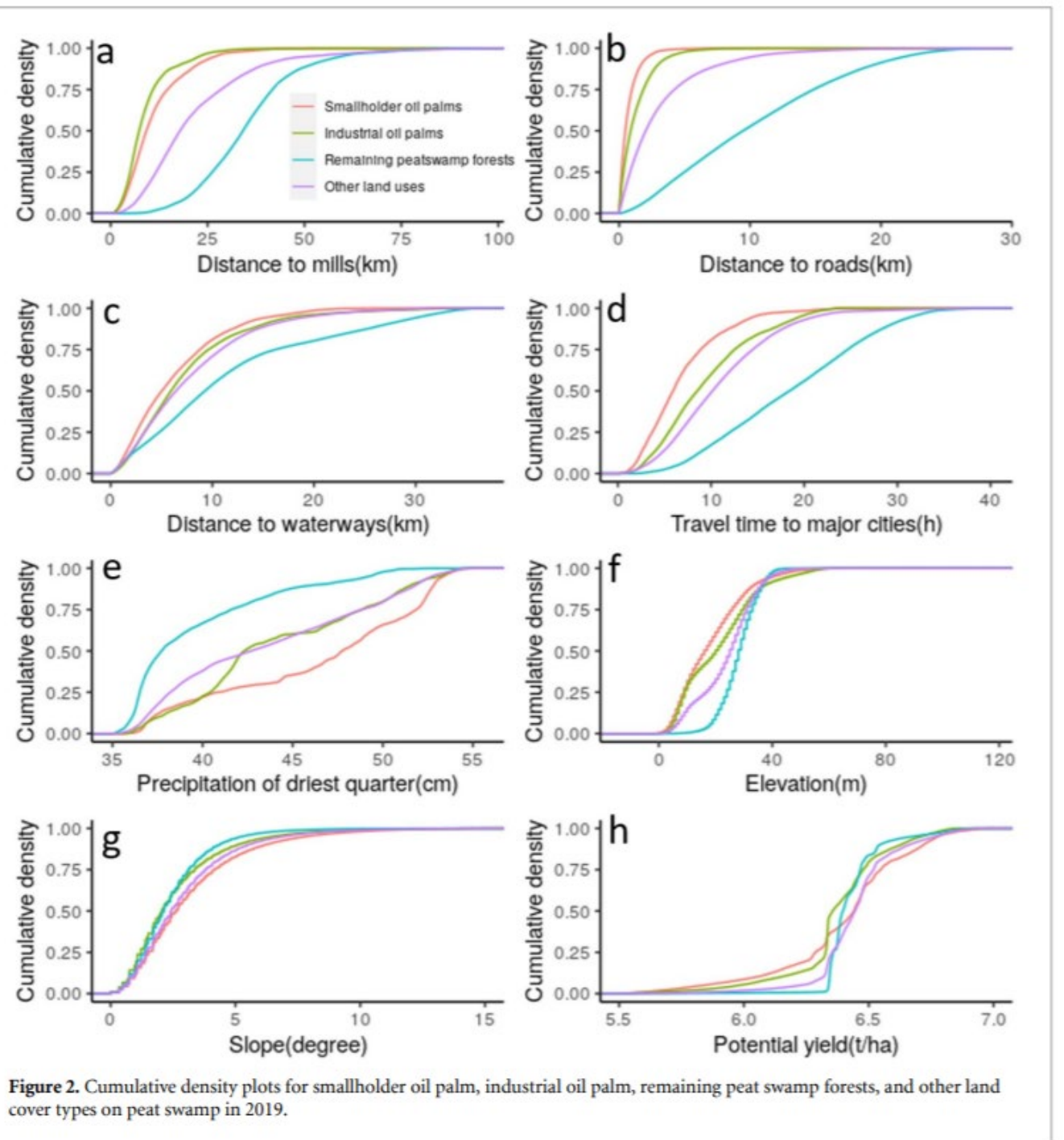
Class	Description
Mature oil palm	Oil palm plantation with high canopy closure (>4 years old)
Young oil palm*	Oil palm plantation with open canopy (1 to 4 years old)
Open dry land	Other land use types including open area, crops and pasture
Forest	Natural forest
Bare soil/Impervious	Bare ground after deforestation and replacement of oil palm trees and crop harvest. Impervious surface such as urban area, roads and other constructions
Other vegetation	Coconut palm, grass, vegetation in riparian zone, rubber trees, recovery and other unknown vegetation surfaces
Pulpwood	<i>Acacia</i> and <i>Eucalypt</i>
Water**	Water body

Results: Forest loss and expansion of Oil Palm

Table 2. Total area (M ha) of forest, oil palm and pulpwood plantation area in 1990, 2000, 2010 and 2020.
Note: Numbers in parentheses are proportions of each land cover type on mineral soil and peatland in Riau.

	1990	2000	2010	2020
Forest	6.28	4.20	2.43	1.65
Overall coverage	68.5%	45.8%	26.5%	18.0%
Mineral Soil	3.03 (48%)	1.65 (39%)	0.88 (36%)	0.58 (35%)
Peatland	3.25 (52%)	2.55 (61%)	1.55 (64%)	1.07 (65%)
Oil Palm	0.59	1.21	2.06	3.52
Overall coverage	6.4%	13.1%	22.5%	38.4%
Mineral Soil	0.063 (91%)	1.22 (84%)	1.87 (80%)	2.68 (71%)
Peatland	0.06 (9%)	0.24 (16%)	0.47 (20%)	1.08 (29%)

Spatial patterns of smallholder oil palm expansion over peat swamp forest since 1990 are different with other land cover types.



Drivers of smallholder oil palm expansion over peat swamp forests

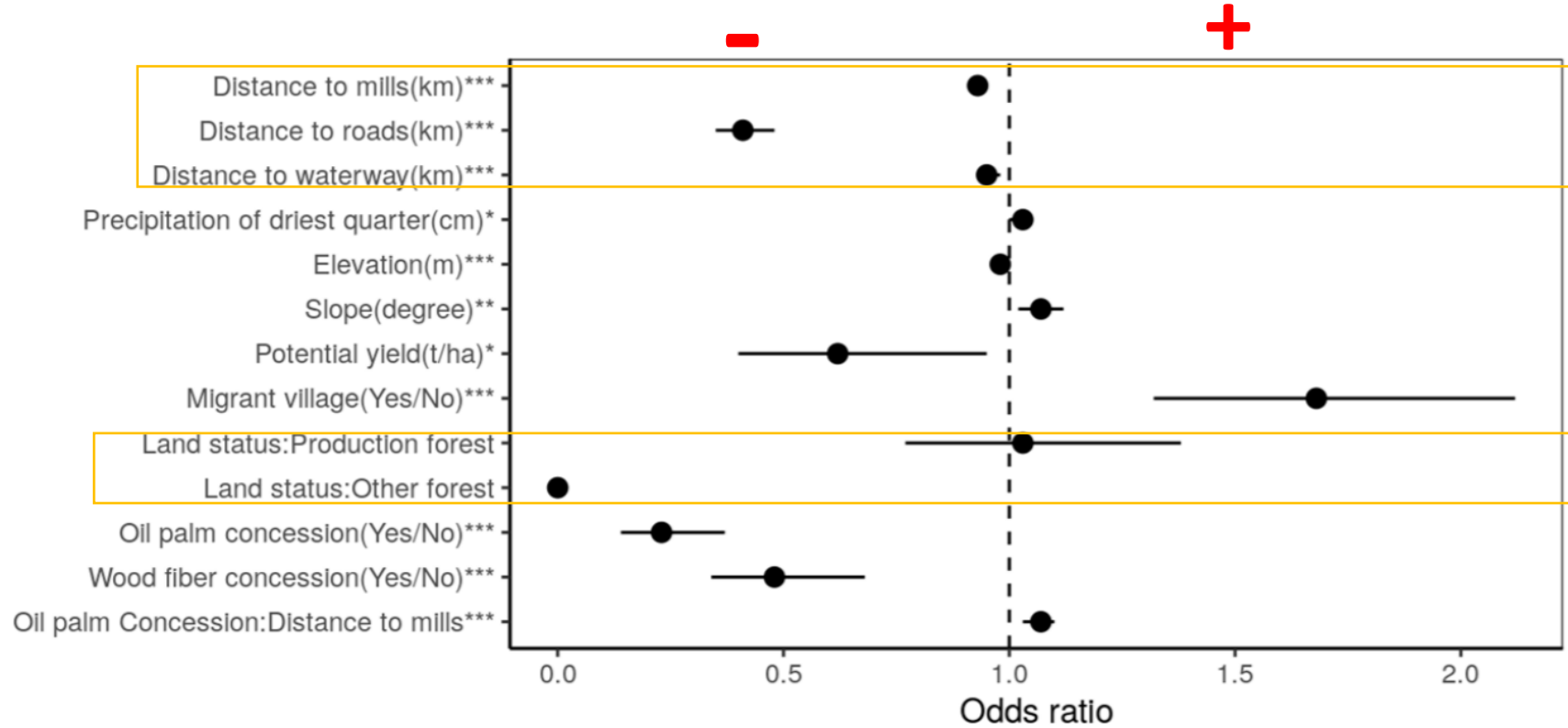


Figure 4. Relative influences of socioeconomic and biophysical variables on smallholder oil palm expansion into peat swamp forest in Riau. Results from the final model after selecting variables with stepwise AIC. All displayed variables are statistically significant with *, **, *** showing significance at 5%, 1%, 0.1%, respectively. Variables with odds ratios to the right of the dotted line indicates that increasing that variable is associated with greater odds of conversion from peat swamp forests to smallholder oil palm, while odds ratios to the left of the dotted line indicate that increasing that variable decreases the odds of conversion. Bars correspond to the 95% confidence interval for odds ratios calculated using White–Huber standard errors based on a spatial logistic regression model with 9000 samples.

Oil palm cut and replantation

More smallholder oil palms are located on illegal forest area that were covered by peat swamp forest in 1990.

	Industrial OP	Smallholder OP
Non-forest land(APL)	232217	63900
Convertible production forest(HPK)	36830	30304
Permanent Production forest(HP)	32913	36411
Limited Production Forest(HPT)	10665	18644
Nature Reserve/Conservation area(KSA/KPA)	147	85
Protected forest(HL)	51	67
Wildlife reserve(SM)	0	8
Total area (ha)	312823	149419
Area on forest (ha)	80606	85519
Ratio of area on forest over total area	0.26	0.57